การซึมผ่านผิวหนังนอกร่างกายของไลโคปีนนาโนพาร์ทิเคิลที่มีไคโตซานเป็นสารเพิ่มความคงตัว

นางสาว สุฎา ลิ่มวงศ์สุวรรณ

วิทยานิพนธ์นี้เป็นส่วนหนึ่งของการศึกษาตามหลักสูตรปริญญาวิทยาศาสตรมหาบัณฑิต

สาขาวิชาเทคโนโลยีเภสัชกรรม คณะเภสัชศาสตร์ จุฬาลงกรณ์มหาวิทยาลัย

ปีการศึกษา 2548

ISBN 974-14-1896-5

IN VITRO PENETRATION OF LYCOPENE-LOADED NANOPARTICLES USING CHITOSAN AS A STABILIZER

Miss Suda Limvongsuwan

A Thesis Submitted in Partial Fulfillment of the Requirements
for the Degree of Master of Science Program in Pharmaceutical Technology
Faculty of Pharmaceutical Sciences
Chulalongkorn University
Academic Year 2005

ISBN 974-14-1896-5

Thesis Title	*IN VITRO* PENETRATION OF LYCOPENE-LOADED NANOPARTICLES USING CHITOSAN AS A STABILIZER
By	Miss Suda Limvongsuwan
Field of Study	Pharmaceutical Technology (International)
Thesis Advisor	Associate Professor Ubonthip Nimmannit, Ph.D.

Accepted by the Faculty of Pharmaceutical sciences, Chulalongkorn University in Partial Fulfillment of the Requirements for the Master's Degree

Pornpen Pramyothin ..... Dean of the Faculty of Pharmaceutical Sciences

(Associate Professor Pornpen Pramyothin, Ph.D.)

THESIS COMMITTEE

Papavadee Klongpiyapong ..... Chairman

(Associate Professor Papavadee Klongpiyapong)

Ubonthip Nimmannit ..... Thesis Advisor

(Associate Professor Ubonthip Nimmannit, Ph.D.)

Parkpoom Tengamnuay ..... Member

(Associate Professor Parkpoom Tengamnuay, Ph.D.)

Sunanta Pongsamart ..... Member

(Associate Professor Sunanta Pongsamart, Ph.D.)

N. Vardhanabhuti ..... Member

(Nontima Vardhanabhuti, Ph.D.)

สุฎา ลิ่มวงศ์สุวรรณ : การซึมผ่านผิวหนังนอกร่างกายของไลโคปีนนาโนพาร์ทิเคิลที่มีไคโตซานเป็นสารเพิ่มความคงตัว (*IN VITRO* PENETRATION OF LYCOPENE-LOADED NANOPARTICLES USING CHITOSAN AS A STABILIZER) อ. ที่ปรึกษา: รศ. ดร.อุบลทิพย์ นิมมานนิตย์, 134 หน้า. ISBN 974-14-1896-5

ไลโคปีนนาโนพาร์ทิเคิลเตรียมจาก 2 วิธี คือ ไคโตซานไลโปโซมนาโนพาร์ทิเคิล และไคโตซานอัลจิเนตนาโนพาร์ทิเคิล โดยใช้ไคโตซานเป็นสารเพิ่มความคงตัว การวิเคราะห์ขนาด ลักษณะของอนุภาคและ เปอร์เซ็นต์การกักเก็บไลโคปีนในนาโนพาร์ทิเคิลได้ผลดังนี้ ขนาดอนุภาคของไลโคปีนในไคโตซานไลโปโซมนาโนพาร์ทิเคิลและไคโตซานอัลจิเนตนาโนพาร์ทิเคิลอยู่ระหว่าง 320-463 นาโนเมตร และ 323-500 นาโนเมตร ตามลำดับ จากภาพถ่ายอิเล็กตรอนไมโครสโคป พบลักษณะอนุภาคของไคโตซานไลโปโซมนาโนพาร์ทิเคิลมีรูปร่างกลมหรือรี มีผนังซ้อนเรียงเป็นชั้น และลักษณะอนุภาคของไคโตซานอัลจิเนตนาโนพาร์ทิเคิลมีรูปร่างกลม และมีลักษณะเป็นรูพรุน ความเข้มข้นของไลโคปีนที่ใช้เตรียมมีผลต่อเปอร์เซ็นต์การกักเก็บไลโคปีนในนาโนพาร์ทิเคิล ซึ่งเมื่อเพิ่มความเข้มข้นของไลโคปีนที่ใช้เตรียม ทำให้เปอร์เซ็นต์การกักเก็บไลโคปีนในนาโนพาร์ทิเคิลเพิ่มขึ้น พบว่า เปอร์เซ็นต์การกักเก็บไลโคปีนในไคโตซานไลโปโซมนาโนพาร์ทิเคิลมีค่าสูงที่สุดเมื่อเตรียมที่ความเข้มข้นของไลโคปีนเท่ากับ 200.28 ไมโครกรัมต่อมิลลิลิตร และ เปอร์เซ็นต์การกักเก็บไลโคปีนในไคโตซานอัลจิเนตนาโนพาร์ทิเคิลมีค่าสูงที่สุด เมื่อเตรียมที่ความเข้มข้นของไลโคปีนเท่ากับ 234.16 ไมโครกรัมต่อมิลลิลิตร การศึกษาความคงตัวพบว่าไคโตซานอัลจิเนตนาโนพาร์ทิเคิลมีความคงตัวดีกว่าเมื่อเก็บในตู้เย็นเปรียบเทียบกับการเก็บในที่มืด และ ที่แสงปกติ ในอุณหภูมิห้อง ในการศึกษาการซึมผ่านของไลโคปีนนาโนพาร์ทิเคิลผ่านผิวหนังคน พบว่าไคโตซานไลโปโซมนาโนพาร์ทิเคิลและไคโตซานอัลจิเนตนาโนพาร์ทิเคิล มีอัตราการซึมผ่าน 0.71$\pm$0.03 และ 1.67$\pm$0.07 ไมโครกรัมต่อชั่วโมงต่อตารางเซนติเมตร ตามลำดับ ภาพถ่ายอิเล็กตรอนไมโครสโคปแสดงการซึมผ่านผิวหนังกำพร้าของไลโคปีนนาโนพาร์ทิเคิลหลังการทดสอบเป็นเวลา 3 ชั่วโมง พบไคโตซานไลโปโซมนาโนพาร์ทิเคิลอยู่ระหว่างเซลล์ชั้นผิวหนังกำพร้าร่วมกับมีการโป่งออกของไขมันระหว่างเซลล์และพบไคโตซานอัลจิเนตนาโนพาร์ทิเคิลอยู่ในเซลล์ของชั้นผิวหนังกำพร้า

สาขาวิชา เทคโนโลยีเภสัชกรรม ลายมือชื่อนิสิต.....สุฎา ลิ่มวงศ์สุวรรณ.....

ปีการศึกษา.....2548..... ลายมือชื่ออาจารย์ที่ปรึกษา.....

4776854033: MAJOR PHARMACEUTICAL TECHNOLOGY (INTERNATIONAL) PROGRAM
KEY WORD: LYCOPENE / NANOPARTICLES / LIPOSOMES / CHITOSAN / ALGINATE / *IN VITRO* PENETRATION / HUMAN SKIN / STABILITY / ENCAPSULATION

SUDA LIMVONGSUWAN: *IN VITRO* PENETRATION OF LYCOPENE-LOADED NANOPARTICLES USING CHITOSAN AS A STABILIZER. THESIS ADVISOR: ASSOC. PROF. UBONTHIP NIMMANNIT, Ph.D. 134 pp. ISBN 974-14-1896-5.

Lycopene nanoparticles were prepared by two different methods, chitosan coated liposome nanoparticles and chitosan alginate nanopaticles. The chitosan was used as a stabilizer. The particle sizes, morphology and encapsulation efficiency were investigated. The results showed that the mean particle sizes were in range of 320-463 nm and 323-500 nm for chitosan coated liposome nanoparticles and chitosan alginate nanoparticles, respectively. TEM analysis showed that lycopene loaded chitosan coated liposome nanoparticles had a spherical or ellipsoidal shape with some lamellar patterns of liposomes. Lycopene loaded chitosan alginate nanoparticles presented a spherical shape with a highly porous structure. The percentage of encapsulation efficiency was significantly affected by the lycopene loading concentration. When lycopene loading concentration was increased, the percentage of encapsulation efficiency increased. The highest percentage of encapsulation efficiency of chitosan coated liposome nanoparticles was obtained at lycopene loading concentration of 200.28 µg/mL, while the highest percentage of encapsulation efficiency of chitosan alginate nanoparticles was obtained at lycopene loading concentration of 234.16 µg/mL. Lycopene loaded chitosan alginate nanoparticles exhibited greater stability after storage for 12 weeks in refrigerator than storage in dark and visible light at room temperature. The *in vitro* penetration through the human skin showed the flux of lycopene loaded chitosan coated liposome and lycopene loaded chitosan alginate nanoparticles were 0.71 ± 0.03 and 1.67 ± 0.07 µg/cm^{2}h, respectively. TEM micrographs showed the penetration of lycopene loaded nanoparticles into epidermis after 3 h treatment. lycopene loaded chitosan coated liposome nanoparticles was found between the corneocyte with swelling of the intercellular lipid and lycopene loaded chitosan alginate nanoparticles was found in corneocyte at stratum corneum.

Field of study Pharmaceutical Technology Student's signature Suda Limvongsuwan.
Academic year……2005…… Advisor's signature Ubonthip Nimmannit

ACKNOWLEDGEMENTS

I am deeply indebted to many people who have made their kind contributions to much study. First of all, I would like to express my profound gratitude and appreciation to my advisor, Associate Professor Dr. Ubonthip Nimmannit for her valuable comments and suggestions, her kindness and constant encouragement throughout my study. I am very much obliged to the members of my thesis committee for their scrutiny and discussion.

I am most grateful to Dr. Pranee Lertsutthiwong of the Center for Chitin-Chitosan Biomaterials, Chulalongkorn University, for supply of chitosan and her invaluable advice in this thesis. Also, I am very thankful to Mr. Pisuth Lertvilai of Rovithai Limited, for providing lycopene (10% FS Redivivo™) used in this thesis. Moreover, I would like to thank Yanhee Hospital for giving the human skin sample.

My special thanks and highly regard is extended to Associate Professor Somporn Swadison, DDS of Department of Oral Pathology, Faculty of Dentistry, for her helpful assistance to prepare histological slide. My sincere appreciation also goes to Dr. Naree Warnnissorn of Faculty of Medicine, Thammasart University, for her kindness, consideration and excellent guidance in the histological observation. I am deeply honored to Associate Professor Kleophant Thakerngpol of Department of Clinical Pathology, Faculty of Medicine, Siriraj Hospital for her consideration and invaluable discussion.

I also would like to thank Mr. Boonlaer Ngotrawornchai, Miss. Siripen Vethchagarun and Miss. Kaew kajornchaiyakul of the Scientific and Technological Research Equipment Center of Chulalongkorn University for the useful suggestion and data of TEM and particle size analysis to my thesis.

Above all, my deep appreciation goes to my friends and other people, whose names have not been mentioned, for helping me in anyway during the time of my study.

I would like to express appreciate to all the faculty members in the Pharmaceutical Technology (International) Program for their help and encouragement. Finally, I would like to express my sincerest and deepest gratitude to my family for their love, care, understanding and support.

CONTENTS

PAGE

PAGE

LIST OF TABLES

TABLE **PAGE**

TABLE **PAGE**

LIST OF FIGURES

FIGURE **PAGE**

FIGURE **PAGE**

FIGURE **PAGE**

FIGURE **PAGE**

FIGURE **PAGE**

LIST OF ABBREVIATIONS

cm	centimeter
g	gram
h	hour
HPLC	high performance liquid chromatography
LUVs	large unilamellar vesicles
M	mole per liter
mg	milligram
μg	microgram
min	minute
mL	milliliter
μl	microliter
MLVs	multilamellar vesicles
mM	millimole per liter
μm	micrometer
μM	micromole per liter
nm	nanometer
nM	nanomole per liter
R^2	coefficient of determination
ROS	reactive oxygen species
rpm	revolution per minute
RSD	relative standard deviation
SD	standard deviation
sec	second
SUVs	small unilamellar vesicles
T_c	phase transition temperature
TEM	transmission electron microscope
UV	ultraviolet

CHAPTER I

INTRODUCTION

Long-term exposure of UVA and UVB radiation to the skin cause degenerative effect such as sunburn, phototoxicity, photoallergy, photoaging and photocarcinogenesis. The use of antioxidants to inhibit photooxidative toxicity has been suggested as an important strategy in preventing and treating photodamage. Recently, scientists have tried to find a natural compound that can act as an antioxidant. Carotenoids are the pigments responsible for the colors of vegetables and fruits. Many carotenoids are known as an antioxidant and the most predominant carotenoid in human plasma is lycopene.

Lycopene is a phytochemical, synthesized by plants and microorganisms. It is the compound responsible for red color found in tomatoes, watermelons and other fruits, particularly concentrated in tomatoes, processed tomato products, such as juice, ketchup paste, sauce, and soup. Lycopene is a C_{40}-acyclic carotenoid. It is one of the most effective quenchers of a free radical called singlet oxygen. There are many researches that support the role of lycopene in human health such as prevention of cancer of the prostate, breast and lung, as well as in the prevention of cardiovascular disease, and protection skin from ultraviolet (UV) damage (Blum et al., 2005; Stahl and Sies, 2004).

Because lycopene can protect skin against oxidative stress, it is desirable to be applied directly into skin. Although lycopene can be absorbed and circulated to skin by diet and oral supplementation, physiological processes which related to absorption, solubility and transport also limited the amount that can be delivered into skin. Direct application of lycopene has the added advantage of its targeting to the area of skin needing the protection. For topical application of lycopene, several obstacles must be

overcome. However, lycopene is inherently unstable compounds, susceptible to oxidants, light and heat. These make them difficult to formulate in stable composition and acceptable for cosmetic use. Therefore, lycopene should be protected from environment and chemical damage. In addition, lycopene is deeply colored, adding to the complexity of producing an acceptable aesthetic product. For delivery, lycopene loaded nanoparticles should be formulated to overcome their problems.

Liposomes have been evaluated by many researchers as delivery system for drugs, vitamins and cosmetic materials. Liposomes consist of amphiphilic lipid, having a polar head group and one or two long hydrophobic chains. They consist of one or several concentric lipid bilayers enclosing an aqueous core. Liposomes are used to overcome solubility problem in the delivery of active compounds and for improving topical absorption of poorly absorbed drug. Encapsulation of drug into liposomes can lead to the enhancement or prolongation of therapeutic efficacy of drugs, reducing toxicity (Grit and Crommelin, 1993; Singh and Das, 1998) and also increasing stability (Bergstrand, 2003; Brisaert et al., 2001).

Nowadays, nanoparticles as submicron (<1μm) drug colloidal carriers have attracted more and more interest in the last decade, since these systems were found to be able to increase efficacy, stability and reduce toxicity of potent drug. Nanoparticles are able to adsorb and/or encapsulate drugs, thus protecting them against chemical and enzymatic degradation.

Nanoparticles generally, but not necessarily, made of both biodegradable and nonbiodegradable polymers. A basic requirement for these polymers to be used in humans or animals is that they have to degrade into molecules with no toxicity for biological environments. For this biocompatibility reason a very limited numbers of polymers can be used to prepare biodegradable nanoparticles. Recently, natural material chitosan has attracted great attention in pharmaceutical and biomedical fields because of its advantage in biodegradability, biocompatibility and low toxicity. It is also commercially available (Agnihotri et al., 2004).

Chitosan can also be used as a stabilizing constituent of liposomes. Chitosan was then applied as a coated membrane to increase the mechanical strength and stabilize the liposome membrane (Henriksen et al., 1994; Wu et al., 2004).

For most drug delivery application, chitosan could be crosslinked due to its cationic properties (Agnihotri et al., 2004). Due to the toxicity of crosslinking reagents, only the ionic gelation technique can be used for pharmaceutical application (López-León et al., 2004). Chitosan hydrogel can be also formed by means of electrostatic interaction between the positively charged chitosan chain and polyanions employed as cross-linkers (Douglas and Tabrizian, 2005).

Calcium alginate is commonly used and forms a matrix for various delivery systems including gels, film, beads, microparticles and sponges. Addition of chitosan increases the mechanical strength of alginate nanoparticles (De and Robinson, 2003). Chitosan can be used as an alternative cationic polymer to form stable uniform alginate nanosphere by enveloping the negatively charged calcium alginate complex (Douglas and Tabrizian, 2005; Polk, 1994).

In this study lycopene nanoparticles were designed for skin delivery to improve penetration of lycopene through the stratum corneum into the deeper skin layers thus providing internal UV protection of the skin. Direct application of lycopene has the added advantage of targeting the antioxidants to the area of skin needing the protection. Due to lycopene is unstable compound. The encapsulations of lycopene into chitosan coated nanoparticles are chosen to overcome its instability in cosmetic application. Chitosan has many advantages, particularly for the developing nanoparticles. The cationic polymer is critically important in stabilizing the calcium alginate and liposomes. Addition of cationic molecule allowed strengthening of this system to obtain small and well-defined particles (López-León et al., 2004). The two different techniques employed to prepare nanoparticles were chitosan coated liposome and chitosan alginate nanoparticles. The determination of particle size, encapsulation efficiency, morphology and penetration through the skin were investigated. The *in*

vitro penetration through skin was investigated using franz diffusion cell. Finally, this research will be useful for further development of lycopene in skin care products.

Objectives

The purposes of this study were as follows:

1. To prepare lycopene-loaded nanoparticles using chitosan as a stabilizer
2. To study the effect of lycopene concentration on physicochemical properties of nanoparticles
3. To study the stability of lycopene-loaded nanoparticles during storage
4. To study the *in vitro* penetration of lycopene-loaded nanoparticles through the skin

CHAPTER II

LITERATURE REVIEW

1. Lycopene

1.1 Structural properties of lycopene

Lycopene is a C40-acyclic carotenoid with 11 conjugated double bonds. It is the isomer of β-carotene. Lycopene lacks a beta-ionone ring structure , therefore it is not converted into vitamin A as same as β-carotene. The all-trans isomer of lycopene is the most predominant isomer in fresh tomatoes and is the most thermodynamically stable form. Each conjugated double bond can undergo isomerization to produce various cis isomers, particularly during food processing and storage (Bramley, 2000; Omoni and Aluko, 2005). In human serum and tissue found a mixture of approximately 50% all–trans lycopene and 50% cis –isomers (5-cis, 9 -cis, 13 –cis and 15 –cis). It is generally accepted that the all-trans isomers have the highest bioactivity and the cis-isomers have the lowest bioactivity (Shi et al., 1999). The long chromophore in the polyene chain accounts for the red colour of lycopene (λ_{max} 472 nm) and also makes it a potentially powerful antioxidant. The many conjugated is a characteristic believed to be responsible for its beneficial effects (Bramley, 2000).

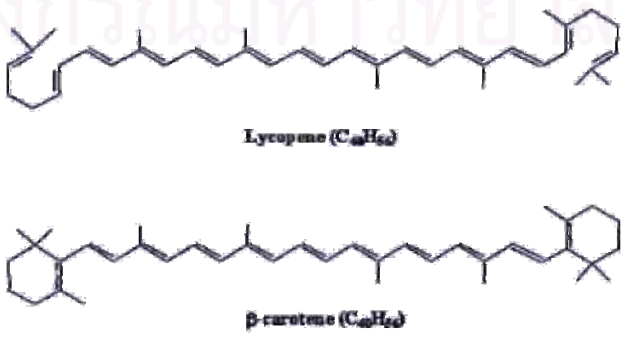

Figure 1 Basic structure of lycopene and β-carotene (Nijhawan and Holt, 1999).

1.2 Bioavailability and absorption of lycopene

Since humans are unable to synthesis carotenoids. They can be obtained exclusively from the diet. At least 85% of our dietary lycopene comes from tomato fruit and tomato-based products, the remainder being obtained from watermelon, pink grapefruit, guava and papaya (Table 1). Of the tomato products, juice, ketchup, soup and pizza and spaghetti sauces are the major contributors in the diet. The bioavailability of dietary lycopene appears to be dependent upon several factors. It is absorbed better from heat processed foods than unprocessed sources and also from lipid-rich diets. The different isomeric forms of lycopene have been suggested to be important factors that influence its bioavailability and adsorption (Bramley, 2000).

Table 1 Lycopene content of fruit and tomato products (Bramley, 2000).

Fruit or tomato Product	**Lycopene content (μg/g wet weight)**
Fresh tomato	8.8-42.0
Watermelon	23.0-72.0
Pink guava	54.0
Pink grapefruit	33.6
Papaya	20.0-53.0
Tomato sauce	62.0
Tomato paste	54.0-1500.0
Tomato juice	50.0-116.0
Tomato ketchup	99.0-134.4
Pizza sauce	127.1

The physical form of lycopene presents in foods is also an important factor influencing its adsorption. Carotenoids in fruit and vegetable are generally present as crystals. They may also be present bound as protein complexes and entrapped in cellular matrix. Thermal processing may facilitate the disruption of cellular structure

resulting in the dispersion or dissolution of crystalline carotenoids in to the lipid portion of the food matrix. Furthermore, Heat, along with chopping and processing, induces cis–isomerization and promotes its absorption thereby increasing their bioavailability (Bramley, 2000; Omoni and Aluko, 2005).

The cis form of lycopene found in processed tomato products has been shown to be more bioavailable than the all-trans from found in fresh tomatoes. This may be because cis-isomers are more soluble in bile acid micelles and so preferentially incorporated into chylomicrons. Lycopene is also distributed in the human body. It is one of the major carotenoids found in the human serum with plasma levels ranging from 0.22 to 1.06 nmol/mL (Omoni and Aluko, 2005). It is also found in various tissues throughout the body such as the liver, kidney, adrenal gland, testes, ovaries, and the prostate gland but is not deposited uniformly (Table 2). These differences suggest that there are specific mechanisms for the preferential deposition of lycopene, particularly in the adrenals and testis.

Table 2 Lycopene levels in human tissues (Bramley, 2000).

Tissue	**Lycopene (nmol/g wet weight)**
Adipose	0.2-1.3
Adrenal	1.9-21.6
Brainstem	Not detectable
Breast	0.8
Colon	0.3
Liver	1.3-5.7
Lung	0.2-0.6
Ovary	0.3
Prostate	0.8
Skin	0.4
Stomach	0.2
Testis	4.3-21.4

In vivo once the lycopene is taken up by the intestinal cells. It has high bioavailability, represents as much as 50 % of carotenoids found in human serum. Lycopene is a lipophilic compound thus lipids could increase the absorption of lycopene. Due to being fat soluble and has relatively small molecules, lycopene appears to be particularly effective in tissues with high fat and lipid content. It is transported by lipoproteins in blood and is concentrated in the prostate gland, adrenal testes, skin, liver and kidneys. A dynamic equilibrium exists between tissue and blood levels of lycopene (Omoni and Aluko, 2005). The skin is a lipid rich organ. But when lycopene was ingested, it was distributed through out the entire body and only relatively small amount was found in the skin.

The absorption and antioxidant properties of lycopene were investigated using liposome model system to simulate intestinal cells. Liposomes prepared from egg yolk phosphatidylcholine. Concentration of lycopene in the incubation medium had a significant effect on its uptake into the liposomes. Low concentration of lycopene (100 μM) showed a maximum percent uptake after incubate with liposomes 4 h, compared with higher concentration (200 μM). This can be explained by the saturation of lycopene on the absorptive site at higher concentration. There was time dependent increase in its absorption. Additionally, lipid soluble vitamin E also inhibit lycopene uptake by the liposomes presumably by competitive mechanism (Balachandran and Rao, 2003).

1.3 Antioxidant activity

Reactive oxygen species (ROS) have been implicated in playing a major role in the causation and progression of several chronic diseases including cancer and cardiovascular diseases. These ROS are highly reactive oxidant molecules that are generated endogenously through regular metabolic activity. The production of these free radicals in the body is much higher in response to several situations, for example exposure to sunlight, X-rays, smoking and environmental pollutants. Free radicals damage cell membranes and DNA, and alter various biochemical compounds within

the cells. It seems that they play a significant role in the development of heart and blood vessel diseases and the induction of malignancies.

Scientists believe that oxygen free radicals enhance the process of aging in various body systems, by their gradual and cumulative effect (Pinnell et al., 2003). Antioxidants are protective agents that inactivate ROS and, significantly delay or prevent oxidative damage associated with chronic disease risk.

Lycopene has the highest antioxidant activity among all carotenoids. It is a more effective at quenching a free radical called singlet oxygen, highly reactive free radical formed during normal metabolic processes that reacts with polyunsaturated fatty acid which are the major constituents of cell membranes (Stahl and Sies, 2004; Toor and Savage, 2005). During singlet oxygen quenching, energy is transferred from singlet oxygen to the lycopene molecule, converting it to the energy-rich triplet state. Lycopene in the triplet state can return to the ground state by dissipating the energy as heat or by physical quenching, leaving the lycopene molecule intact and ready for further quenching events (Wertz et al., 2004). The ability of antioxidant to prevent ROS (reactive oxygen species) mediated cellular damage depends on the ability of these molecules to be incorporated and transported across the cellular membranes. The effectiveness of lycopene as an antioxidant depends on concentration and interaction with other co–antioxidants such as vitamin E and C.

The antioxidant activity of lycopene is highlighted by its singlet oxygen-quenching property and its ability to trap peroxyl radicals. The previous study showed that the quenching constant of lycopene was found to be more than that of β–carotene and α–tocopherol (Heber and Lu, 2002). It also has ability to inhibit the oxidation of DNA, lipid peroxidation and may suppress tumor growth by stimulate gap junction communication between two cells (Wertz et al., 2004). As a result, to regulate cell to cell junction might provide an additional benefit of improving skin texture (Stahl and Sies, 2004).

The additional of lycopene in liposomes significant dose dependent decrease in the formation of thiobarbituric acid-reactive substances (TBARS), indicated the lipid peroxidation. However, inhibition of TBARS formation was less as the concentration of lycopene was increased. The protective properties of lycopene on lipid peroxidation at higher concentration may be due to aggregation or crystallization of lycopene out of solution. The antioxidant effect of lycopene was also found to be significantly higher than for α-tocopherol at the equimolar concentration (Balachandran and Rao, 2003).

Several recent studies have shown that a dietary intake of tomatoes and tomato products was associated with a decreased risk of chronic diseases such as cancer and cardiovascular disease. Serum and tissue lycopene levels have also been inversely related with the risk of chronic disease (Blum, 2005).

Several epidermiological studies have suggest that a high consumption of tomatoes and tomato products containing lycopene can protect against cardiovascular diseases (Das et al., 2005; Sesso et al., 2004; Visioli et al., 2003; Willcox et al., 2003) and reduce risk of several types of cancer, most notably those of the prostate (Klein, 2005; Stacewicz-Sapuntzakis and Bowen, 2005; Wertz et al., 2004), breast (Sesso et al., 2005), and lung (Liu et al., 2003). Evidence from the studies suggests that lycopene has anti-carcinogenic and anti-atherogenic effects both *in vitro* and *in vivo* (Blum, 2005).

1.4 Skin protection potential in UV induced photo-damage

Ultraviolet light affects the eyes and the skin. Upon UV-irradiation, the skin was exposed to photooxidative damage which was induced by the formation of reactive oxygen species and peroxyl radicals that damage DNA, lipids and proteins. In the eyes, photooxidative stress results in cataracts and age related mucula degeneration. In the skin, sunburn, skin aging, photosensitivity disorders and skin cancer can be resulted.

The most severe consequence of photodamage is skin cancer. Less severe photoaging changes result in wrinkling, scaling, dryness and mottled pigment abnormalities consisting of hyperpigmentation and hypopigmentation. The use of antioxidants to inhibit photooxidative toxicity has been suggested as an important strategy in preventing and treating photodamage (Pinell et al., 2003).

Lycopene may reduce the damaging effect of UV light on the skin and can boots protection against both the short term (sunburn, erythema formation) and cumulative effects of sun expose (skin cancers, photoaging). Several *in vivo* and *in vitro* studies have examined the potential of lycopene to protect skin from UV induced photo-damage, sunburn, inflammatory response, photo aging and skin cancer.

Lycopene may be an important defense mechanism against adverse effects of UV irradiation on the skin (Stahl and Sies, 2004). When human skin is expose to UV light *in vivo*, skin lycopene concentration is lowered compared with non–exposed area and not significant changes in skin β–carotene concentration, indicated that lycopene may have superior antioxidant properties compared with β–carotene (Ribaya-Mercado et al., 1995).

Erythema formation, an indicator of the sunburn reaction was 40% lower in subjects who ingested tomato paste for 10 weeks compared with the control. Consequently, long–term oral lycopene supplement was also shown to protect against UV–induced erythema in humans (Stahl et al., 2001). Therefore, dietary intake lycopene can use as the internal sun protection to provide the basal prevention.

Protection against UV-induced erythema was observed for topically applied lycopene in gel emulsion. The lycopene-based product proved to have a grater protective activity than the product containing the mixture of vitamins E and C (Andreassi et al., 2004). Fazekas et al., 2003 suggested that topical lycopene in acetone is able to exert its protective effects against acute UVB-induced photodamage and aids in the maintenance of normal epidermal regeneration.

1.5 Stability

Carotenoids are very sensitive to light–catalyzed air oxidation. The product containing lycopene should be protected from exposure to light and heat if it is intact but poorly sealed the content starts degradation due to exposure to oxygen in the air (Sharma and Maguer, 1996).

Nanoparticles formulation using gelatin as wall materials were found to be delivering system to carry lycopene and vitamin E into human dermal fibroblasts in monolayer cultures. The lycopene nanoparticles are stabilized with vitamin E to protect against oxidative degradation and provide a well–defined form of carotenoids that is physically (against precipitation) and chemically (against degradation) stable. In addition, vitamin E in nanoparticles also enhanced the cellular uptake of lycopene.

Lycopene was significantly stabilized in the nanoparticle formulation compared to a preparation in dimethylsulphoxide (DMSO) but less stable than vitamin E or β-carotene. As a result of, when lycopene dissolved in DMSO, its crystals were observed on the cell surface whereas no visible crystal was found on the cell surface with lycopene when formulated as nanoparticles (Offord et al., 2002).

2. Liposomes

Liposomes constitute an important potential as drug delivery systems, not only for intravenous delivery but also particularly for topical applications.

Liposomes are spherical self-closed structures, composed of curved lipid bilayers, which enclose part of the surrounding solvent into their interior. The range in size of liposomes is from 10 nm up to several micrometers in diameter and they may be composed of one or several concentric membrane, each with a thickness of about 4 nm. Liposomes are made up of amphiphiles, which are characterized by hydrophilic, or water-soluble, head and hydrophobic tail.

Liposomes form spontaneously when phospholipids are hydrated in which an aqueous volume is entirely enclosed by a membrane composed of phospholipids. When mixed in water under low shear condition the phospholipids arrange themselves in sheets, these sheets then join tails-to-tails to form a bilayer membrane, which enclosed some of water in a phospholipid sphere. Particles containing only one bilayer have been termed “unilamellar vesicles” (ULVs), while these containing many bilayers have been termed “multilamellar vesicles” (MLVs). In the case of unilamellar vesicles, one can differentiate between small unilamellar vesicles (SUVs) and large unilamellar vesicles (LUVs) (Bergstrand, 2003).

2.1 Type of liposomes (New, 1997)

Liposomes can be characterized by their size and shape. They are range in size from the smallest vesicle (diameter approximate 25 nm) and which are visible under light microscope with a diameter of 1000 nm or greater. Liposomes of different size often require completely different method of manufacturing.

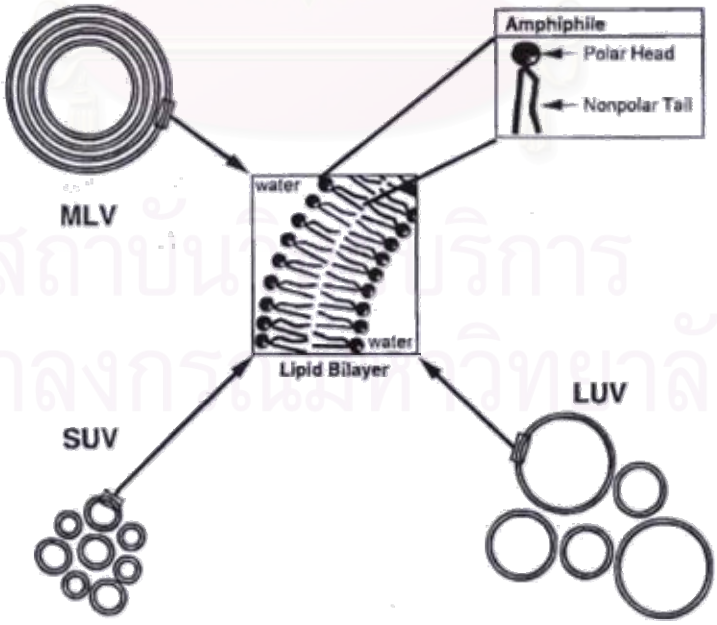

Figure 2 Structures of SUVs, MLVs and LUVs (Lasic, 1997).

2.1.1 Small unilamllar vesicles (SUVs)

They are the lowest limit of size possible for phospholipids vesicles. The ranges of sizes are 15-25 nm. They require high-energy input for production, the best method that does not kinetics or thermodynamics. SUVs are well characterized vesicles population, homogeneous in size and lamellarity. They are thermodynamic unstable, susceptible to aggregation and fusion particularly below the phase transition temperature. The entrapped volume is small; % entrapment of aqueous solute is low. Therefore, SUVs are not recommended for efficacy of entrapment, retention of materials. SUVs are appropriate choice when a high surface area need.

2.1.2 Multilamellar vesicles (MLVs)

The simplest type of liposomes is prepared. They consist of population of vesicles covering a wide range of sizes (100-1000 nm). Each vesicle generally consists of five or more concentric lamellae. Mechanically stable upon storage for long period of time. The internal space occupied by lipid membrane, suitable to acting as a carrier for lipophilic compound.

MLVs can be prepared by hand shaking of lipid in aqueous media and can be included in lipid mixture at time of dry down. The ultimate size can be control by extrusion. Percentage capture of aqueous compartment is not very high. The higher value can be achieved (>50%) by very large MLVs.

2.1.3 Large unilamellar vesicles (LUVs)

LUVs show large size of vesicles (1000 nm), they have a high aqueous: lipid compartment ratio, larger volume. So, they are suitable for entrapment of aqueous materials. LUVs can be prepared by REV technique.

2.2 Materials used in the preparation of liposomes

2.2.1 Phospholipids

A phospholipid has two acyl chains linked to a headgroup by means of glycerol-backbone. Phosphotidylcholines or PC-lipids are the most widely used lipids in liposome work (Bergstrand, 2003).

Phospholipids are the major structural components. The most common are phosphatidylcholine molecule (PC). It is an amphiphilic molecule. There is a glycerol bridge links a pair of hydrophobic acyl hydrocarbon chain with hydrophilic polar head group. The molecules of PC are not soluble in water. They can be derived from both natural and synthetic sources, readily extracted from egg yolk and soya bean but less readily from bovine heart and spinal cord. They are often used because of low cost, neutral charge and chemical inertness. Lecithin from natural sources is a mixture of phosphatidylcholines, each with chains of different length and varying degree of unsaturation. Lecithin from plant consists of high level of polyunsaturated in fatty acid chain whereas lecithin from mammalian consists of a higher proportion of fully saturated chain (New, 1997).

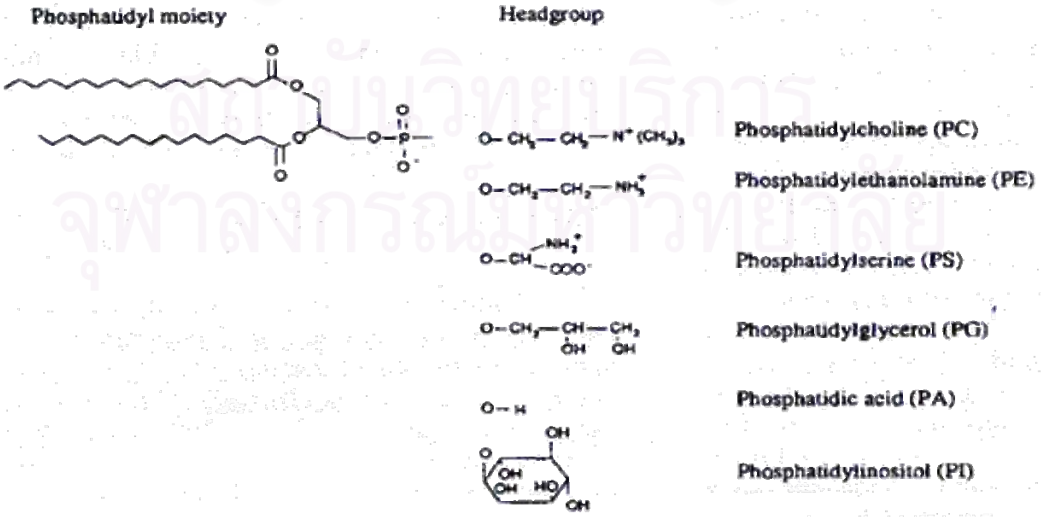

Figure 3 Structure of a number of phospholipids regularly used in liposomes (Grit and Crommelin, 1993).

2.2.2 Phosphatidylcholines membranes

At different temperature, lecithin membranes can exist in different phase, and transition from one phase to another as the temperature is increased. That one occurring at the highest temperature is the membrane passes from a tightly ordered ‘gel’ or ‘solid’ phase to liquid-crystal phase, where the freedom movement is higher. The method for determining the phase transition temperature (T_c) is microcolorimetry. The hydrocarbon chain length and unsaturation as well as head group influence on the value of T_c. Generally, increasing the chain length or increasing the saturation of the chain length increase the transition temperature.

The liposome membranes are semi-permeable membrane. For molecule with a high solubility in both organic and aqueous media, phospholipid membranes are a weak barrier. On the other hand, for polar solute and high molecular weight compound slowly pass through the membrane. A smaller molecule with neutral charge (water, urea) can diffuse across quite rapidly. Proton and hydroxyl ion cross the membrane fairly quickly

2.2.3 Other neutral phospholipids

Neutral lipid bilayers may be composed of sphingomyelin or alkyl ether lecithin analogues. Replacement of ester grouping by ether linkages increases the resistance of the lipid to hydrolysis, while not affecting the physical properties. When the content of saturated fatty acid increased, the phase transition temperature was increased. Mixtures of different chain lengths give a combined phase transition temperature below that of individual components. Sphingomyelin membranes are more stable and tightly packed than lecithin, decreased value for permeability to solute, greater resistance to lyses and lower membrane fluidity.

2.3 Method of preparation

The main point of preparation of liposomes is to getting the membranes to form vesicles of the right size and structure. Moreover, to entrap materials with high efficiency and in such a way that these materials do not leak out of the liposomes once formed.

The standard manufacturing procedure of liposomes is the film-forming method. Alternatively, solvent injection and reverse phase dialysis are appropriate procedure for the formulation of SUVs and LUVs.

Properties of lipid formulations can vary depending on the composition (cationic, anionic, neutral lipid species), however, the same preparation method can be used for all lipid vesicles regardless of composition. The general elements of the procedure involve preparation of the lipid for hydration, hydration with agitation, and sizing to a homogeneous distribution of vesicles.

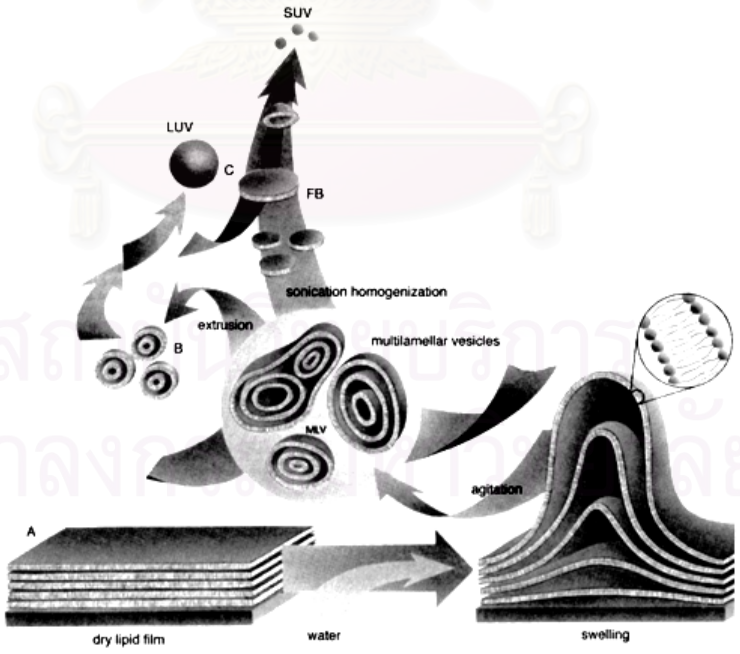

Figure 4 The general procedure involves preparation of liposomes, hydration with agitation, and sizing by sonication and extrusion to a homogeneous distribution of vesicles (Lasic, 1997).

The four basic stages for making liposomes are

1. Drying down of lipids from organic solvents onto the solid support
2. Dispersion of the lipids in aqueous media and then, shaking
3. Purification of the resultant liposomes.
4. Analysis of the final product.

The solvent should be used in the highest purity. Lipid should be stored either as solids or in organic solution at -20^{o}C, or at -70^{o}C to reduce the chance of oxidation to a minimum. All lipid solution should be stored in the dark, in glass vessels with a securely fastened ground-glass stopper, keep even under refrigeration. Flush the gaseous volume above the liquid in the container with inert gas prior storage. Rapid rotation of solvent containing flask is in order to increase the surface area for evaporation (New, 1997).

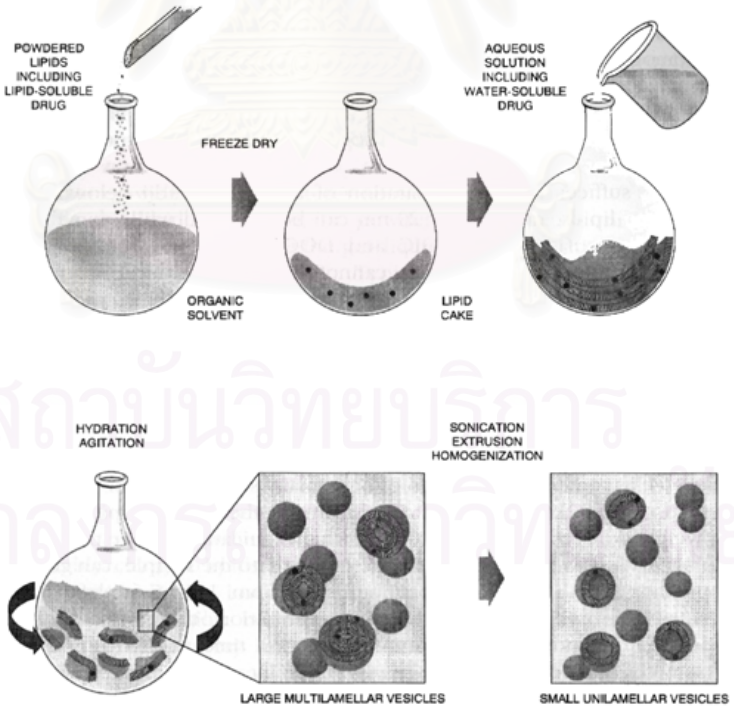

Figure 5 The method for preparation liposomes (Lasic, 1997).

When preparing liposomes with mixed lipid composition, the lipids must first be dissolved and mixed in an organic solvent to assure a homogeneous mixture of lipids. Usually this process is carried out using chloroform or chloroform: methanol mixtures. The intent is to obtain a clear lipid solution for complete mixing of lipids. Once the lipids are thoroughly mixed in the organic solvent, the solvent is removed to yield a lipid film. For small volumes of organic solvent (<1mL), the solvent may be evaporated using a dry nitrogen or argon stream in a fume hood. For larger volumes, the organic solvent should be removed by rotary evaporation yielding a thin lipid film on the sides of a round bottom flask. The lipid film is thoroughly dried to remove residual organic solvent by placing the vial or flask on a vacuum pump overnight.

Hydration of the dry lipid film/cake is accomplished simply by adding an aqueous medium to the container of dry lipid and agitating. The temperature of the hydrating medium should be above the gel-liquid crystal transition temperature (T_c or T_m) of the lipid with the highest T_c before adding to the dry lipid. After addition of the hydrating medium, the lipid suspension should be maintained above the T_c during the hydration period. For high transition lipids, this is easily accomplished by transferring the lipid suspension to a round bottom flask and placing the flask on a rotory evaporation system without a vacuum. Spinning the round bottom flask in the warm water bath maintained at a temperature above the T_c of the lipid suspension allows the lipid to hydrate in its fluid phase with adequate agitation. Hydration time may differ slightly among lipid species and structure, however, a hydration time of 1 h with vigorous shaking, mixing, or stirring is highly recommended. It is also believed that allowing the vesicle suspension to stand overnight (aging) prior to downsizing makes the sizing process easier and improves the homogeneity of the size distribution. Aging is not recommended for high transition lipids as lipid hydrolysis increases with elevated temperatures. The hydration medium is generally determined by the application of the lipid vesicles. Suitable hydration media include distilled water, buffer solutions, saline, and nonelectrolytes such as sugar solutions. Generally accepted solutions with meet these conditions are 0.9% saline, 5% dextrose, and 10% sucrose.

The product of hydration is a large, multilamellar vesicle analogous, with each lipid bilayer separated by a water layer. The spacing between lipid layers is dictated by composition with poly hydrating layers being closer together than highly charged layers which separate based on electrostatic repulsion.

Disruption of LMVs suspensions using sonic energy (sonication) typically produces small, unilamellar vesicles (SUVs) with diameters in the range of 15-50nm. The most common instrumentation for preparation of sonicated particles is bath or probe tip sonicators. Bath sonicators are the most widely used instrumentation for preparation of SUVs. Sonication of a LMVs dispersion is accomplished by placing a test tube containing the suspension in a bath sonicator (or placing the tip of the sonicator in the test tube) and sonicating for 5-10 minutes above the T_c of the lipid. The lipid suspension should begin to clarify to yield a slightly hazy transparent solution. The haze is due to light scattering induced by residual large particles remaining in the suspension. These particles can be removed by centrifugation to yield a clear suspension of SUVs. Mean size and distribution is influenced by composition and concentration, temperature, sonication time and power, volume, and sonicator tuning. Since it is nearly impossible to reproduce the conditions of sonication, size variation between batches produced at different times is not uncommon. Also, due to the high degree of curvature of these membranes, SUVs are inherently unstable and will spontaneously fuse to form larger vesicles when stored below their phase transition temperature.

Lipid extrusion is a technique in which a lipid suspension is forced through a polycarbonate filter with a defined pore size to yield particles having a diameter near the pore size of the filter used. Prior to extrusion through the final pore size, LMVs suspensions are disrupted either by prefiltering the suspension through a larger pore size (typically 0.2µm-1.0µm). This method helps prevent the membranes from fouling and improves the homogeneity of the size distribution of the final suspension. As with all procedures for downsizing LMVs dispersions, the extrusion should be done at a temperature above the T_c of the lipid. Attempts to extrude below the T_c will be unsuccessful as the membrane has a tendency to foul with rigid membranes which

cannot pass through the pores. Extrusion through filters with 100 nm pores typically yields large, unilamellar vesicles (LUVs) with a mean diameter of 120-140 nm. Mean particle size also depends on lipid composition and is quite reproducible from batch to batch.

2.4 Liposomes for drug delivery

Liposomes possess unique properties owing to the amphiphilic character of the lipids, which make them suitable for drug delivery. These phospholipid vesicles are capable of encapsulating both hydrophilic and hydrophobic drugs. The entrapment of materials into liposomes depends on whether the molecule is hydrophilic or hydrophobic. Liposomes can encapsulate water-soluble actives within the aqueous compartment. Additionally a lipid-soluble or amphiphilic ingredient can be embedded within the bilayer membrane. Figure 6 shows the position of drug are located in the liposome. Compounds can probably be accommodated in the membrane to concentration of about 1-10% by weight with out serious disruption of the bilayer structure, although the fluidity or permeability may be altered. The large liposomes entrap a far greater aqueous volume than do small liposomes.

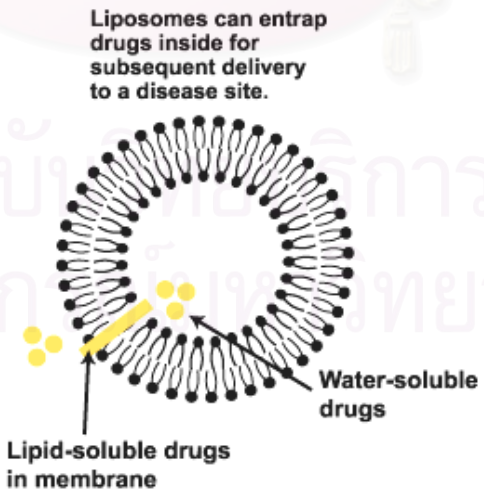

Figure 6 The positions of drugs which are located in the liposomes (Zhang, 2005).

The effective of liposomes for enhancement of therapeutic efficacy should be considered to retain their content as long as possible, suitable for interaction with some biological system, have ability to take up material of all shape, size and for immunological effect. Inclusion of other membrane component may be considered useful in view of the specific interaction may occur which could modify the behavior of liposomes with regard to either its contents or it mode of action (Ranade and Hollonger, 2003).

Encapsulation of drug into liposomes can lead to the enhancement of therapeutic efficacy of drugs by reduction of toxicity and prolongation of their therapeutic effect. Tretinoin which was entrapped in liposomal preparation was more stable to photodegradation than when dissolved in caster oil (Brisaert et al., 2001).

Retinol has the length of 15.5 Å, while the thickness of bilayers is approximate 40 Å thus retinol can be stabilized in the lipid bilayers of liposomes to exhibit greater stability and reduce toxicity (Singh and Das, 1998).

Photolabile agent may be protected from UV-light by incorporating barriers to light and presence of antioxidants into a liposome-based multicomponent system. The entrapment of riboflavin into DRVs increases it half-life. When incorporated lipid soluble UV-absorbers, oil red O, and/or β-carotene produce increasing half-life (Loukas et al., 1995).

3. Nanoparticles

Encapsulation using nanoparticles system is an increasingly implemented strategy in drug targeting and delivery. Such systems have also been proposed for topical administration to enhance percutaneous transport into and across the skin barrier.

Nanoparticles as drug carriers have attracted more and more interest in the last decade, since these systems were found to be able to increase efficacy and/or to

reduce toxicity of potent drugs. Nanoparticles have become an important area of research in the field of drug delivery because they have the ability to deliver a wide range of drugs to varying areas of the body for sustained periods of time. Nanoparticles may be defined as submicron (<1μm) colloidal systems, can be formed from different materials. Both biodegradable polymers and nonbiodegradable polymers have been used as carrier materials (Hans and Lowman, 2002). According to the process used for the preparation of nanoparticles, nanospheres or nanocapsules can be obtained. Nanocapsules are vesicular systems in which the drug is confined to a cavity surrounded by a unique polymeric membrane. Nanospheres are matrix systems in which the drug is dispersed throughout the particles (Beniha, 1996).

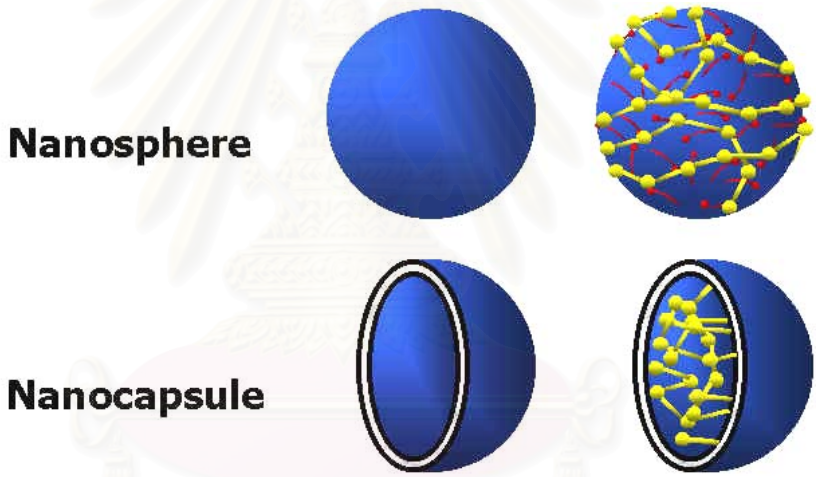

Figure 7 Nanosphere and nanocapsule (Lambert, 2002).

Several methods have been developed for preparing nanoparticles. Polymer nanoparticles are most commonly prepared by precipitation via solvent displacement, salting-out and pH variation. In the last years several synthetic as well as natural polymers have been examined for pharmaceutical applications. A basic requirement for these polymers to be used in humans or animals is that they have to degrade into molecules with no toxicity for biological environments. For this biocompatibility reason a very limited numbers of polymers can be used to prepare biodegradable materials.

The molecular weight and concentration of the polymer used will also affect the nanoparticles. The molecular weight of the polymer has opposite effects on nanoparticle size and encapsulation efficiency. Smaller size nanoparticles, approximately 100 nm, can be prepared with lower molecular weight polymer, however, at the expense of reduced drug encapsulation efficiency. When considering a particular polymeric nanoparticles for a given drug delivery application, particle size and encapsulation efficiency are two of the most important characteristics of the nanoparticles. For example if the goal is rapid dissolution in the body or arterial uptake then the size of nanoparticles should be approximately 100 nm or less. If prolonged dissolution is required, or targeting the mononuclear phagocytic system (MPS), larger particles around 800 nm would be preferable. It appears that encapsulation efficiency increases with the diameter of the nanoparticles

Nanoparticles can be used to deliver hydrophilic drugs, hydrophobic drugs, proteins, vaccines, biological macromolecules, etc. They can be formulated for targeted delivery to the lymphatic system, brain, arterial wall, lungs, liver, spleen, and skin or made for long-term systemic circulation. Therefore, numerous protocols exist for synthesizing nanoparticles based on the type of drug used and the desired delivery route. Once a protocol is chosen, the parameters must be tailored to create the best possible characteristics of nanoparticles. Four of the most important characteristics of nanoparticles are their size, encapsulation, zeta potential (surface charge), and release characteristics.

The use of polymers for skin preparations is manifold. Requirements of such polymers are dependent on the formulation types. The most applied polymers on skin belong to various classes, for example to cellulose derivatives, chitosan, carageenan, polyacrylate, polyvinyl alcohol, polyvinylpyrrolidone and silicones (Han and Lowman, 2002).

Additionally, numerous methods exist for incorporating drugs into the particles. Nanoparticles can also be made from hydrophilic polysaccharides like chitosan. Chitosan nanoparticles can be formed by the spontaneous ionic gelation

process. The resulting nanoparticles have small sizes and positive surface potentials. This technique is promising as the particles can be prepared under mild conditions without using harmful organic solvents.

4. Chitosan

Chitosan [(1, 4)-2-acetamido-2-deoxy-β-D-glucan)] is a copolymer of glucosamine and N-acetylglucosamine. Chitosan is obtained from the deacetylation of chitin, a naturally occurring and abundantly available (in marine crustaceans). Acetamide group of chitin can be converted into amino group to give chitosan, which is carry out by treating chitin with concentrated alkali solution. Chitosan represent long-chain polymers having molecular mass up to several million Daltons. Commercially available chitosan has average molecular weigh ranging between 3,800 and 20,000 Daltons and is 66% to 95% deacetylated.

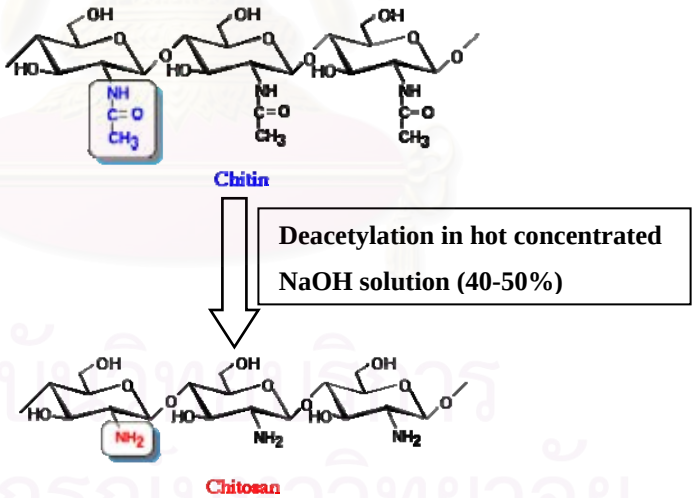

Figure 8 Scheme of preparation of chitosan (Agnihotri et al., 2004).

Chitosan being a cationic polysaccharide in neutral or basic pH conditions contains free amino groups and hence, is insoluble in water. In acidic pH, amino groups can undergo protonation thus, making it soluble in water. Solubility of chitosan depends upon the distribution of free amino and N-acetyl groups. Usually 1-3% aqueous acetic acid solutions are used to solubilize chitosan.

Chitosan is biocompatible with living tissues since it does not cause allergic reactions. It breaks down slowly to harmless products (amino sugar), which are completely absorbed by the human body. If degree of deacetylation and molecular weight of chitosan can be controlled, then it would be a material of choice for developing micro/nanoparticles.

Chitosan has many advantages, particularly for developing micro/nanoparticles. These include: its ability to control the release of active agents, it avoids the use of hazardous organic solvents while fabricating particles since it is soluble in aqueous acidic solution, it is linear polyamine containing a number of free amine groups that are readily available for crosslinking, its cationic nature allows for ionic crosslinking with multivalent anions, it has mucoadhesive property, which increases residual time at the site of absorption.

Chitosan have very low toxicity, LD_{50} of chitosan in laboratory mice is 16g/kg body weight. Chitosan is proven to be safe in rat up to 10% in the diet. The primary amine groups render special properties that make chitosan very useful in pharmaceutical applications. Various sterilization methods such as ionizing radiation, heat and chemical methods can be suitably adopted for sterilization of chitosan in clinical application (Agnihotri et al., 2004).

Recently, natural chitosan material has attracted great attention in pharmaceutical and biomedical fields. Because of its advantageous biological properties such as biodegradability, biocompatibility and low toxicity, chitosan has frequently been applied for drug delivery systems. Many reports are available on the preparation of chitosan nanoparticles.

Several methods used to prepared chitosan nanoparticles. Selection of any methods depends upon factors such as particle size requirement, thermal and chemical stability of the active agent, reproducibility of the release kinetic profiles, stability of the final product and residual toxicity associated with the final product. However, selection of any of these methods depends upon the nature of the active molecule as

well as the type of the delivery device. Two different techniques are usually employed to obtain chitosan micro/nanoparticles: chitosan chains can be chemically cross-linked leading to quite stable matrixes, where the strength of the covalent bonds stands out. Glutaraldehyde is broadly used as a cross-linking molecule in covalent formulations. On the other hand, chitosan hydrogel can be also obtained by ionic gelation, where micro- or nanoparticles are formed by means of electrostatic interactions between the positively charged chitosan chains and polyanions employed as cross-linkers. For most drug delivery application, chitosan should be crosslinked due to its cationic properties. Studies reported in recent users have shown that the glutaraldehyde crosslinked chitosan microsphere have a long acting ability suitable for the controlled delivery of many drugs. Due to the proved toxicity of glutaraldehyde and other organic molecules used in the synthesis of gels covalently stabilized, only the ionic gelation technique can be used for pharmaceutical applications (López-León et al., 2005).

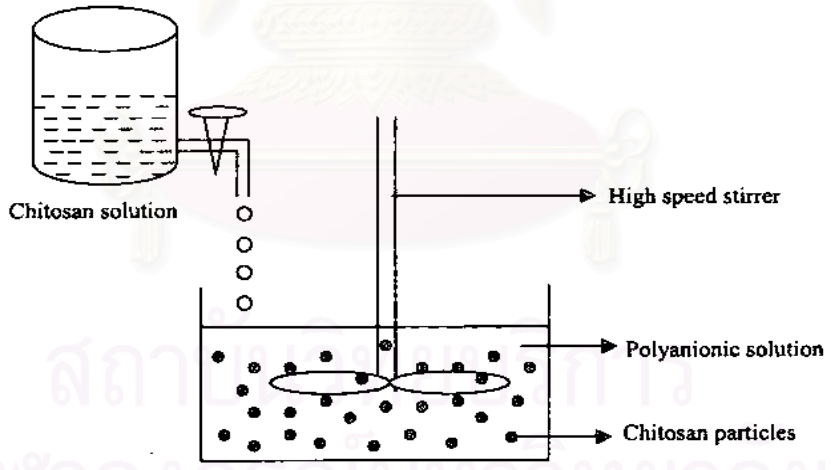

Figure 9 Schematic representation of preparation of chitosan particulate systems by ionic gelation method (Agnihotri et al., 2004).

Table 3 Chitosan-based drug delivery systems prepared by different methods for various kinds of drugs (Agnihotri, 2004).

Type of system	Method of preparation	Drug
Tablets	matrix	diclofenac sodium, pentoxyphylline, salicylic acid, theophylline
	coating	propranolol HCl
Capsules	capsule shell	insulin, 5-amino salicylic acid
Microspheres/ Microparticles	emulsion cross-linking	theophylline, cisplatin, pentazocine, phenobarbitone, insulin, 5-fluorouracil, diclofenac sodium, griseofulvin, aspirin, diphtheria toxoid, pamidronate, subroylbisphosphonate, mitoxantrone, progesterone
	coacervation/precipitation	prednisolone, interleukin-2, propranolol-HCl
	spray-drying	cimetidine,famotidine, nizatidine, vitamin D-2, diclofenac sodium, ketoprofen, metoclopramide-HCl, bovine serum albumin, ampicillin, cetylpyridinium chloride, oxytetracycline, betamethasone
	ionic gelation	felodipine
	sieving method	clozapine
Nanoparticles	emulsion-droplet coalescence	gadopentetic acid
	coacervation/precipitation	DNA, doxorubicin
	ionic gelation	insulin, ricin, bovine serum albumin, cyclosporin A
	reverse micellar method	doxorubicin
Beads	coacervation/precipitation	adriamycin, nifedipine, bovine serum albumin, salbutamol sulfate, lidocaine-HCl, riboflavin
Films	solution casting	isosorbide dinitrate, chlorhexidine gluconate, trypsin, granulocyte-macrophage colony-stimulating factor, acyclovir, riboflavine, testosterone, progesterone, beta-oestradiol,
Gel	cross-linking	chlorpheniramine maleate, aspirin, theophylline, caffeine, lidocaine-HCl, hydrocortisone acetate, 5-fluorouracil

5. Chitosan Alginate Nanoparticles

Recently, polyelectrolyte complexes have been proposed for the design of drug delivery systems. Cationic chitosan can form gels with non-toxic multicovalent anionic counterions such as polyphosphate (Wu et al., 2005; Xu and Du, 2003) and sodium alginate (Anal and Stevens, 2005; Ribeiro et al., 1999) by ionic cross-linking.

Alginate is derived from brown seaweeds. Sodium alginate is widely used in the food industry. In a great number of food and pharmaceutical applications, the now well-known reactivity of alginates with calcium ions is utilized. Alginate is an anionic polysaccharide consisting of linear co-polymer of two monomeric units, D-mannuronic acid (M) and L-guluronic acid (G), each of which has different conformational preferences and behavior. These monomers occur in the alginate molecule as regions

made up exclusively of one unit or the other, referred to as M-blocks or G-blocks, or as regions in which the monomers approximate an alternating sequence (Goddard and Gruber, 1999).

The calcium reactivity of alginates is a consequence of the particular molecular geometries of each of these regions. The D-mannuronic acid exists in the 1C conformation and in the alginate polymer is connected in the β-configuration through the 1-and 4-position; the L-guluronic acid has the 1C conformation and is α-1, 4-linked in the polymer. Because of the particular shapes of the monomers and their modes of linkage in the polymer, the geometries of the G-blocks are buckled while the M-blocks have a shape referred to as an extended ribbon, as shown in Figure 10. If two G-block regions are aligned side by side, a diamond hole shaped results. This hole has dimensions that are ideal for the cooperative binding of calcium ions (Douglas and Tabrizian, 2004).

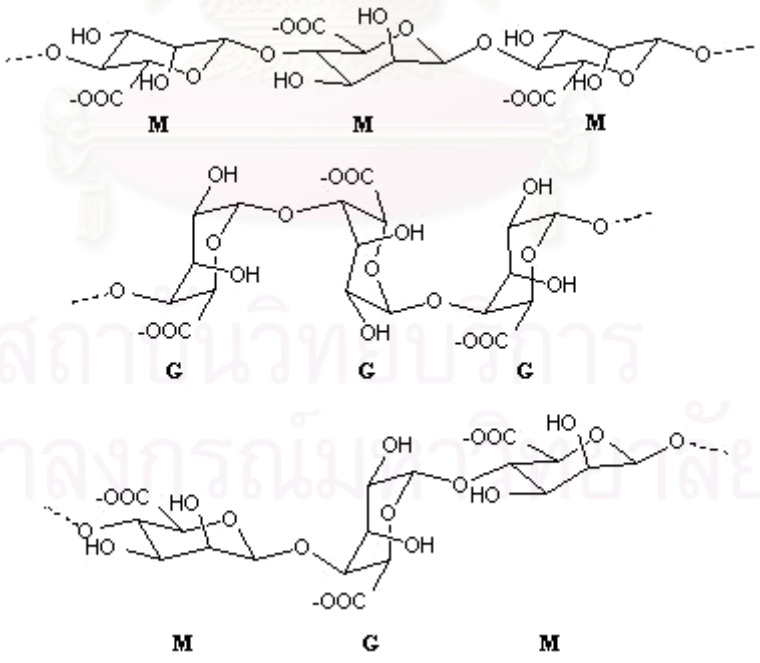

Figure 10 The structure of alginates (Kjønikson, 2006).

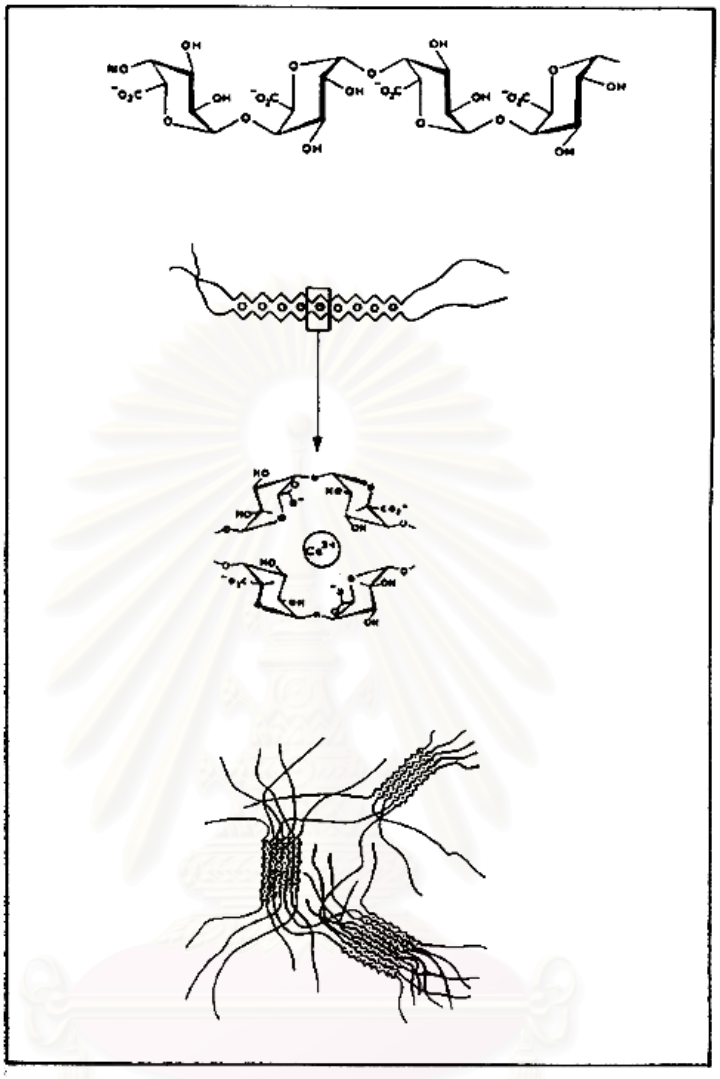

Figure 11 The egg box for alginate gelation when adding calcium ion (Barbaroux, n.d.).

When calcium ions are added to a sodium alginate solution, such an alignment of the G-blocks occurs; and the calcium ions are bound between the two chains like eggs in an egg box, as shown in Figure 11. Thus the calcium reactivity of aligns is the result of calcium-induced dimeric association of the G-block regions. Depending on the amount of calcium present in the system, these inter-chain associations can be either temporary or permanent. With low levels of calcium, temporary associations are obtained, giving rise to highly viscous, thixotropic solutions. At higher calcium levels, precipitation or gelation results from permanent associations of the chains (Goddard and Gruber, 1999).

The properties of calcium-alginate gel beads make them one of the most widely used carriers for controlled release systems. Coating of these beads with other polymers, including chitosan, has been shown to improve their stability during storage and in biological fluids. The encapsulating membrane may be formed by reacting chitosan with alginate (Douglas and Tabrizian, 2005). The electrostatic interaction of carboxyl groups of alginate with the amino groups of chitosan and resulting entanglement of polymer forms a membrane that encloses the active material (Polk et al., 1994). The complex protects the encapsulant, has biocompatible and biodegradable characteristics, and limits the release of encapsulated materials more effectively than either alginate or chitosan alone.

6. Drug Loading into Nanoparticles of Chitosan

Drug loading in nanoparticulate systems can be done by two methods, during the preparation of particles (incorporation) and after the formation of particles (incubation). In these systems, drug is physically embedded into the matrix or adsorbed onto the surface. Various methods of loading have been developed to improve the efficiency of loading, which largely depends upon the method of preparation as well as physicochemical properties of the drug. Maximum drug loading can be achieved by incorporating the drug during the formation of particles, but it may get affected by the process parameters such as method of preparation, presence of additives, etc (Swarbrick and Boylan, 1994).

Both water-soluble and water-insoluble drug can be loading into chitosan-base particulate systems. Water-soluble drug are mixed with chitosan solution to form a homogeneous mixture, and then, particles can be produced by the methods for preparation. Water-insoluble drugs and drugs that can precipitate in acidic pH solution can be loaded after formation of particles by soaking the preformed particles with the saturation of drug.

Water-insoluble drugs can also be loaded using the multiple emulsion technique. In this method, drug is dissolved in a suitable solvent and then emulsified

in chitosan solution to form an oil-in-water (o/w) type emulsion. Sometimes, drug can be dispersed into chitosan solution by using a surfactant to get the suspension. Thus, prepared o/w emulsion or suspension can be further emulsified into liquid paraffin to get the oil-water-oil (o/w/o) multiple emulsions. The resulting droplets can be hardened by using a suitable cross-linking agent (Agnihotri et al, 2004).

7. Skin Structure

The skin is the largest organ of the human body and consists of a complex layered structure, which forms a barrier between the body and the outside environment. It major roles are to regulate body temperature, protect tissues from infection, prevent fluid loss, and cushion internal structure. The skin can be divided into three distinct layers: the epidermis, dermis and hypodermis. The epidermis is a multilayer structure consisting of cells in various stages of differentiation. The layer that interacts with the environment is the stratum corneum, or horny layer (Shai et al., 2001).

The stratum corneum is the skin's primary defense against invasion and is a composite of corneocytes or terminally differentiated keratinocytes, which are surrounding by crystalline lamellar lipid regions. The corneocytes suspended in this lipid matrix, in addition to the lipid envelope surrounding the cells, form a 'brick-and-mortar' barrier that permits retention of water within the corneocytes in addition to hampering the penetration of foreign particles. The major lipid classes within the stratum corneum are ceramides, cholesterol, and fatty acids. Below the stratum corneum lies the stratum granulosum, or granular layer, followed by the stratum spinosum. The stratum spinosum has an abundance of desmosomes that give a spiny appearance to the cells, hence its byname, the prickly layer. The lowest layer of the epidermis is the basal layer, also known as the stratum basale.

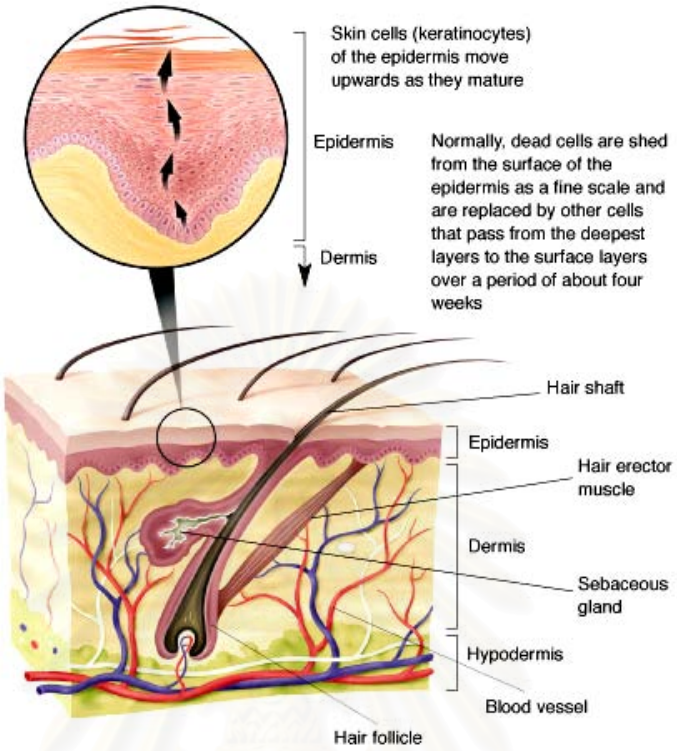

Figure 12 Basic diagram of skin structure (de Berker, n.d.).

The stratum basale is a single layer of columnar basal cells that are attached to the basement membrane, or basal lamina, via hemidesmosomes. The stratum basale is the regenerative layer composed of undifferentiated keratinocytes and stem cells. As the keratinocytes, connected together by desmosomes and gap junctions, mature and migrate through the epidermal layers, they transform from spinous cells to granular cells and finally the flattened corneocytes of the stratum corneum. Along the way the keratinocytes continually gain the protein keratin so that by the time they reach the stratum corneum, they are the fully differentiated cornified cells. Overall, the approximate composition of the viable epidermis is 90% keratinocytes, with the remaining 10% of cells consisting of melanocytes, Langerhans cells, which play and important immunoregulatory role, and merkel cells.

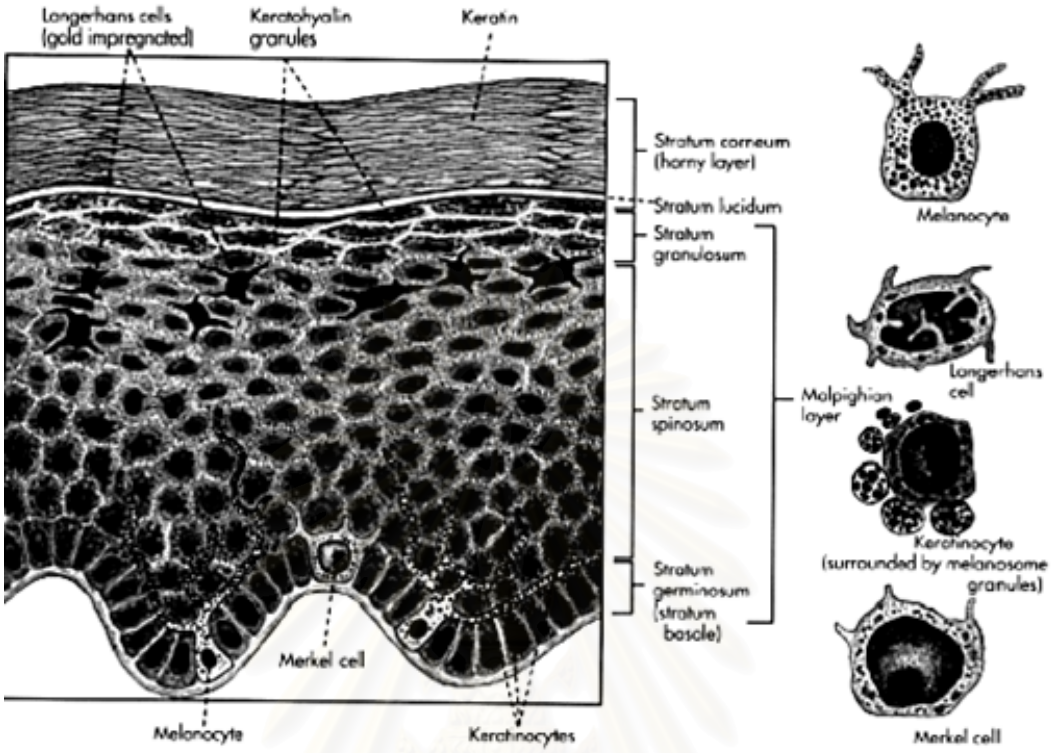

Figure 13 Layer of the epidermis (Murley, 2003).

The dermis consists of two regions, the papillary, or adventitial that interfaces the basil lamina, and the lower region, the reticular dermis. The reticular dermis makes up the bulk of the structural dermis. The dermis, approximately 2-3 mm thick, forms the bulk of the skin and is made up primarily of fibroblasts. It consists of a network of collagen and elastin fibers with interweaving blood and lymph vessels, sweat and sebaceous glands, hair follicles and nerve endings. The collagen fibers give the skin's strength. Elastin fibers are thinner than collagen fibers. They are responsible for the skin's elasticity. If these fibers are damaged as a result of aging, or from excessive, cumulative exposure to the sun, the skin becomes loose, does not return to its original state when stretched, and looks thin and wrinkled.

The lowest layer of the skin is the hypodermis, which is primarily composed of fibroglasts and adipocytes. The hypodermis binds skin to the underlying structures,

in addition to serving as a thermoregulator and a cushion to internal organs against trauma (Carpenter, 2004; Junqueira et al., 1986).

7.1 Functions of the skin

The function of skin are acts as a protective layer, transmits sensations, help to regulate the body's temperature, produces vitamin D and plays a role in social interactions. The skin serves not only to protect the body from the external environment; another important function of the skin is to prevent loss of water from the body. When the water content of the skin is normal, the skin appears soft, smooth, supple and glowing (Shai et al., 2001).

7.2 Permeability barrier

The skin is a complex transport barrier with special anatomical organization and chemical structure. Most important in the respect is the outer most skin region, the stratum corneum, which comprises columns of tightly packed corneocytes organized into clusters up to a dozen cells per corneocyte layer. Individual corneocytes are merged together with desmosomes and sealed tightly with special inter-cellular lipids that are attached to cell membrane.

From the permeant point of view, the skin barrier resembles a lipid layer along which individual molecules migrate via diffusion. Key factors that control molecular permeation through the horny layer of the skin, in decreasing sequence of importance, are molecular hydrophobicity, size, and the ability to interact with the other molecules, e.g. via hydrogen bond formation. As a consequence, molecules larger than a few hundred dalton and/or highly polar compounds cannot efficiently pass through the skin by diffusion. This is also suitable to the small water molecules. The much larger colloids and typical colloid components do not enter the skin in a practically meaningful quantity, except though transport shunts.

Single molecules and other entities smaller than pore diameter diffuse, that is permeate, through a barrier freely, limited just by incomplete barrier porosity. The resulting diffusive trans-barrier flux is proportional to the permeant concentration or water activity difference between the two sides of an obstacle (Cevc, 2004).

Maintenance of the normal internal environment of the body depends on the relative impermeability of the epidermis. Without this layer, there would very soon be an evaporative water loss equal to the total blood volume. Although the cells of the stratum corneum contribute to the barrier, it is now known that the complex intercellular lipids play a major role. The lipid bilayers liberated from discoid granules released in the transition from the stratum granulosum to the stratum corneum coalesce to form continuous intercellular lamellae in which the dense and lucent layers. These lipid lamellae constitute an essential component of the permeability barrier. They have an unusual composition, the major lipid consists of the ceramide (40%), cholesterol (25%), free fatty acids (25%) and triglyceride (5%), and this mixture is more resistant to bacterial attack and oxidation from exposure to the atmosphere than other lipid bilayers in the body that are composed mainly of phospholipids

In addition to protecting against loss of water and electrolytes, the barrier also prevents entry of water-soluble toxins from the environment. It does, however, permit entry of lipid-soluble substances. The rate of penetration of a substance depends on its oil/water partition coefficient; compounds that are equally soluble in oil and water penetrate best. Anything that can cross the epidermal barrier may enter into the blood circulation. Advantage is now taken of this for percutaneous administration of some drugs. Enzymes of the epidermis are capable of transforming certain compounds from an inactive to an active form. Present of lipid-rich extracellular material in the stratum corneum clearly provide some degree of protection against mechanical damage, fluid loss, and entry of noxious substances from the environment (Fawcett, 1994).

7.3 Effect of Solar radiation and ultraviolet radiation on the skin

The wavelength of ultraviolet radiation is adjacent to that of visible violet light. Ultraviolet-B (UVB) rays are high-energy emissions, which can cause significant damage to living tissues and cells. This is the main type of radiation that is responsible for skin redness burns, tanning and skin tumors following prolonged, cumulative exposure to the sun.

There has been increasing awareness of the damage caused to skin by cumulative sun exposure. Solar radiation is responsible for most of the harmful skin conditions that are sometime erroneously attributed to aging, such as the appearance of brown spots and wrinkles, enlargement of blood capillaries on the face and development of various skin tumors

The energy level off ultraviolet-A (UVA) rays is less than that of UVB rays, so they cause less skin damage. Moreover, UVA rays penetrate deeper into the skin than do UVB rays, causing damage to the elastin fibers locate deeper in the skin, and thus accelerate skin aging (Pinnell et al., 2003).

7.4 Passage of drugs through the skin

Skin delivery has become increasingly popular for the following reasons (Carpenter, 2004)

1. The skin presents a relatively large and readily accessible surface area for absorption
2. It is an alternative to more invasive administration routes which leads to greater patient compliance
3. Allows a more controlled drug delivery, which may allow for a lower frequency in dosing
4. Drugs do not have to go through the systematic metabolic pathway

Many factors govern the delivery of drugs and cosmetics into the skin from topically applied formulations. These factors include the size of the molecule, the lipophilicity of the component, type of formulation, presence of penetration enhancers and physical state of the stratum corneum.

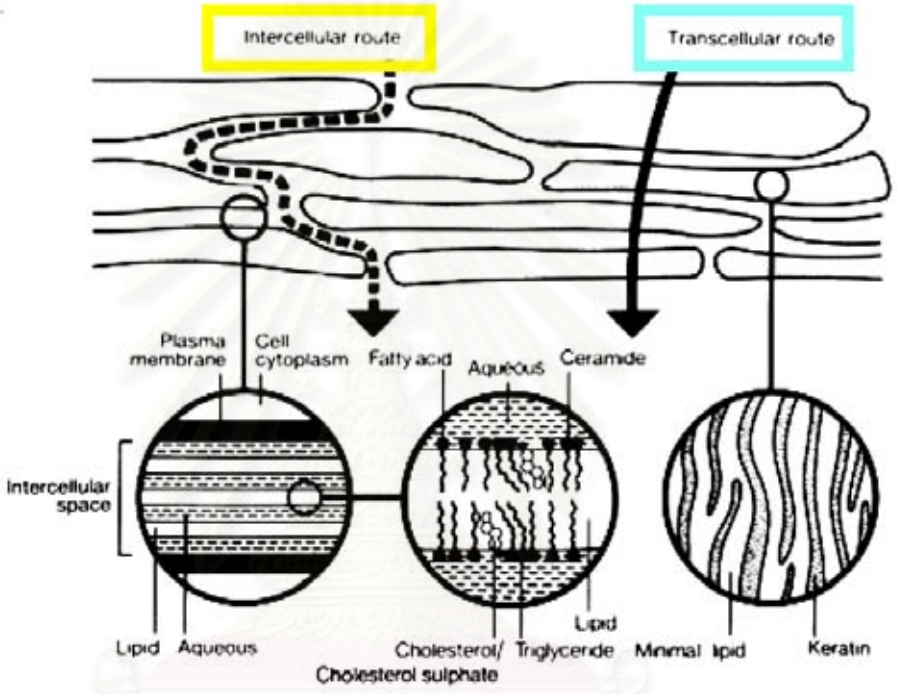

Figure 14 The possible pathways of drug penetration through the stratum corneum (Moghimi, 1999).

The transports mechanisms by which drugs cross the intact skin have not yet been completely elucidated. However, possible major routes may comprise the transepidermal pathway, across the horny layer either intra- or intercellularly, or via the hair follicles and sweat glands (appendageal route). The appendageal route may be of significance for short diffusional times and for polar molecules. Recently, it was believed that, for polar molecules, the probable route was via the hydrated keratin of the corneocyte. However, it now seems more probable that the dominant pathway is via the polar region of intercellular lipid, with the lipid chains providing the non polar route (Ranade and Hollinger, 2003).

For molecule to passively penetrate the epidermis, they can either pass through the corneocytes and lipid matrix in a transcellular route, or by intercellular travel between the corneocytes in the lipid matrix. The latter, lipophilic route is the proposed mechanism for most drugs as it is the pathway of least resistance (Wilson and Washington, 1989). This route is restricted by the molecule's size and charge with the presence of tight junctions. The transcellular route involves the movement of the solute through the cell's interior and across the basolateral membrane by either active or passive processes.

Lipophilic molecules are better accepted by the stratum corneum. Ideally, a drug must possess both lipoidal and aqueous solubilites. If drug is too hydrophilic, the molecule will be unable to transfer into the stratum corneum, however if it is too lipophilic, the drug will tend to remain in the stratum corneum layers.

Two main strategies for the formulation of dermatological preparations have been described. In the first strategy, a vehicle or device is utilized in order to maximize drug partition into the skin without significantly affected the physicochemical properties of the stratum corneum. The alternate strategy incorporates materials such as penetration enhancers into formulation. These enhancers are chemicals that enter the skin and reversibly alter it to promote the penetration of a drug. They should be pharmacologically inert, not interacting with receptors in the skin, should not be toxic, irritating, or allergenic and the skin should show an immediate and full recovery of its normal properties when the enhancer leaves the tissue (Ranade and Hollinger, 2003).

Liposomes, small vesicles composed of phospholipids, have been used for years to bring active ingradients into the skin. Several factors such as lamellarity, lipid composition, charge on the liposomal surface (Song and Kim, 2005), mode of application and the total lipid concentrations have been proven to influence drug deposition into the deeper skin layers (Verma et al., 2003).

Many studies performed in the last decade showed significantly higher absorption rates, as well as greater pharmacological effects for drugs applied to the skin entrapped in liposomes, as compared to conventional topical formulations. It is supposed that once in contact with skin, some budding of liposomal membrane might occur. These could cause a mixing of the liposome bilayer with intracellular lipids in the stratum corneum, which may change the hydration conditions and thereby the structure of lipid lamellae. This may enhance the permeation of the lipophilic drug into the stratum corneum and ease the diffusion of hydrophilic drugs into the interlamellar spaces (Sinico et al., 2005).

8. *In Vitro* Skin Diffusion Cells

There have been several methods reported in literature for percutaneous penetration enhancement and its quantification. These include diffusion experiments (Biruss and Valenta, 2005; Contreras et al., 2005; Fočo et al., 2005; Venter et al., 2001), visualization by electron microscopy (Bhatia and Singh, 1999; Sinico et al., 2005; van den Bergh et al., 1999).

In vitro diffusion cells, method for determining topical absorption have been used to understand and/or predict the delivery of drug from the skin surface into the body of living animals or humans. The advantages of in vitro experiments are easier to perform, less expensive and easier to control the environment factors, such as temperature. Accurate absorption rates can be determined, since sampling can be done frequently directly beneath the skin (Venter et al., 2001). Although a potential disadvantage is that little information on the metabolism, distribution, and effects of blood flow on permeation can be obtained (Brain et al., 1998).

8.1 Diffusion cell design

The diffusion cell consists of an upper donor and a lower receptor chamber, separated by a skin preparation. The cells are made preferably from an inert non-adsorbing material, and glass is most common, although Teflon and stainless steel are also used. In all case excised skin is mounted as a barrier between a donor chamber and a receptor chamber, the stratum corneum faces the donor chamber. Temperature control of the receptor fluid is crucial throughout the experiment. The skin surface temperature in the diffusion cell should be kept at the *in vivo* skin temperature of 32^{o}C. Additional dermal absorption studies may be required in some specific case (e.g. exposure to a higher skin temperature). Efficient mixing of the receptor fluid (and sometimes the donor fluid) is essential, and sample removal should be simple. The amount of compound permeating from the donor to the receptor side is determined as a function of time. Continuous agitation of the receptor medium, sampling from the bulk liquid rather than the side arm, and accurate replenishment after sampling, are important practical considerations. It is essential that air bubbles not be introduced below the membrane during sampling.

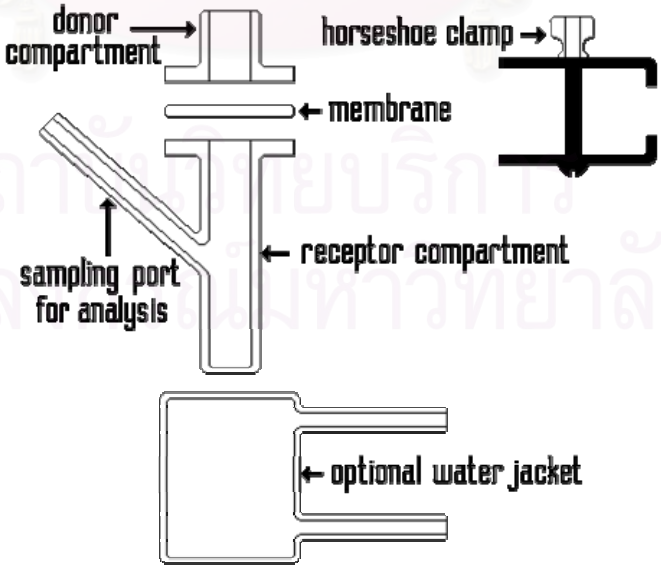

Figure 15 The diagram of diffusion cell experiment (Wilt, 2005).

To summarize, a well-designed skin diffusion cell should:

1. Be inert.
2. Be robust and easy to handle.
3. Allow the use of membranes of different thicknesses.
4. Provide through mixing of the receptor chamber contents.
5. Ensure intimate contact between membrane and receptor phase.
6. Be maintainable at constant temperature.
7. Have precisely calibrated volumes and diffusion areas.
8. Maintain membrane integrity.
9. Provide easy sampling and replenishment of receptor phase.
10. Be available at reasonable cost.

8.2 Receptor chamber and medium

A large receptor volume may ensure sink conditions but will reduce analytical sensitivity unless large samples can be taken and subsequently concentrated. The ideal receptor phase provides an accurate simulation of the conditions pertaining to in vivo permeation of the test compound. Excessive receptor phase concentration can lead to a decrease in the rate of absorption, which may result in an underestimate of bioavailability. The most commonly used receptor fluid is pH 7.4 phosphate-buffered saline (PBS), although this is not always the most appropriate material. It has been postulated that if a compound has a water solubility of < 10 μg/mL, then a wholly aqueous receptor phase is unsuitable and the addition of solubilizers becomes necessary. One particularly useful receptor fluid is 25% (v/v) aqueous ethanol, which provides a reasonable “sink” for many permeants, whilst removing the need for other antimicrobial constituents. Other examples of modified receptor phase include 3% bovine serum albumin (Bronaugh et al., 1999; Cintreras et al., 2005), 50% aqueous ethanol (Sinico et al., 2005), 1.5% to 6% Triton X-100 and 6% Poloxamer 188. A nonionic polyethylene glycol-20-oleyl ether surfactant did not disrupt the barrier function of rat skin to hydrophilic compounds.

The composition of the receptor fluid is chosen so that it does not limit the extent of diffusion of the test substance, such as the solubility and the stability in the receptor fluid of the chemical under investigation have to be guaranteed. Saline or bufferd saline solutions are commonly used for hydrophilic compounds. For lipophilic molecules, serum albumin or appropriate solubilizers/emulsifiers are added in amounts which do not interfere with membrane integrity (Brain et al., 1998).

8.3 Selection, variation, and preparation of skin membranes

Human skin would be the obvious choice but is not always readily available. Pig skin is used because it shares essential permeation characteristics with human skin. Rat skin is grossly 2 to 10 times more permeable than human skin leading to overestimation of human dermal absorption. Skin sample that may be used are split-thickness (200-500 μm) or full-thickness (500-1000 μm) skin preparations. Dermatomed skin is often used (SCCNFP, 2003).

Different methods can be used to prepare human skin. The membrane is one of the following:

1. Full-thickness skin, incorporating the SC, viable epidermis, and dermis.
2. Dermatomed skin, in which the lower dermis has been removed.
3. Epidermal membranes, comprising the viable epidermis and the SC (prepared by heat separation).
4. SC alone (prepared from 3 by enzyme treatment).

The most suitable type of tissue is dependent on the nature of the permeant. The environment of skin in vivo differs somewhat from that in vitro. In vivo the continuously perfused subcutaneous vasculature, which penetrates the dermis to a significant degree, can rapidly remove permeants reaching the epidermal-dermis junction. These vessels, if still present, are not perfused in simple in vitro models. In vitro, the relatively aqueous environment of the dermis will inhibit the penetration of lipophilic compounds, whereas in vivo this barrier is circumvented by the capillary.

Hence the use of dermatomed, epidermal or stratum corneum membranes is more appropriate for particularly lipophilic permeants. The preparation of epidermal membranes and stratum corneum is time-consuming, and the necessary processing increases the possibility of damage to the skin membrane. With animal skin, full-thickness membranes are usually used, because it is difficult to isolate intact epidermis or stratum corneum due to the presence of numerous hair follicles, which may also compromise dermatomed tissue.

For human skin the separation of the dermis from the epidermis (stratum corneum and viable epidermis) is a relatively simple technique. First, the subcutaneous fat is removed by blunt dissection. The full-thickness skin membrane is then totally immersed in water at 60^{o}C for ~45 sec. Following removal from the water, the skin is pinned; dermal side down, to a dissecting board and the epidermis is gently peeled back using a pair of blunt curved forceps. The epidermal membrane can then be floated onto warm water and taken up on to support membrane (membrane or paper filter). It is then ready to be mounted in a diffusion cell. To isolate the stratum corneum from the epidermal membranes, the latter are placed in trypsin solution, incubated at 37^{o}C for 12 h, rubbed (with a cotton bud) to remove the epidermal cells, rinsed in distilled water, and air-dried on a surface from which they can be removed easily (Brain et al., 1998).

8.4 Experiment Duration

The normal exposure time is 24 h. The longer duration may result in membrane deterioration and requires membrane integrity to be carefully checked. Sample intervals should be of an appropriate frequency to allow realistic assessment of such parameters as lag time and steady state. For a compound with unknown permeation characteristics, samples should ideally be taken at 2 h intervals for the duration of the experiment. In vitro skin diffusion experiments are normally conducted with a skin temperature of 32^{o}C (the *in vivo* value). This is achieved by maintaining the receptor solutions at 37^{o}C, either by immersing cells in a water bath or by using cell jackets perfuse at the correct temperature (SCCNFP, 2003).

CHAPTER III

MATERIALS AND METHODS

Materials

1. Acetonotrile HPLC grade (Lab-Scan Co., Ltd, Ireland)
2. Calcium chloride (Srichand United Dispensary Co., Ltd., Thailand)
3. Chitosan (MW 1.48 milliondaltons, 76.905 %deacetylation)
4. Disodium phosphate, heptahydrate (Merk, Germany)
5. Ethanol AR grade (Mallinckrod, Maxico)
6. Glacial acetic acid (Lab-Scan Co., Ltd, Ireland)
7. Lycopene (Redivivo® 10%FS, Roche, Switzerland)
8. Lycopene from tomato (Approx. 98%, Sigma, USA. Lot 034K7005)
9. Methanol HPLC grade (Lab-Scan Co., Ltd, Ireland)
10. Monosodium phosphate, monohydrate (Ajax Finechem, Australia)
11. n-Hexane AR grade (Lab-Scan Co., Ltd, Ireland)
12. L-α-Phosphatidylcholine (from fresh egg yolk, type XVI-E, Sigma, USA Lot 90K5220)
13. Propan-2-ol HPLC grade (Lab-Scan Co., Ltd, Ireland)
14. Sodium alginate (Srichand United Dispensary Co., Ltd., Thailand)
15. Triethylamine(Carlo Erba, France)
16. Tri-sodium citrate (Ajax Finechem, Australia)
17. Tween 80 (Acros Organics, USA)

Equipment

1. Analytical balance (Sartorius GMPH, Germany)
2. Centrifuge (Model K3 system, Centurion, UK)
3. High performance liquid chromatography (HPLC, Shimadzu, Japan) instrument equipped with the following:
   System controller (SCL-10AVP)
   Pump (LC 10ADVP)
   Diode array detector (SPD-M10AVP)
   Autoinjector (SIL-10ADVP)
4. Mastersizer (S long bed version 2.11, Malvern, UK)
5. Modified franz diffusion cell (Crown Glass Company, Inc, USA)
6. Optical light microscope (Olympus, Japan)
7. pH meter (C832, Consort, Belgium)
8. Rotary evaporator (Model R-200, Buchi, Switzerland)
9. Transmission Electron Microscope (Model JEM-2100, JOEL, Japan)
10. Ultracentrifuge (L-80, Beckman, USA)
11. Ultrasonic bath (Cavitator, Ultrasonic Mettler Electronic, USA)
12. UV-visible spectrophotometer (UV-160A, Shimadzu, Japan)
13. Vortex mixer (Vortex-genie, model G650E, USA)

Methods

1. Methods of Quantitative Analysis of Lycopene

1.1 UV spectrophotometry

In order to determine the maximum absorption wavelength, lycopene was dissolved in n-hexane and then transferred to cells for UV detection. The n-hexane solvent was used as the blank.

The concentrations of the standard solutions were precisely measured by spectrophotometry against n-hexane at the corresponding absorption maximum (472 nm) in a 1 cm cell. % Purity was calculated as follows:

$$\% \text{ Purity} = \frac{\text{Absorbance} \times 10{,}000 \times 100}{3450 \times C}$$

Where:

C = Concentration of standard in μg/ml

3450 = $A^{1\%}_{1cm}$ (Specific absorption coefficients) of all-trans lycopene in n-hexane

10,000 = Scaling factor

The spectrophotometric purity was used to correct the concentration of the chromatographic calibration solutions.

1.2 High Performance Liquid Chromatography (HPLC) assay for lycopene analysis

Concentration of lycopene in nanoparticles was determined using HPLC as following.

1.2.1 HPLC conditions

The high performance liquid chromatography technique was used for analysis of lycopene. The system was composed of two pumps able to generate the variable flow of mobile phase, an autoinjector, an adjustable wavelength UV detector, system controller and degasser. All of these were operated by the data station softwere. The mobile phase used for analyzing lycopene consisted of methanol, acetronitrile and propan-2-ol.

The HPLC condition used was as follows:

Column : Reverse phase column C18, Inertsil ODS, 5 μm (4.6x150 mm) with guard column, Inertsil ODS, 5 μm
Mobile phase : Propan-2-ol: Methanol: Acetronitrile (50:25:25 v/v) + TEA 0.1%
Flow rate : 1.2 mL/min
Detector : UV-visible (SPD-M10AVP) detector at wavelength 472 nm.
Injection volume: 20 μL
Run time : 10 min
Retention time : 7.6-7.8 min

The mobile phase was filtered through a 0.45 μm membrane, and degassed ultrasonically prior to use. The presence of TEA improves the response of lycopene and reduces or eliminates on-column degradation (Olives Barba et al., 2006).

1.2.2 Preparation of standard solutions

A stock standard solution of lycopene was prepared by dissolving 1 mg of lycopene (Sigma, USA) in n-hexane and adjusted to 25 ml in a volumetric flask.

Standard solution was prepared by pipetted 2.0 mL of this stock standard solution into a 25 mL volumetric flask and adjusted to volume using n-hexane. The resulting standard solutions contain approximately 0.32 μg/mL lycopene. Aliquots of lycopene standard solution 0.2, 0.4, 0.6, 0.8, 1.0, 2.0 and 3.0 mL were pipetted and transferred to volumetric flask. The solutions were adjusted to volume with mobile phase so that the final concentrations of lycopene were 0.0128, 0.0256, 0.0384, 0.0512, 0.0128, 0.0256 and 0.384 μg/mL, respectively.

1.2.3 System suitability for quantitative determination of lycopene by HPLC

System suitability must be demonstrated to ensure that the validity of the analytical method is maintained whenever used. Replicate injections of the standard preparation required to demonstrate adequate system precision may be made before the injection of sample. The system suitability parameters used to evaluate were reproducibility (S_R) and tailing factor (T). Reproducibility is expressed in relative standard deviation, five replicate injections of the standard were used to calculate the relative standard deviation if the requirement is 2.0% or less. The tailing factor, a measure of peak symmetry, is unity for perfectly symmetrical peaks. These tests were performed by collecting data from five replicates injection of standard (USP 27, 2004).

20 μl of the standard solution (0.0128 μg /ml) were repeatedly injected into the HPLC system. Then, reproducibility (S_R) and tailing factor (T) were calculated.

2. Preparation of Lycopene Loaded Nanoparticles

2.1 Preparation of lycopene stock solution.

Accurately weighing approximately 150 mg of 10% lycopene (Redivivo® 10% FS) into a 50 mL clear glass volumetric flask. Adjusted to volume by ethanol and sonicated for 30 min or until dissolved. The concentration of stock solution was 300 μg/mL of lycopene. From the stock solution 2:10, 4:10, 6:10, 8:10 dilution in ethanol were prepared so that the final lycopene concentration were approximately 60, 120, 180, 240 μg/mL, respectively.

2.2 Preparation of chitosan solution.

The solution of 0.2% and 0.03% w/v chitosan in 1.0%v/v acetic acid was prepared and stirred overnight. The solution was filtered through No.1 filtered paper to remove particulates.

2.3 Preparation of chitosan coated liposome nanoparticles

Liposomes were prepared by thin film method. The amount of 30 mg phospholipid was dissolved in 10 mL of ethanol, 1 mL of lycopene stock solution was incorporated into the mixture, then shaking and sonicated. Ethanol was evaporated using rotary evaporator in 30^{o}C water bath under reduced pressure to 100 mbar until the thin film was obtained. Ten mL of phosphate buffer (1.0 mM, pH 7.4) were added and shaking for 30 min at 30 ^{o}C and sonicated for 45 min. Then the liposomes suspension was allowed to swell for 2 h at room temperature. Chitosan coated liposomes were prepared by dropwise addition of 10 mL of liposomal suspensions into 20 mL chitosan solution (0.2% in acetic acid) and leaving the mixture incubated in a refrigerator for at least 1 h. The liposomal suspensions were centrifuged at 3,500 rpm for 1 h to remove any large aggregates and the supernatant was harvested. The precipitant were washed with 10 ml phosphate buffer by centrifugation. Centrifugation under these conditions allowed the aggregates to precipitate, leaving nanoparticles suspended in the supernatant. The lycopene-loaded nanoparticles were isolated from supernatant by ultracentrifugation at 60,000 rpm for 2 h at 4^{o}C. The nanoparticles were redispersed in phosphate buffer by sonication for 30 min and washed twice in phosphate buffer by ultracentrifugation.

A phosphate buffer (1.0 mM), pH 7.4 was prepared from monosodium phosphate, monohydrate and disodium phosphate, heptahydrate. The final pH was adjusted using a pH meter.

2.4 Preparation of chitosan alginate nanoparticles

Using a method modified from De and Robinson (2003). A stock solution of lycopene in ethanol (1 mL) was added to 10 mL of sodium alginate solution (0.6mg/mL) containing 0.5 g of Tween 80. An aqueous calcium chloride solution (2 mL of 0.67 mg/mL) was added dropwise to the mixture of sodium alginate and lycopene. The mixtures were continuously sonicated for 30 min. Then, 2 mL of an aqueous chitosan solution (0.3mg/mL) were added and stirred for additional 30 min.

The suspensions were equilibrated overnight to allow nanoparticles to form. The ethanol and acetic acid were removed by evaporator at 50 mbar, 30^{o}C for 1 h. The concentrated solution was redispersed in deionized water and adjusted to 15 mL. The particulate of alginate and chitosan were isolated by centrifugation at 3,500 rpm for 1 h at 4^{o}C to remove any large aggregates. Then, the nanoparticles in supernatant were isolated from aqueous solution by ultracentrifugation at 60,000 rpm for 60 min at 4^{o}C. The resultant pellets were redispersed in deionized water by sonication for 30 min and the nanoparticles were washed twice in deionized water by ultracentrifugation.

2.5 Effect of lycopene concentration on the physicochemical properties of nanoparticles

To study the effect of lycopene concentration on the physicochemical properties, lycopene concentrations were varied between 60 to 300 μg/mL, each of them were added to prepare chitosan coated liposome and chitosan alginate nanoparticles. The amount of phospholipids was constant. The particle size and morphology of nanoparticles were determined by Mastersizer and TEM, respectively. The percentage of encapsulation efficiency and percentage of recovery were determined using HPLC.

3. Physical Characterization of Lycopene Loaded Nanoparticles

Lycopene loaded nanoparticles prepared from two different methods were characterized in size and morphology.

3.1 Particle size determination

The particle sizes of lycopene loaded nanoparticles were measured by means of the laser light scattering. The measurements were repeated three times for each sample.

The Mastersizer is based on the principle of laser ensemble light scattering. The instrument is composed of lens 300 RF counting the size in the range of 0.05-3480 μm. The light from a 2-mW Helium-Neon laser (633 nm wavelength) is used to form an analyzer beam. The transmitter and receivers units mounted on an optical bed. The Fourier lens mount receiver and any particles introduced by the sample presentation modules present within it will scatter this laser light.

The unscattered light is brought and passes through the detector and out of the optical system. The total laser power passing out of the system in this way is monitored allowing the sample volume concentration to be determined and shown on computer (Scientific and Technology Research Equipment Center [STREC])

3.2 Morphology

The shape and the surface morphology of lycopene loaded nanoparticles were investigated by means of the transmission electron microscope (TEM). They were normally characterized under optical microscopes and scanning electron microscopes. However prepared nanoparticles have noticeably small sizes that can not be characterized under optical microscopes and scanning electron microscopes. Thus, these particles were characterized under transmission electron microscopy.

The procedure for negative staining of a nanoparticles preparation sample was as follows. A drop of nanoparticles suspensions was applied onto carbon coated grids. After leaving for 1-3 min to allow adsorption of nanoparticles to a grid, the excess was removed by filter paper. A drop of 2% phosphotungstic acid was applied onto the grid, leaving for 1 min, drawn off by filter paper. Then the grid was air-dried and examined under a transmission electron microscope.

4. Determination of Lycopene Encapsulation Efficiency

4.1 Separation of lycopene nanoparticles

In order to separate unencapsulated lycopene from nanoparticle suspensions, the nanoparticle suspensions were centrifuged at 3,500 rpm at 4^{o}C for 1 h. Unencapsulated lycopene can be observed as the red droplet located both precipitant and at the upper part of the centrifuge tube. Then, both encapsulated lycopene in nanoparticles (supernatant) and unencapsulated lycopene were analyzed by HPLC with suitable condition. The quantitative lycopene analysis was shown in the percentage of encapsulated lycopene and compared among those sets of preparation with the varied amount of lycopene for each of two methods of preparations.

To separate nanoparticles from the suspensions ultracentrifuge method was used. The ultracentrifuge tube containing 8 ml of lycopene nanoparticle suspensions was put in the rotor. The maximum speed of the ultracentrifuge was 60,000 rpm at which the ultracentrifuge tube can tolerate. The temperature was set at 4^{o}C. The ultracentrifugation process took about 2 h to separate them efficiently.

4.2 Quantitative analysis of encapsulated lycopene in chitosan coated liposome nanoparticles

After separation using centrifugation at 3,500 rpm at 4^{o}C for 1 h, 2 ml of supernatant was collected to analyse encapsulated lycopene. The nanoparticles were lysed by addition 5 ml of ethanol to obtain the encapsulated lycopene solution. Then,

5 ml of n-hexane was added. The mixture was shaken with vortexed-mixer for 30 sec, and sonicated for 30 min, and then left undisturbed for 2 h to separate the two phases. The extraction was repeated twice. The n-hexane in upper part was analyzed for lycopene by HPLC method. The aliquot of the n-hexane solution from each preparation was pipetted and transferred in to 10 ml volumetric flask and was adjusted to volume with the mobile phase and ready for HPLC analysis.

4.3 Quantitative analysis of encapsulated lycopene in chitosan alginate nanoparticles

After separation using centrifugation at 3,500 rpm at 4^{o}C for 1 h, 1 ml of supernatant was collected to analyze encapsulated lycopene. The nanoparticles were lysed by addition 4 mL of 1.12 M sodium citrate to obtain the encapsulated lycopene solution. Then, 5 ml of n-hexane was added. The mixture was shaken with vortexed-mixer for 30 sec and sonicated for 30 min, and then left undisturbed for 2 h to separate the two phases. The extraction was repeated twice. The n-hexane upper part was analyzed for lycopene by HPLC method. The aliquot of the n-hexane solution from each preparation was pipitted and transferred in to 10 ml volumetric flask and was adjusted to volume with the mobile phase and ready for HPLC analysis.

4.4 Quantitative analysis of unencapsulated lycopene

The unencapsulated lycopene was diluted with distilled water and adjust to volume in a 10-ml volumetric flask. Two ml of the solution was transferred to test tube. Then, 5 ml of n-hexane was added. The mixture was shaken with vortexed-mixer for 30 sec and sonicated for 30 min. After phase separation, the n-hexane in upper part was analyzed for lycopene by HPLC method. The aliquot of the n-hexane solution from each preparation was pipitted and transferred in to 10 ml volumetric flask and was adjusted to volume with the mobile phase and ready for HPLC analysis.

4.5 Calculation of the percentage of encapsulation efficiency and the percentage of recovery

The encapsulation efficiency was calculated as the ratio between the amount of lycopene in the nanoparticles and initial amount of lycopene used to formulate. The percentage of encapsulation efficiency and the percentage of recovery of lycopene of each preparation were determined from the following equation:

$$\% \text{ Encapsulation efficiency} = \frac{\text{Amount of lycopene in the nanoparticles}}{\text{Initial amount of lycopene used to formulate}} \times 100$$

$$\% \text{ Recovery} = \frac{\text{Sum of amount of lycopene in nanoparticles and unencapsulated lycopene}}{\text{Initial amount of lycopene used to formulate}} \times 100$$

5. Stability Studies of Lycopene Loaded Nanoparticles

The physical stability (size and morphology) and chemical stability (encapsulation efficiency) of lycopene loaded nanoparticles were examined in the preparations that presented the best encapsulation efficiency. The samples were stored in a well-closed amber vial in the refrigerator ($5 \pm 1\ ^{o}C$), in dark and visible light at room temperature ($25 \pm 1\ ^{o}C$). The samples were taken immediately after preparation as 0 and then 1, 2, 3, 4, 8, 12 weeks. The amounts of undegraded lycopene in sample were determined quantitatively by HPLC. The result was shown as the remaining percentage of lycopene in nanoparticle suspensions.

The remaining percentage of lycopene in nanoparticle suspensions was calculated from the following equation:

$$\% \text{ Remaining} = \frac{\text{The amount of lycopene in suspensions at various time}}{\text{The amount of lycopene in suspensions were analyzed at time 0}} \times 100$$

5.1 Quantitative analysis of undegraded lycopene in chitosan alginate nanoparticles suspensions

Sodium citrate was added to 1 ml of lycopene loaded chitosan alginate nanoparticles, then vortex and sonicated for 30 min followed by added n-hexane to separate lycopene from aqueous solution. The n-hexane solution was diluted with mobile phase before analyzed by HPLC.

5.2 Quantitative analysis of undegraded lycopene in chitosan coated liposome nanoparticles suspensions

Ethanol was added to 5 ml of lycopene loaded chitosan coated liposome nanoparticles, then vortex and sonicated for 30 min followed by added n-hexane to separate lycopene from aqueous solution. The n-hexane solution was diluted with mobile phase before analyzed by HPLC.

6. *In Vitro* Skin Penetration Experiments

Both lycopene loaded chitosan coated liposome nanoparticles and lycopene loaded chitosan alginate nanoparticles were investigated for the penetration through the human stratum corneum. The most useful apparatus for drug penetration studies was franz diffusion cell.

6.1 Preparation and treatment of membranes

The experiment was carried out according to the Song and Kim (2006). Briefly, human skin samples were obtained from the abdominal region after plastic surgery. Then underlying fat and subcutaneous tissue was removed. The human skin from hospital was placed in transport medium and moved to the laboratory, where it was processed as soon as possible. The skin samples were cut into small pieces and were stored in freezer at -20 ^{o}C. Before used, the skin samples were thawed for 1 h at

room temperature and skin disk with a diameter of 35 mm was punched. This protocol was approved by the Faculty Ethic Committee.

The epidermis was isolated at 60^{o}C for 2 min to remove the dermis, leaving the stratum corneum and intact epidermal layers. Epidermis was isolated by incubation in 1% solution of trypsin in PBS (pH 7.4) for 2-4 h at 37^{o}C. Then, stratum corneum and epidermis (SCE) was carefully peeled off using two forceps, the skin samples were used immediately. Before being mounted in a diffusion cell, the epidermis was soaked in the receptor medium for at least 10 min. Then, the epidermis was clamped in place between the donor and the receptor compartment of the cell.

After the experiment, the skin samples were in freezer and were eliminated by Public Cleansing Service Division of Bangkok Metropolitan Administration.

6.2 *In vitro* penetration studies

A franz diffusion cell was used for the *in vitro* penetration studies. The diffusion cell was made up from glass. It consists of two compartments with the donor compartment in the upper and the receptor compartment in the lower which has double jacket around it. The diameter of the franz cell was 1.5 cm corresponding to an effectively permeable area of 1.76 cm^{2}. Epidermis from human skin prepared from 6.1 was mounted between the donor and receiver compartments of the diffusion cell with the stratum corneum side up. The receptor compartment was filled with about 14 ml of phosphate buffer solution with Tween 80 (3%w/v) and was stirred continuously during the experiment. The water bath was maintained at 37$\pm$1^{o}C then circulating water through a jacket surrounding the receptor compartment throughout the experiment which resulted in a temperature on the skin surface of 32$\pm$2^{o}C. The receptor compartment was stirred by magnetic stirring at 500 rpm with 0.5 cm magnetic bar. All bubbles were carefully removed between the underside of the skin and solution in the receptor compartment. The two ml of each nanoparticle suspensions were carefully filled in the dornor compartment of the diffusion cells. At the beginning of each penetration experiment, initial lycopene concentration in the

donor compartment was determined. The penetration experiments were carried out for 12 h. The two ml of receptor fluid was removed at appropriate time intervals and immediately replaced with an equal volume of fresh receptor medium. Each experiment was run in triplicate.

The amount of lycopene in the receptor fluid sample was determined by HPLC method. The method of lycopene analysis for penetration studies was similar to that for encapsulation studies.

Amount of penetrated were plotted as a function of time and linear portion of the curve determined as s steady-state flux (J_s). The penetration coefficient (k_p) were calculated as $k_p = J_s/C_o$, Where: C_o is the initial concentration of lycopene in the donor compartment.

6.3 Histological observation

The small pieces human skin samples, used as full thickness skin, were used in this experiment. Each previously prepared lycopene loaded nanoparticles were applied on the skin and performed the penetration studies. The skin was thawed and clamped into position between the donor and receptor compartment of diffusion cell thermostated at $32\pm2^{o}C$. The donor was filled with 2 ml of either a suspension of chitosan alginate nanoparticles or the chitosan coated liposome nanoparticles solution. After 3 h of penetration experiments, the excess formulation was removed from the skin surface. The skin samples were washed three times with phosphate buffer (pH 7.4) before drying gently with a cotton swab. The treated skin area was cut in order to perform the histological observation.

At the end of the penetration experiments the pieces of skin treated with lycopene loaded chitosan coated liposome nanoparticles and lycopene loaded chitosan alginate nanoparticles were observed by TEM. The skin samples incubated for 3 h with lycopene loaded nanoparticles were then cut into small ribbon approximately of 2x4 mm. in size. The ribbons were fixed with 2.5% glutaraldehyde

in 0.1 M cacodylate buffer solution overnight, wash with 0.1 M cacodylate buffer and then fixed with 1% osmium tetroxide in 0.1 M cacodylate buffer (1:1) for 2 hour. Following post fixation, the samples were dehydrated in 30%, 50%, 70%, 95%, and 100% ethanol and embedded in epon-araldite resin.

Ultrathin sections were cut by an ultramicrotome, collected on formvar-coated grids and intensified with uranyl acetate and lead acetate. Finally samples were examined and photographed in a JEM-2100 (JOEL®) transmission electron microscope.

CHAPTER IV

RESULTS AND DISCUSSION

1. Methods of Quantitative Analysis of Lycopene

1.1 UV spectrophotometry

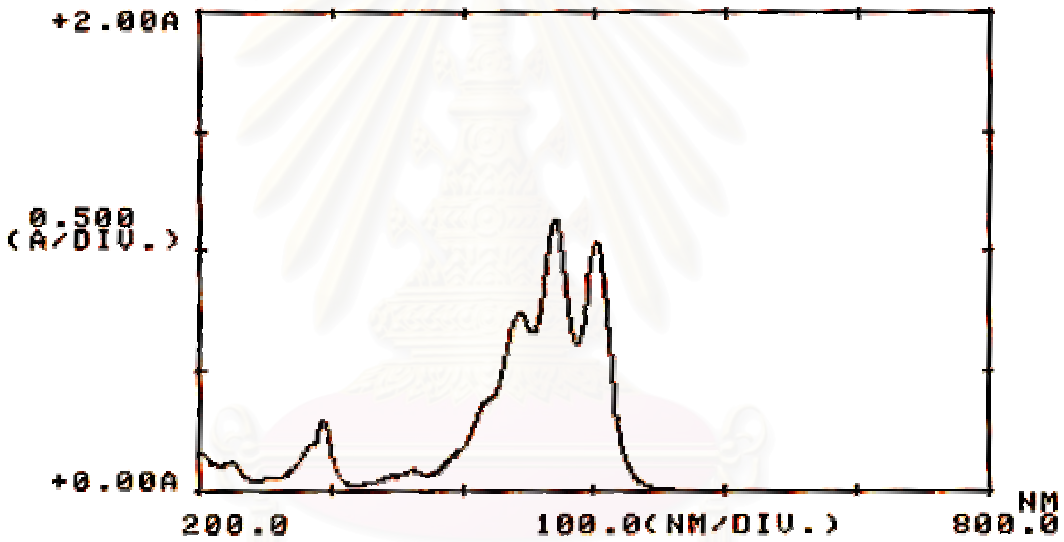

Figure 16 The UV spectrum of lycopene standard solution.

Lycopene in n-hexane solution showed the maximum absorption wavelength at 472 nm as demonstrated in Figure 16. Therefore, the UV detector of HPLC was set at 472 nm in order to obtain the accurate quantitative analysis of lycopene. The standard solution of 3.2 μg/mL was freshly prepared and followed by the spectrophotometric determination of the exact concentration. A spectrophotometric purity check of the standard is necessary because of the instability of lycopene. The exact concentration of the standard solution was found to be 3.23 μg/mL. So, the percentage of purity of standard solutions was 100.93 %.

1.2 HPLC assay for lycopene analysis

The use of mixtures of methanol and acetronitrile, at any ratio, resulted in prolonged retention time of the lycopene. Therefore, the addition of third solvent, in which lycopene is more soluble, was found to be essential. The optimum mobile phase composed of propan-2-ol, methanol, acetronitrile in the ratio of 50:25:25 %v/v, respectively. The concentration of lycopene was determined by an isocratic reverse phase HPLC. The flow rate was 1.2 mL/min. The injection volume was 20 μl, and the retention time was found to be 7.646 min. The column effluent was detected at 472 nm. The calibration curve for the quantification of lycopene was linear over the range of concentration of 0.0129 – 0.3876 μg/mL with correlation coefficient (R^2) of 0.9993 as shown in Figure 17. The data of peak area of lycopene standard are shown in Table 4.

Lycopene may undergo losses or degradation on the column. Some studies have indicated that solvent modifiers improve the recovery of lycopene from the column and reduce or eliminate on-column degradation. The addition of 0.1% v/v triethylamine (TEA) to the mobile phase could increase the recovery of lycopene and also had the effect of reducing retention times but the lycopene peaks were still baseline resolved. The exact action of these solvent modifiers is unclear, but it is suggested that the improvement in recovery is caused by the buffering of acidity in the mobile phase, or more likely the acidity of the free silanols in the stationary phase or preventing reactions with free metal ions (Hart and Scott, 1995).

Table 4 The concentration and peak area of lycopene standard solutions by HPLC analysis.

Concentration (μg/mL)	Peak area
0.0129	3716
0.0258	8794
0.0388	12414
0.0517	16069
0.0646	21206
0.1292	43712
0.2584	88339
0.3876	134138

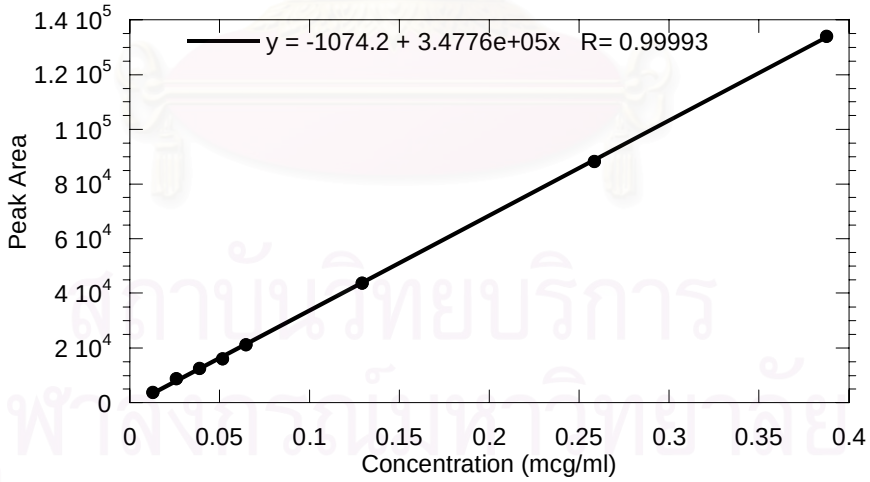

Figure 17 The calibration curve for lycopene.

1.3 System suitability

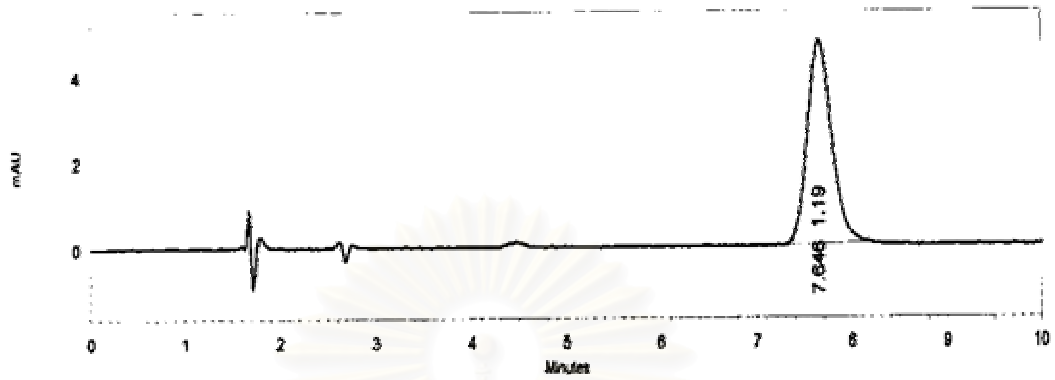

Figure 18 The chromatogram of lycopene standard solution.

Table 5 Reproducibility (% RSD) and tailing factor of five replicate injections of the standard solution.

Number of Replication	Concentration (μg/mL)	Peak Area	Tailing Factor
1	0.128	32623	1.18
2	0.128	32308	1.19
3	0.128	32184	1.20
4	0.128	32401	1.20
5	0.128	32609	1.21
Mean		32381.5	1.196
SD		201.08	0.011
% RSD		0.62	0.95

The % RSD obtained from this method was 0.62%. This result was within acceptable range (< 2.0%). Asymmetrical was evaluated by the calculation of tailing factor, using the width of the peak at 5% height. The tailing factor was 1.196 $\pm$ 0.011 (Table 5) which was in acceptable range ($\leq$1.2) (Snyder et al., 1997). In conclusion, the system of HPLC was suitable for quantitative analysis of lycopene in nanoparticles.

2. Preparation of Lycopene Loaded Nanoparticles

2.1 Preparation of lycopene loaded chitosan coated liposome nanoparticles

In this study, lycopene loaded chitosan coated liposome nanoparticles could be prepared by the method modified from Wu et al. (2004). The organic solvent, the sonication time, and the temperature for evaporation of organic solvent were adjusted to obtain suitable conditions of preparation of lycopene nanoparticles. The liposomal suspensions were clear pink to colorless dispersion (see Appendix I).

Chitosan can be used to influence the penetration and stability by forming a stable layer around the vesicles in dependence on their concentration and type. To avoid extensive aggregation, it appears to be necessary to have a certain excess of chitosan in the solution during coating. Thus, the procedure for the additional liposomes into a 0.2% w/v of chitosan was chosen (Henriksen et al., 1994). When liposomes are added to a solution with excess of high molecular weight chitosan polymer, the chitosan will adhere to the liposomal surface and produce coated vesicles.

2.2 Preparation of lycopene loaded chitosan alginate nanoparticles

Previous report described the preparation of nanospheres using combination of alginate and a cationic natural polymer, poly-L-lysine or chitosan. These researchers proposed that the addition of cationic polymer is essential to form stable, uniform alginate nanospheres by enveloping the negatively charged calcium alginate complex. The calcium chloride to alginate mass ratio was necessary to prepare nanospheres. A ratio below 0.2 was required to maintain the critical pre-gel state essential for the preparation of nanospheres. Additionally, chitosan alginate nanospheres were formed when the ratio of calcium chloride to sodium alginate ratio was 0.1 (De and Robinson, 2003).

In this study, lycopene loaded chitosan alginate nanoparticles could be prepared by the gelation method modified from De and Robinson (2003) at the ratio calcium chloride to alginate of 0.2. Chitosan alginate nanoparticles were prepared in a two step procedure, base on the ionotropic gelation of polyanion with calcium chloride followed by polycationic crosslinking. The nanoparticle suspensions were yellow to pink clear dispersion (see Appendix I).

3. Physical Characterization of Lycopene Loaded Nanoparticles

3.1 Determination of particle size

The particle size of nanoparticles was measured by Mastersizer, which is the most convenient method for particle size analysis. The particle size was described by the volume-weighted mean diameter ($D_{4,3}$).

Table 6 Mean particle size and span of lycopene loaded chitosan coated liposome and lycopene loaded chitosan alginate nanoparticles with varying of initial lycopene concentrations (Mean ± SD, n=3).

Initial lycopene concentration (μg/mL)	**Chitosan coated liposome nanoparticles**		**Chitosan Alginate nanoparticles**	
	Mean particle size ($D_{4,3}$, nm)	**Span**	**Mean Particle size ($D_{4,3}$, nm)**	**Span**
60	463.33±11.55	3.11±0.06	323.33±5.77	0.79±0.05
120	360.00±17.32	2.98±0.05	500.00±10.00	4.78±0.18
180	320.00±0.00	4.16±0.01	500.00±0.00	4.32±0.22
240	366.67±5.77	2.40±0.08	373.33±5.77	2.57±0.07
300	420.00±0.00	3.47±0.06	350.00±0.00	3.28±0.06

The mean particle size of lycopene loaded chitosan coated liposome and lycopene loaded chitosan alginate nanoparticles were in range of 320-463 nm and 323-500 nm, respectively. The polydispersity of particles were expressed by the span.

The span value of lycopene loaded chitosan coated liposome and lycopene loaded chitosan alginate nanoparticles being approximately in the range of 2.40-4.16 and 0.79-4.78, respectively. The high span value indicated a wide particle size distribution. The influences of lycopene concentration on the particle size and particle size distribution (span) of lycopene loaded nanoparticles are shown in Table 6. However, the mean particle size and particle size distribution of both preparations were not related to the lycopene concentration.

3.2 Transmission electron microscope

The TEM image of the lycopene loaded chitosan coated liposome nanoparticles and lycopene loaded chitosan alginate nanoparticles are illustrated in Figure 19 and 20, respectively. It could be found that lycopene loaded chitosan coated liposome nanoparticles showed a spherical or ellipsoidal shape with 100-200 nm in diameter. There was some aggregation and overlapping of liposomes. In Figure 19A, TEM micrograph shows the majority of liposomes consisted of one phospholipids bilayer but others as shown in Figure 19B appears to have several bilayers.

Transmission electron microscope showed some deformed structures, apparently due to osmotic pressure change during the staining process. In Figure 19B shows some lamellar patterns on liposomes. It might be multilamellar but it is usually difficult to report for multilamellar vesicle from transmission microscopy. It has been suggested that the apparent multilamellarity might be an artifact of negative staining and that multilamellations were seen when liposomes were partially overlapping thus do not reflect the actual internal structure. However, if an isolated multilamellar structure was seen, it could highly suggestive that the sample could be multilamellar (New, 1997).

When negative staining was performed properly, a monolayer of liposomes embedded in negative stain could be spread across the grid. This would result in the formation of artefactual aggregates of liposomes. These aggregates could be indistinguishable from those formed prior to staining.

A. B.

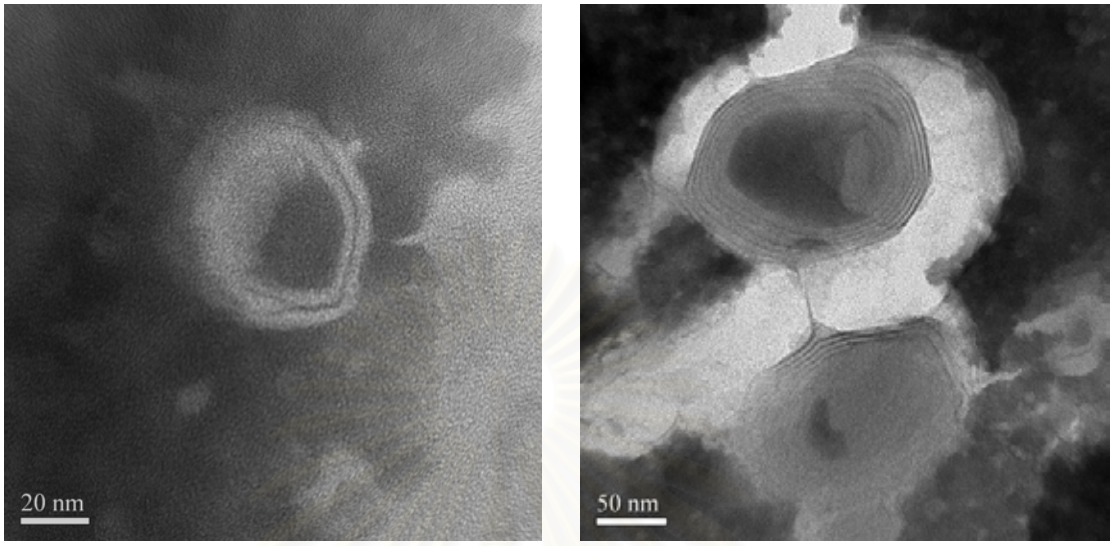

Figure 19 Transmission electron micrographs of lycopene loaded chitosan coated liposome nanoparticles, A: presence of unilamellar vesicles (x 450,000) and
B: presence of multilamellar vesicles (x 180,000).

A. B.

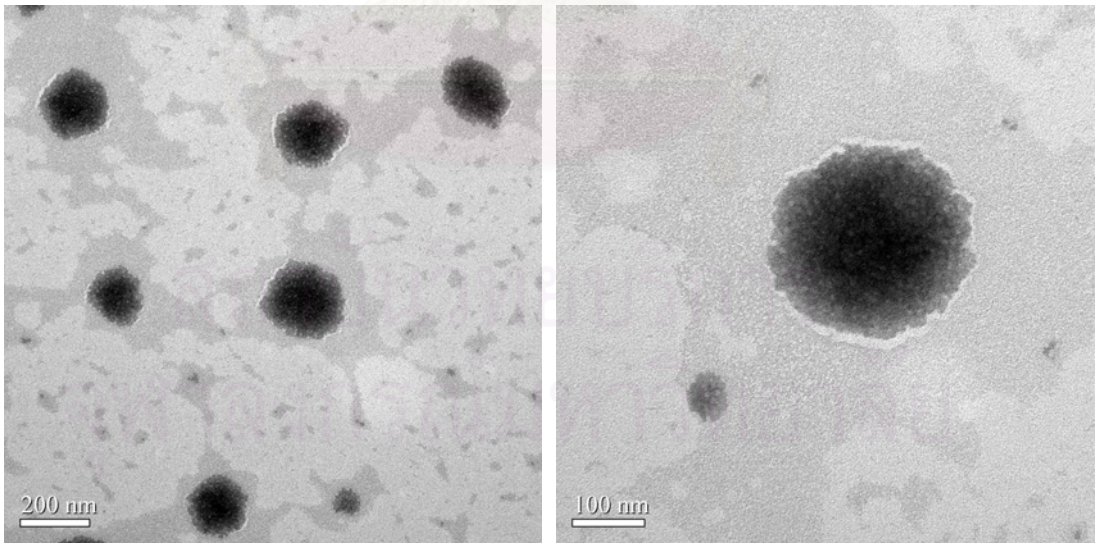

Figure 20 Transmission electron micrographs of lycopene loaded chitosan alginate nanoparticles, A: an overview of spherical shape of nanoparticles (x 45,000),
B: a high magnification of individual particles (x 90,000).

TEM micrographs in Figure 20 confirm the presence of lycopene loaded chitosan alginate nanoparticles and provided morphological information. A relatively homogeneous population with spherical shape and highly porous structure of lycopene loaded chitosan alginate nanoparticles was obtained. Each particle was arrangement in separately. Lycopene loaded chitosan alginate nanoperticles were considerably smaller when viewed with TEM than when measured by Mastersizer. TEM images showed particle size between 50 and 200 nm, whereas Mastersizer indicated that the smallest population has average diameter of at least 320 nm. This apparent discrepancy can be explained by the dehydration of the hydrogel particles during sample preparation for TEM imaging. Additionally, Mastersizer measured the apparent size of a particle, including hydrodynamic layers that form around hydrophilic particles such as those composed of chitosan alginate, leading to an overestimation of particle size (Douglas and Tabrizian, 2005).

4. Determination of Lycopene Encapsulation Efficiency

4.1 Effect of lycopene concentration on encapsulation efficiency

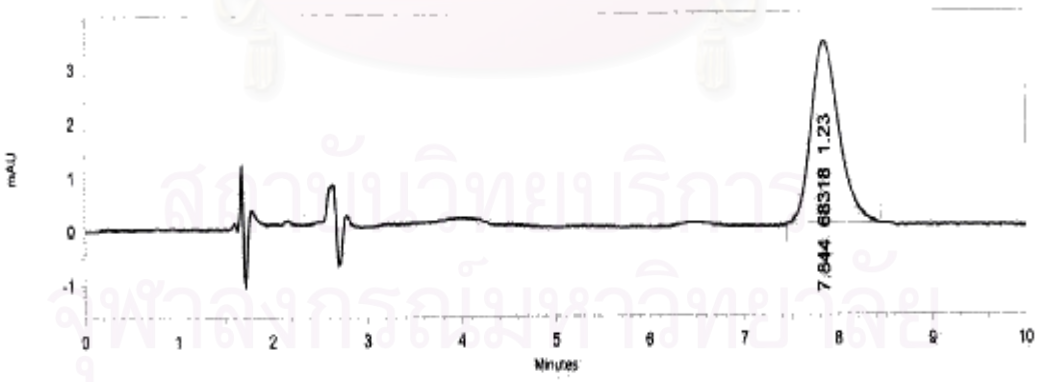

Figure 21 The chromatogram of lycopene sample.

To separate lycopene loaded nanoparticles from the nanoparticle suspensions, both lycopene loaded chitosan coated liposome nanoparticles and lycopene loaded chitosan alginate nanoparticles suspension were ultracentrifuged at 60,000 rpm for 2 h.

Then, the upper part or supernatant with pink to colorless and the precipitant with red to yellow were obtained (see in appendix I). Interestingly, the TEM images presented the nanoparticles characteristic both in the supernatant and the precipitant with the particle size of the upper part were smaller than the precipitant. The TEM images of supernatant and precipitant of lycopene loaded chitosan coated liposome nanoparticles and lycopene loaded chitosan alginate nanoparticles are shown in appendix I. In Figure I-18, the supernatant of the lycopene loaded chitosan liposome nanoparticles, small spherical particles of vesicles with a homogeneous distribution of 10 nm diameter was observed. In Figure I-19, the precipitant of lycopene loaded chitosan liposome nanoparticles showed a spherical or ellipsoidal shape with diameter about 100-200 nm and presented lamellarity characteristic of liposomes. In case of lycopene loaded chitosan alginate nanoparticles, Figure I-20 shows a spherical shape with highly porous structure with particle sizes up to 200 nm in diameter was found in the supernatant. Similarly, in Figure I-21 shows spherical structure with homogeneous distribution with 100-200 nm in diameter was found in the precipitant.

Hence, the ultracentrifugation of these nanoparticles preparations was not completely effective to separate nanoparticles from the suspensions. For this reason, the encapsulated lycopene in chitosan coated liposome nanoparticles and lycopene loaded chitosan alginate nanoparticles were calculated from the amount of lycopene in the supernatant after centrifugation at 3,500 rpm for 1 h.

The experiment was set by varying the amount of lycopene added in nanoparticles preparation. The encapsulated lycopene and unencapsulated lycopene were separation by centrifugation at 3,500 rpm for 1 h. There were three compartments of nanoparticle suspensions, the upper part of tube that is unencapsulated lycopene, the middle part or the supernatant is the uniform nanoparticles suspensions and the lower compartment locating at bottom of tube is particulates, polymer and unencapsulated lycopene.

The extraction of encapsulated lycopene in chitosan alginate nanoparticles is essential for quantitative analysis. Chitosan alginate nanoparticles were destabilized

when treated with a sequestrant agent such as sodium citrate. This ionic exchange lead to swelling of the gel and started to develop cracks in the surface. Then, membrane ruptured and the dissolved core alginate flowed out immediately (Gaserod et al., 1999).

For extraction of encapsulated lycopene in chitosan coated liposomes, ethanol was added to destroy the lipid bilayer of liposomes and the obtained lycopene was dissolved in hydroalcoholic solution. Then, the lycopene in each preparation was separated from aqueous by addition of n-hexane. n-Hexane was found to be the most efficient and low toxicity. The solubility of lycopene in n-hexane was sufficient for quantitative extraction.

The encapsulation efficiency was expressed as the percentage of encapsulated lycopene in nanoparticles relative to the initial concentration. Lycopene loaded chitosan coated liposome nanoparticles, the higher the initials concentration up to 200.28 μg/mL, increase the encapsulation efficiency. Suggesting that lycopene initial concentration of 200.28 μg/mL may be representing the highest percentage of encapsulation efficiency when 30 mg of phospholipids were used resulted in the core to wall ratio of 1:150 by weight. The reason for reduced the percentage of encapsulation efficiency in chitosan coated liposomes at initial concentration of 234.16 μg/mL may be due to the excess of lycopene was not completely encapsulated in the bilayer. As the lycopene concentration increased, the amount of phospholipid remained constant since limiting the encapsulation of lycopene into the lipid bilayer.

In case of lycopene loaded chitosan coated liposome nanoparticles showed the percentage of encapsulation efficiency in the range of 9.91-47.75%. Whereas lycopene loaded chitosan alginate nanoparticles showed the percentage of encapsulation efficiency in the range of 8.76-69.31%. The amount of encapsulated, unencapsulated lycopene, the percentage of encapsulation efficiency and percentage of recovery of lycopene in chitosan coated liposome and chitosan alginate nanoparticles are summarized in Table 7 and 8, respectively.

Table 7 The amount of encapsulated, unencapsulated, % encapsulation efficiency and % recovery of lycopene in chitosan coated liposome nanoparticles with varying lycopene loading.

Initial amount of lycopene (μg)		Encapsulated (μg)	Unencapsulated (μg)	Total (μg)	% Encapsulation efficiency	% Recovery
Theoretical	Actual					
60	45.7535	4.5360	0.1195	4.6555	9.91	10.18
120	88.9752	16.4560	8.6048	25.0608	18.50	28.17
180	140.5581	45.5440	13.7864	59.3304	32.40	42.21
240	200.2829	95.6381	17.2347	112.8728	47.75	56.35
300	234.1635	65.8800	38.7854	104.6654	28.13	44.70

Table 8 The amount of encapsulated, unencapsulated, % encapsulation efficiency and % recovery of lycopene in chitosan alginate nanoparticles with varying lycopene loading.

Initial amount of lycopene (μg)		Encapsulated (μg)	Unencapsulated (μg)	Total (μg)	% Encapsulation efficiency	% Recovery
Theoretical	Actual					
60	45.7535	4.0060	17.3934	21.3994	8.76	46.77
120	88.9752	46.6860	13.1946	59.8806	52.47	67.30
180	140.5581	89.5040	5.0585	94.5625	63.68	67.28
240	200.2829	130.0860	7.5625	137.6485	63.36	67.14
300	234.1635	162.2900	8.3155	170.6055	69.31	72.86

As a result, initial lycopene concentration also influences the encapsulation efficiency of lycopene loaded chitosan alginate nanoparticles. The higher concentration of lycopene added in chitosan alginate nanoparticle preparations, the

higher the percentage of entrapment efficiency was obtained. Comparatively, the amount of encapsulated lycopene found in chitosan alginate nanoparticles was higher than that in chitosan coated liposome nanoparticles. It may be due to the way of encapsulation were different. The TEM images showed that there was gel matrix of polymer around the droplet of micelle of lycopene and then created the nanospheres or polymer coated micelle, resulted in higher encapsulation efficiency. Whilst, lycopene, a lipophilic compound, was only encapsulated into the lipid bilayers of chitosan coated liposome nanoparticles, resulted in a smaller amount of encapsulated lycopene.

The encapsulation efficiency was determined by liquefying nanoparticles in sodium citrate and extracted lycopene into organic solvent. Some loss of lycopene that occurred during the extraction from the nanoparticles may have resulted in low recovery percentage. The recovery percentage of lycopene loaded chitosan coated liposome and lycopene loaded chitosan alginate nanoparticles were in the range of 10.18-56.35% and 46.77-72.86%, respectively.

However lycopene could not be encapsulated completely. The instability of lycopene during processes of extraction, handling, and elimination of organic solvents makes the preparation of a sample for analysis an extremely delicate task, since successive and complex procedures were required to ensure that all of the lycopene were extracted.

The reproducibility of the two methods of preparation was examined. Preparation of lycopene loaded chitosan coated liposome and lycopene loaded chitosan alginate nanoparticles were repeated in triplicate for the lycopene initial concentration of 200.28 μg/mL. The mean and %RSD of the % encapsulation efficiency and % recovery of lycopene in chitosan coated liposome and chitosan alginate nanoparticles are shown in Table 9.

Table 9 Mean and %RSD of the % encapsulation efficiency and % recovery of lycopene in chitosan coated liposome and chitosan alginate nanoparticles.

Initial lycopene concentration (μg/mL)	Chitosan coated liposome nanoparticles		Chitosan alginate nanoparticles	
	% Encapsulation efficiency	% Recovery	% Encapsulation efficiency	% Recovery
200.28	47.96	56.73	63.13	67.06
200.28	46.27	54.60	62.02	65.51
200.28	49.02	57.74	64.95	68.86
Mean	47.75	56.36	63.37	67.14
SD	1.39	1.60	1.48	1.68
% RSD	2.91	2.84	2.33	2.50

5. Stability Studies of Lycopene Loaded Nanoparticles

The stability of the lycopene-loaded chitosan coated liposome nanoparticles and lycopene-loaded chitosan alginate nanoparticles prepared from initial lycopene concentration of 200.28 μg/mL were investigated during storage.

The physical stability of nanoparticles during storage in refrigerator, in dark and visible light at room temperature was studied in term of particle size and morphology. Particle size and TEM were done after 12 weeks of storage at each condition and the change in particle size of the samples were investigated. The particle size of lycopene loaded chitosan coated liposome nanoparticles increased from the initial states at when keep in dark and visible light at room temperature as shown in Table 10. Moreover, lycopene loaded chitosan coated liposome nanoparticle suspension showed colorless during the storage, which represents their physical instability. However, there was no visible sedimentation or particles in any sample during this period.

On the other hand, the particle size of chitosan alginate nanoparticles decreased, it might be due to the membrane of some nanoparticles was disrupted to a small particles and fraction of polymers. Figure 25-27 present the nanoparticles rupture and fractions of polymer were visualized using TEM after storage for 12 weeks in refrigerator, in dark and visible light at room temperature.

Table 10 Mean particle size and span of lycopene loaded chitosan coated liposome nanoparticles and chitosan alginate nanoparticles after storage for 12 weeks (Mean ± SD, n=3).

Method of preparation	Weeks	Refrigerator		Dark		Visible	
		Mean particle size (D[4,3], nm)	Span	Mean particle size (D[4,3], nm)	Span	Mean particle size (D[4,3], nm)	Span
chitosan coated liposome	0	366.67±5.77	2.57±0.07	366.67±5.77	2.57±0.07	366.67±5.77	2.57±0.07
	12	380.00+0.00	5.54±0.02	453.33+57.74	2.73±0.20	590.00+20.00	2.56±0.01
chitosan alginate	0	373.33+5.77	2.40±0.08	373.33+5.77	2.40±0.08	373.33+5.77	2.40±0.08
	12	376.67+5.77	4.69±0.08	200.00+10.00	1.57±0.03	200.00+0.00	1.52±0.06

In case of chitosan coated liposome nanoparticles as shown in Figure 22-24, the liposomes were aggregated and fused to from large particle. Resulting in increased particle size of nanoparticles and presented wide particle size distribution. Moreover, the changing in characteristic of liposome nanoparticles was observed.

According to Figure 22, the outer layer of the chitosan coated liposome nanoparticles disrupted and might induce the leakage of active compound after storage for 12 weeks in refrigerator. Similar structure had been found in Figure 23, revealed bilayer disintegration with formation of open fragment and characteristic hole on the surface of nanoparticles after storage for 12 weeks in dark at room temperature. From the Figure 24, the appearance of vesicles fusion formed during storage for 12 weeks in visible light at room temperature.

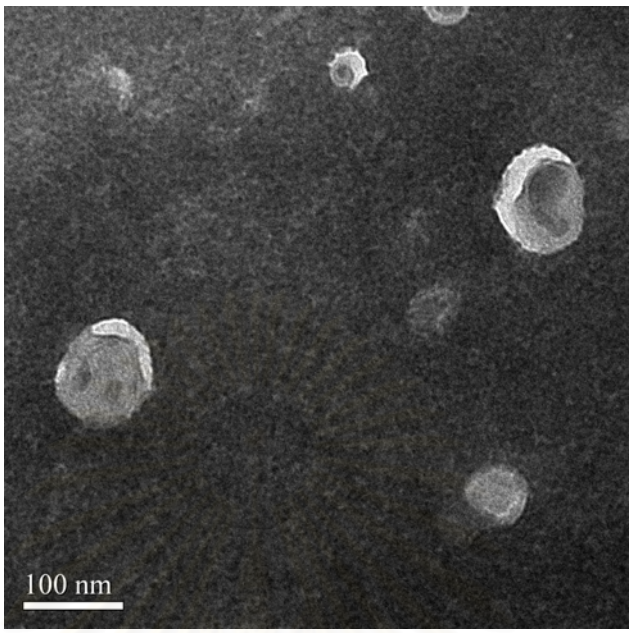

Figure 22 Transmission electron micrograph of lycopene loaded chitosan coated liposome nanoparticles after storage for 12 weeks in refrigerator (x 130,000).

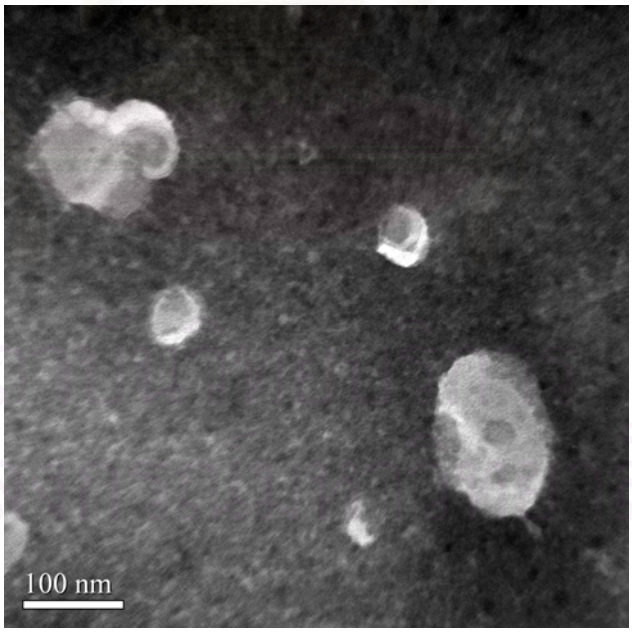

Figure 23 Transmission electron micrograph of lycopene loaded chitosan coated liposome nanoparticles after storage for 12 weeks in dark at room temperature (x 130,000).

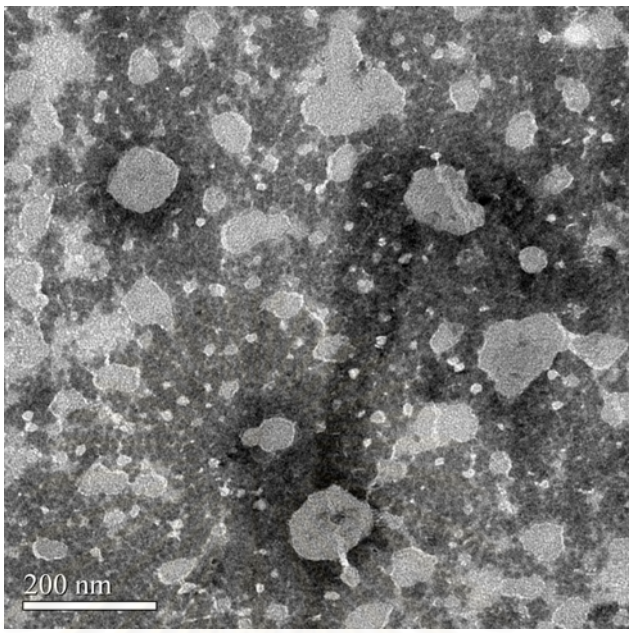

Figure 24 Transmission electron micrograph of lycopene loaded chitosan coated liposome nanoparticles after storage for 12 weeks in visible light at room temperature (x 85,000).

A. B.

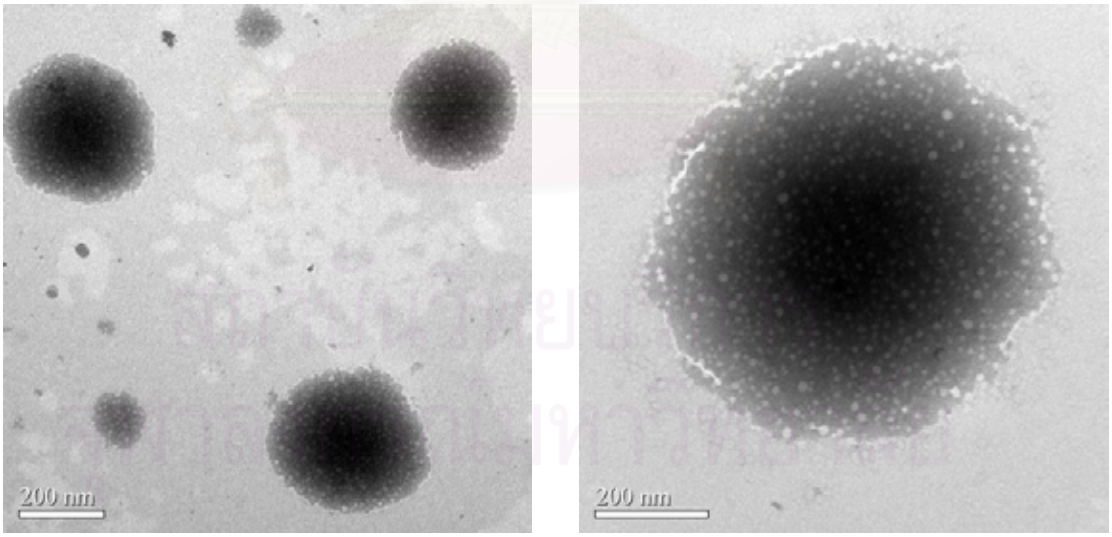

Figure 25 Transmission electron micrographs of lycopene loaded chitosan alginate nanoparticles after storage for 12 weeks in refrigerator.

A: an overview of nanoparticles (x 55,000) and

B: shows cracking on the surface of nanoparticles (x 75,000).

A. B.

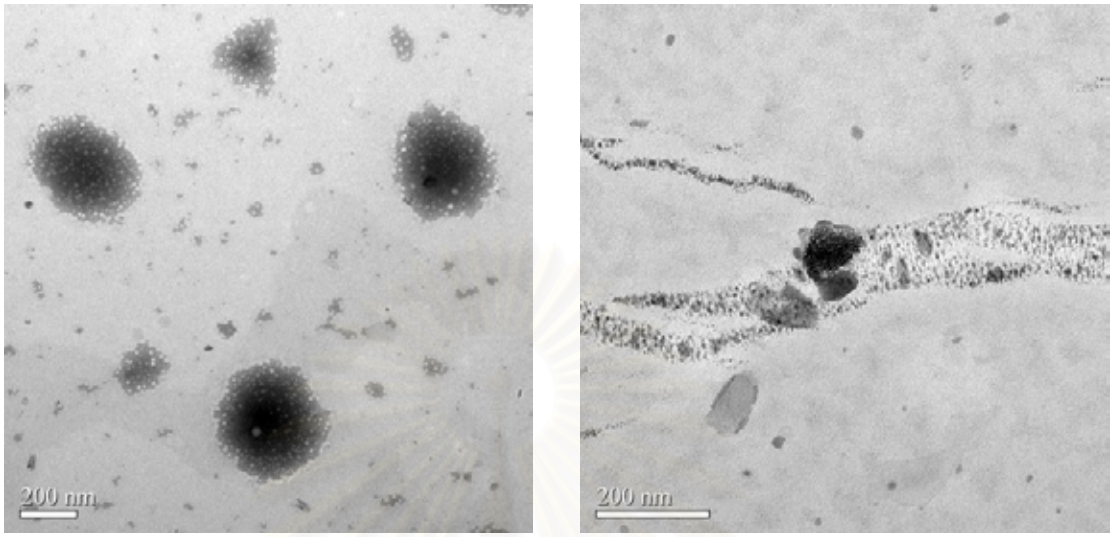

Figure 26 Transmission electron micrographs of lycopene loaded chitosan alginate nanoparticles after storage for 12 weeks in dark at room temperature.
A: shows the erosion on the surface of nanoparticles (x 35,000) and
B: shows the polymer liberated from nanoparticles (x 100,000).

A. B.

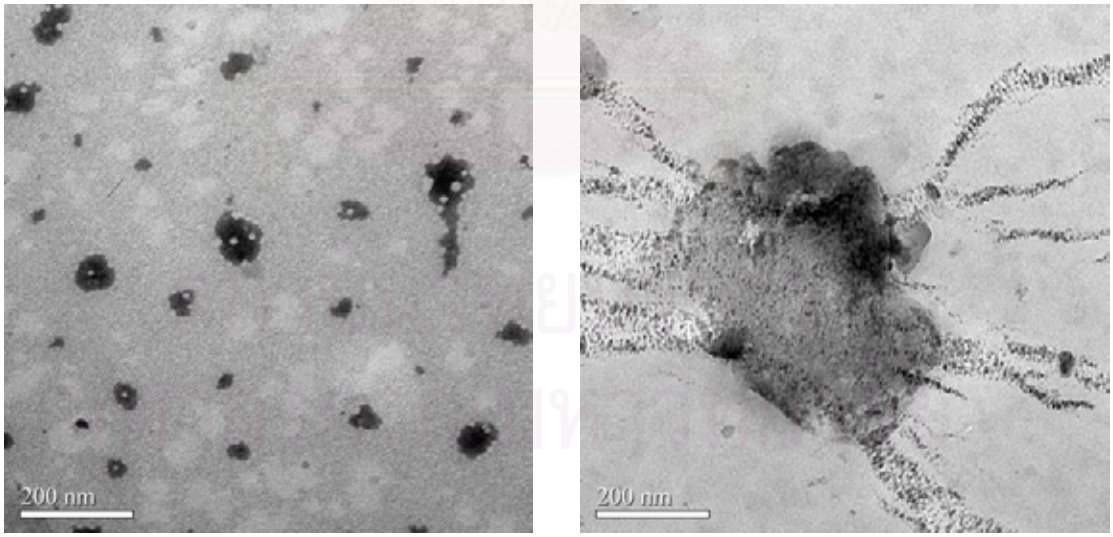

Figure 27 Transmission electron micrographs of lycopene loaded chitosan alginate nanoparticles after storage for 12 weeks in visible light at room temperature.
A: shows the small fragment of nanoparticles (x 75,000) and
B: shows the loose of polymer from nanoparticles (x 75,000).

In Figure 25 presents that lycopene loaded chitosan alginate nanoparticles stored in refrigerator only showed cracking on the membrane of nanopaticles but no any fraction of polymers. The TEM micrographs of lycopene loaded chitosan alginate nanoparticles storaged in dark at room temperature are shown in Figure 26. In Figure 26A, some erosion was found at nanoparticle surfaces; the nanoparticles still exhibited spherical shape but had smaller sizes. In Figure 26B, shows some non-structural of nanoparticles and the polymer liberated from nanoparticle. Similarly, lycopene loaded chitosan alginate nanoparticles stored in visible light demonstrated broken down into small fragments as shown in Figure 27A and presents the disintegrated of polymer from the nanoparticles in Figure 27B.

The chemical stability of chitosan coated liposome nanoparticles and chitosan alginate nanoparticles were presented in terms of lycopene content. The amounts of undegraded lycopene, included a sum of encapsulated and unencapsulated lycopene, were measured as a function of time. The lycopene content of a certain amount of each formulation was analyzed at the day of preparation (time 0), this value was quoted as 100%. The undegraded lycopene content during storage for 12 weeks at different conditions was presented in the percentage remaining of initial lycopene as shown in Table 11.

The stability of lycopene prepared in the two methods of nanoparticles was compared with lycopene in ethanol which used as raw materials. After storage for 12 weeks in the refrigerator 60.93% of lycopene remained in chitosan alginate nanoparticles and 53.58% of lycopene remained in ethanol. On the other hand, no lycopene content was observed in chitosan coated liposome nanoparticles. Accordingly, the greater disruption of the outer layer of lycopene loaded chitosan coated liposome nanoparticles might result in leakage of lycopene from the nanoparticles. Thus any amount of lycopene could not be determined after storage for 12 weeks in all conditions.

Table 11 The lycopene content and % remaining of lycopene in chitosan coated liposome nanoparticles, chitosan alginate nanoparticles and ethanol during storage for 12 weeks in refrigerator, in dark and visible light at room temperature (Mean ± SD, n=2).

Condition	Week	Chitosan coated liposome nanoparticles		Chitosan alginate nanoparticles		Lycopene in ethanol	
		Lycopene content (µg/mL)	% remaining	Lycopene content (µg/mL)	% remaining	Lycopene content (µg/mL)	% remaining
	0	0.08±0.003	100.00±0.00	3.20±0.08	100.00±0.00	6.93±0.09	100.00+0.00
Refrigerator	1	0.07±0.005	91.18±6.17	3.27±0.28	101.93±8.62	6.94±0.11	100.22±1.64
	2	0.07±0.008	92.62±10.21	3.14±0.00	98.31±0.09	6.75±0.06	97.50±0.99
	3	0.06±0.005	82.01±6.24	2.80±0.00	87.65±0.09	6.32±0.10	91.30±1.49
	4	0.05±0.005	66.33±5.88	2.69±0.06	84.25±1.81	4.92±0.13	71.02±1.9
	8	0.13±0.001	16.05±1.36	2.17±0.04	67.79±1.30	3.77±0.11	54.40±1.63
	12	UD	UD	1.95±0.04	60.93±1.28	3.71±0.13	53.58±1.88
Dark	1	0.07±0.000	85.57±0.08	3.12±0.07	97.76±2.21	7.01±0.39	101.25±5.62
	2	0.06±0.007	79.60±8.68	2.88±0.09	90.16±2.86	6.24±0.19	90.12±2.86
	3	0.05±0.008	66.48±10.19	2.77±0.07	86.76±2.16	6.14±0.25	88.63±3.67
	4	0.04±0.003	56.91±3.68	2.47±0.01	77.21±0.21	5.48±0.11	79.06±1.70
	8	0.01±0.000	13.18±0.21	1.58±0.06	49.39±1.96	1.72±0.10	24.85±1.51
	12	UD	UD	1.07±0.02	33.53±0.58	0.97±0.08	13.98±1.20
Visible	1	0.07±0.006	86.00±7.00	2.81±0.006	87.90±0.2	6.08±0.12	87.88±1.83
	2	0.06±0.006	73.30±7.01	2.76±0.03	86.25±1.14	5.64±0.24	81.47±3.48
	3	0.04±0.001	56.73±2.33	2.68±0.05	83.73±1.57	5.29±0.08	76.39±1.29
	4	0.05±0.006	59.29±7.35	2.55±0.01	79.88±0.41	4.63±0.22	66.84±3.12
	8	UD	UD	0.91±0.07	28.40±2.11	1.51±0.07	21.77±1.01
	12	UD	UD	UD	UD	0.85±0.22	12.30±3.16

UD = Undetectable

After 12 weeks of storage in dark at room temperature, the percentage of remaining of lycopene in chitosan alginate nanoparticles and in ethanol was 33.53% and 13.98%, respectively. Whereas lycopene in chitosan coated liposomes preparation could not be detected. The content of lycopene all sample was substantially reduced during storage in visible light at room temperature. Figure 28 shows the degradation profile of lycopene loaded chitosan coated liposome nanoparticles, lycopene loaded chitosan alginate nanoparticles and lycopene in ethanol as a function of storage time in refrigerator (Figure 28A), dark (Figure 28B) and visible (Figure 28C) at room temperature. In comparison, lycopene loaded chitosan alginate nanoparticles showed a highest stability in all condition, whereas lycopene loaded chitosan coated liposome nanoparticles showed very low stability when compared with lycopene in ethanol. The degradation of lycopene in chitosan alginate nanoparticles during storage was due to the erosion of chitosan alginate nanoparticles resulted in losing their spherical shape and lycopene concentration in an aqueous environment as shown in Figure 25, 26 and 27.

Figure 29 shows the percentage of remaining of lycopene in lycopene loaded chitosan coated liposome nanoparticles after storage for 12 weeks with the condition in refrigerator, dark and visible light at room temperature. Lycopene loaded chitosan coated liposome nanoparticles keep in refrigerator presented more stability within 1 month than that of storage in dark and visible light at room temperature. In the same way, Figure 30 shows % remaining of lycopene in lycopene loaded chitosan alginate nanoparticles after storage for 12 weeks with the condition in refrigerator, dark and visible light at room temperature. As can be seen in Figure 30, lycopene loaded chitosan alginate nanoparticles in refrigerator exhibited greater stability within 12 weeks than storage at room temperature in dark and visible light. Similarly, in Figure 31 shows % remaining of lycopene in ethanol compared after storage for 12 weeks with the condition in refrigerator, dark and visible light at room temperature. It appeared that lycopene in ethanol which stored in the refrigerator showed the highest stability than storage at room temperature in dark and visible light. Consequently, it was considered that lycopene was degraded when exposed to visible light and at room temperature much quicker than that was store in refrigerator.

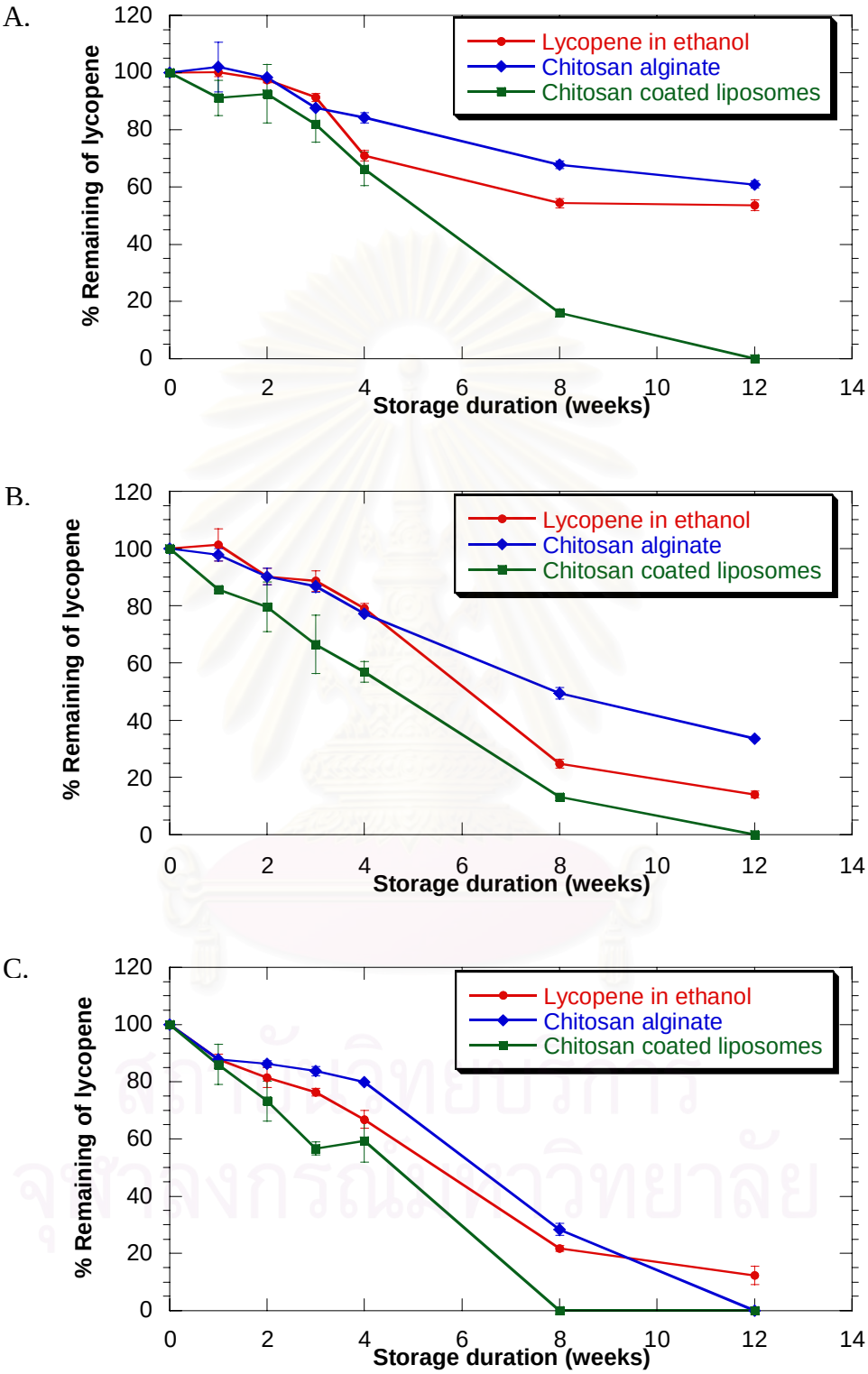

Figure 28 The % remaining of lycopene loaded chitosan coated liposome, lycopene loaded chitosan alginate nanoparticles and lycopene in ethanol after storage for 12 weeks in refrigerator (A), in dark (B) and visible light (C) at room temperature (n=2).

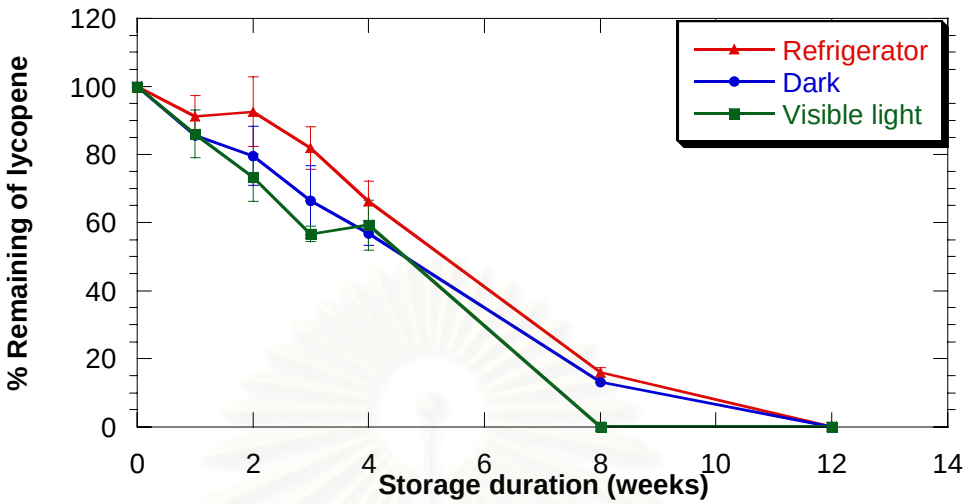

Figure 29 The % remaining of lycopene loaded chitosan coated liposome nanoparticles after storage for 12 weeks in refrigerator, in dark and visible light at room temperature (n=2).

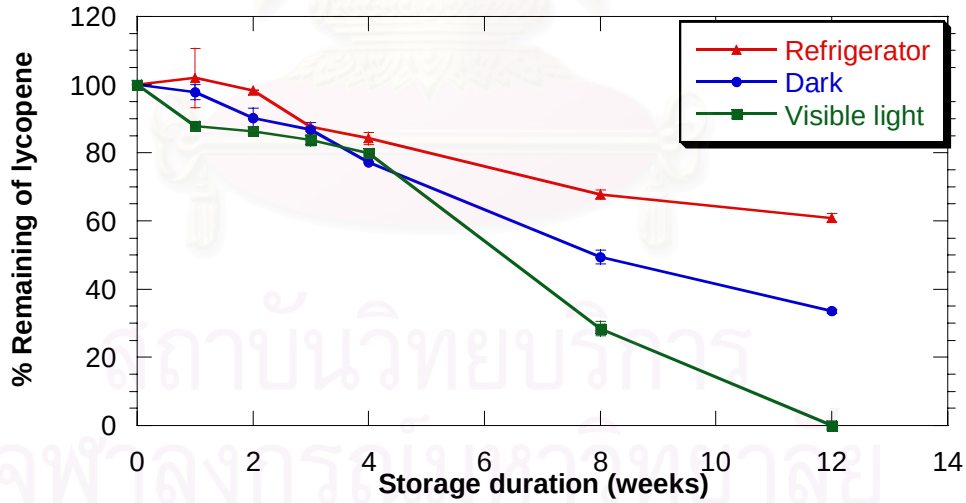

Figure 30 The % remaining of lycopene loaded chitosan alginate nanoparticles after storage for 12 weeks in refrigerator, in dark and visible light at room temperature (n=2).

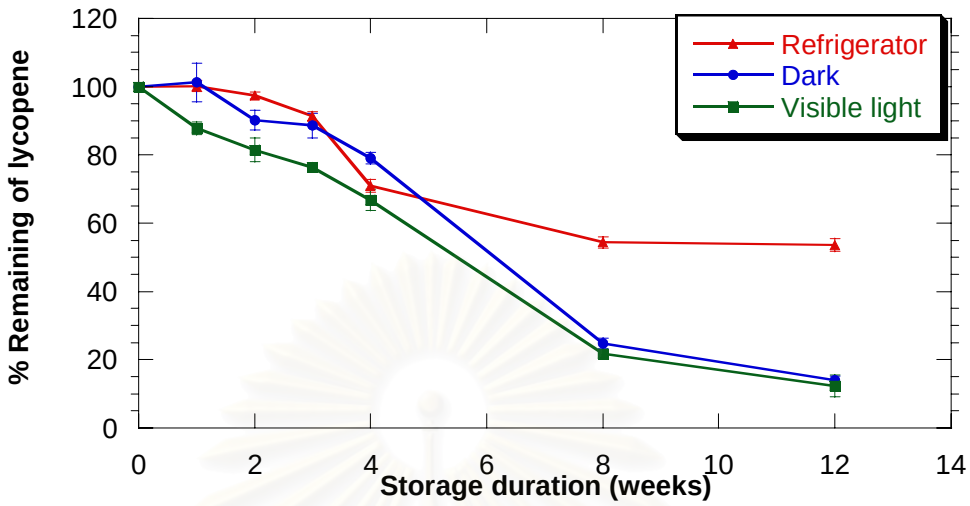

Figure 31 The % remaining of lycopene in ethanol after storage for 12 weeks in refrigerator, in dark and visible light at room temperature (n=2).

It can be concluded that lycopene encapsulated in chitosan alginate nanoparticles is more stable at low temperature. Anyway none of the two samples showed good stability, the amount of undegraded lycopene was very low after storage for 8 and 12 weeks for visible and dark. Such spontaneous disintegration takes place under very mild conditions. This suggests that chitosan alginate nanoparticles behave as a metastable system, and thus, they must be stored lyophilized or fresh nanoparticle suspensions were prepared when required (López-León et al., 2004).

A major disadvantage of liposomes is their chemical instability. One strategy to increase the chemical stability of lycopene in liposomes is the addition of chitosan by forming a stable layer around the vesicles. Referring to stability result it can be noticed that the lycopene incorporated in chitosan coated liposome nanoparticles exhibited very poor chemical stability under storage conditions. The result clearly shows that lycopene loaded chitosan alginate nanoparticles exhibtied greater stability than the lycopene in ethanol and lycopene loaded chitosan liposome nanoparticles under different storage conditions. Within an observation period of 12 weeks, it can be inferred that the temperature has a major influence on the stability of all formulations.

6. *In Vitro* Skin Penetration Experiments

In this study, *in vitro* skin penetration experiments included diffusion experiments and visualization by electron microscopy.

Diffusion experiment provides information about the amount and the rate of drug penetration of the model compound, but do not give any information about the physiological effects of the model drug on cells and lipid organization. The visualization studied using transmission electron microscopy (TEM) provides detailed information about the structure of the cells and lipid organization in the skin, but does not provide information about the penetration pathways (Verma et al., 2003).

Skin is favorite route of drug administration. However, skin has water barrier function which prevents chemicals from penetrating through the skin and entering the body. The stratum corneum is the rate-limiting barrier to percutaneous absorption. In it absence, for example, when skin is denuded by a disease or even after repeated tape stripping; the absorption of drugs into the skin is increased. The stratum corneum is generally composed of dense layers of dead, flattened cells filled with the fibrous protein, keratin, which is produced by the epidermis beneath.

Isolated cutaneous epidermis has many advantages as compared with previously reported reconstructed skin models. It is easier, faster and cheaper to prepare isolated cutaneous epidermis than reconstructed skin models. In addition, isolated cutaneous epidermis is better water barrier function than reconstructed skin models. The separation of epidermis from dermis by enzymes or heat was possible to damage the barrier structure and result in enhanced water penetration through the isolated epidermis. There was minimal damage to water barrier function of the epidermis isolated by the trypsin and culture-heating separating methods. The epidermis was isolated by trypsin and culture-heating methods which can be used as long as one week after separation (Pu and Lin, 1998). Therefore, in this investigation the epidermis isolated by trypsin treatment is an attractive tool to penetration study.

6.1 *In vitro* penetration studies

The experiment was designed for the study of the penetration of two preparations, lycopene loaded chitosan alginate nanoparticles and lycopene loaded chitosan coated liposome nanoparticles using Franz diffusion cell. Lycopene was a lipophilic compound. So it is necessary to add surfactants to increase the solubility of lipophilic compounds in the receptor compartment. Thus, Tween 80 was used to increase the solubility of lycopene in receptor fluid. Under this condition surfactant may have a slight damaging effect on human skin.

The aim of this study was to determine the penetration profile of lycopene loaded nanoparticles through epidermis when it is applied onto the skin. The concentrations of lycopene loaded chitosan coated liposomes and chitosan alginate nanoparticles in donor compartment were 1.67 and 4.48 μg/mL, respectively. The cumulative amount of lycopene in nanoparticles found in receptor compartment was investigated.

The flux at the steady state, J_s (μg/cm^{2}h), was calculated using the linear portion of the correlation between the accumulated quantity of lycopene that diffused through the skin by unit area and time (see in appendix III). The permeability coefficient, K_p (cm/h), of lycopene from the different formulations was obtained from the ratio between the flux of lycopene and its initial concentration in the donor compartment (Contreras et al., 2005). The cumulative amount of lycopene/area (μg/ cm^2), flux and permeability coefficient of lycopene loaded chitosan coated liposome and chitosan alginate nanoparticles are shown in Table 12 and 13, respectively. The flux of lycopene loaded chitosan coated liposome nanoparticles and lycopene loaded chitosan alginate nanoparticles were 0.71$\pm$0.03 and 1.67$\pm$0.07 μg/cm^{2}h, respectively. Lycopene penetration rate is higher at the initial period of the permeation experiments (0-90 min). Afterwards, penetration rates of lycopene nanoparticles were almost constant in all sampling times for both preparations. The penetration profiles of lycopene in chitosan coated liposome and chitosan alginate nanoparticles are shown in Figure 32 and 33, respectively.

Table 12 The cumulative amount of lycopene/area (μg/cm^2), flux and permeability coefficient of lycopene loaded chitosan coated liposome nanoparticles (n=3).

Time (h)	Cumulative amount of lycopene/area (μg /cm^2)			Mean	SD
	n 1	n 2	n 3		
0.5	0.6821	0.7136	0.7285	0.7080	0.02
1	0.7780	0.8384	0.8518	0.8227	0.04
1.5	1.1015	1.1627	1.1822	1.1488	0.04
2	1.1419	1.2314	1.2080	1.1937	0.05
4	1.3156	1.3679	1.3635	1.3490	0.03
6	1.3288	1.4007	1.3900	1.3732	0.04
8	1.3380	1.4260	1.4422	1.4020	0.06
12	1.3651	1.4589	1.4578	1.4273	0.05
J_{ss}	0.6801	0.7226	0.7340	0.7122	0.03
K_p	0.2832	0.3009	0.3056	0.2966	0.01

Table 13 The cumulative amount of lycopene/area (μg/cm^2), flux and permeability coefficient of lycopene loaded chitosan alginate nanoparticles (n=3).

Time (h)	Cumulative amount of lycopene/area (μg /cm^2)			Mean	SD
	n 1	n 2	n 3		
0.5	1.4397	1.4005	1.3843	1.4081	0.03
1	2.0997	1.9637	2.0157	2.0264	0.07
1.5	2.6960	2.5007	2.5295	2.5754	0.10
2	2.9080	2.7882	2.8273	2.8412	0.06
4	3.4039	3.2469	3.1972	3.2827	0.11
6	3.6772	3.4592	3.4560	3.5308	0.13
8	3.6601	3.4930	3.4566	3.5366	0.11
12	3.7040	3.5567	3.5242	3.5950	0.10
J_{ss}	1.7496	1.6131	1.6440	1.6689	0.07
K_p	0.2768	0.2552	0.2601	0.2641	0.01

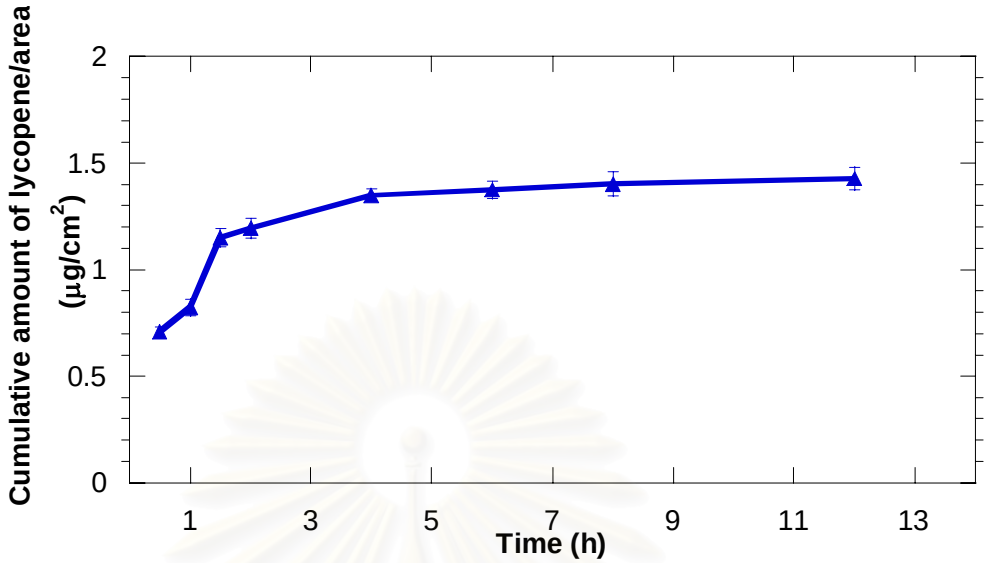

Figure 32 The penetration profile of lycopene in chitosan coated liposome nanoparticles (n=3).

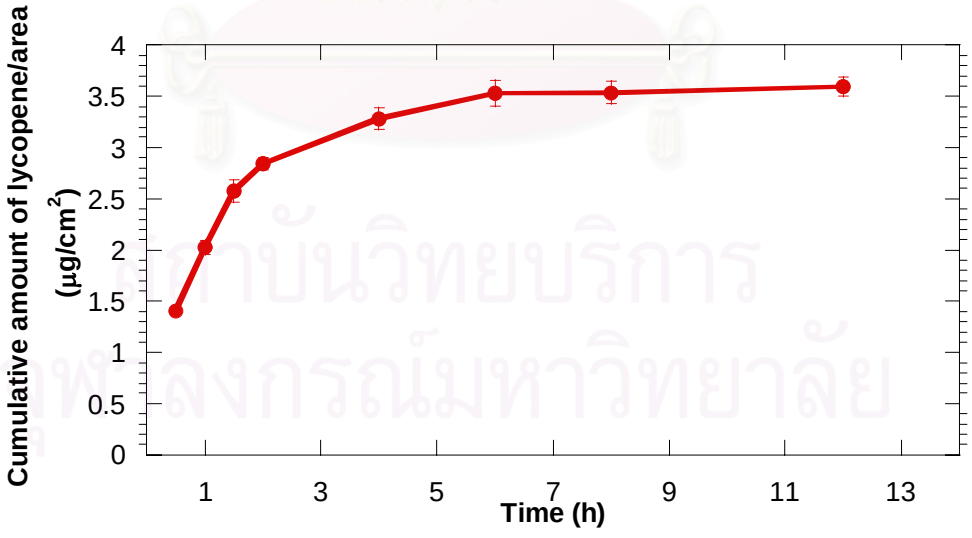

Figure 33 The penetration profile of lycopene in chitosan alginate nanoparticles (n=3).

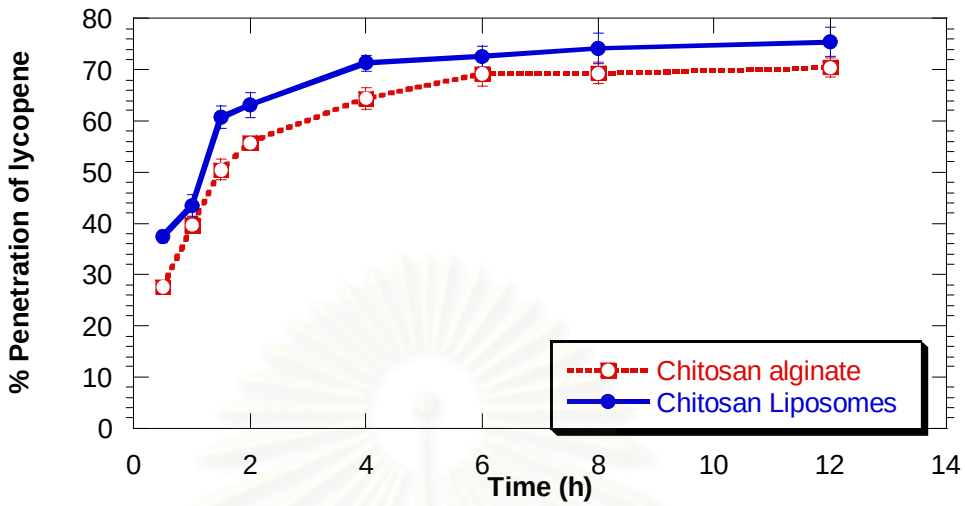

Figure 34 The percentage of penetration of lycopene loaded chitosan coated liposome nanoparticles and lycopene loaded chitosan alginate nanoparticles (n=3).

The cumulative amount of lycopene in receptor medium were compared to the initial dose and expressed as a percentage of penetration of lycopene. The percentage of penetration of lycopene in chitosan coated liposome nanoparticles and chitosan alginate nanoparticles are shown in Figure 34. After the experimental period, the percentage of penetration of lycopene loaded chitosan coated liposomes and lycopene loaded chitosan alginate nanoparticles were 75.46 % and 70.49 %, respectively. The amount of penetrated lycopene from chitosan coated liposome was higher than that from chitosan alginate nanoparticles but not significantly different (Student's t-test, $P>0.05$). The permeability coefficient of lycopene loaded chitosan coated liposome was significantly higher than lycopene loaded chitosan alginate nanoparticles (Student's t-test, $P<0.05$). Consequently, lycopene loaded chitosan coated liposome nanoparticles were more likely to present higher penetration activity through stratum corneum than lycopene loaded chitosan alginate nanoparticles.

Numerous studies reported that the application of liposomes on the skin surface is able to improve permeability for various entrapped drugs through the major barrier (the stratum corneum) (Foco et al., 2005 and Biruss and Valenta, 2005). The penetration enhancing effect of liposomes depends on the liposome size, lipid composition, the lipophilic nature of the drug and on the nature of the skin (Verma et

al., 2003). In general, the small size and amphiphiles characteristic could be important feature which plays a role in its effectiveness penetration across the lipid barrier of skin. The reason of the greater penetration enhancing effect of liposomes may be caused by the interactions between the intercellular lipid in the skin and the liposome bilayer. It is probably due to the composition of the lipid bilayer similar to that of skin lipid thus leading to weaken the highly organized intercellular lipids of stratum corneum in an attempt to more penetration of lycopene transport across the epidermis membrane than chitosan alginate nanoparticles.

6.2 Morphological evaluation of skin after treatment with lycopene loaded nanoparticles

The ultrastructural evaluation under transmission electron microscopy (TEM) allows visualization of the distribution of biodegradable nanoparticles across the human skin. The epidermal layer that could control the absorption is the outermost layer known as stratum corneum. This layer consists of multiple layers of polyhedral cells arranged in a basket-weave pattern. These cells are the most differentiated cells of keratinizing system. They lose their nucleus and cytoplasmic organelles and they are composed almost entirely of high molecular weight birefringent filamentous scleroprotein keratin (Junqueira, 1986). They are the cells that provide a very effective barrier towards penetration; however the impermeability is a considerable problem in the delivery of medicine both to and through the skin (Biruss and Valenta, 2005).

In order to observe the interaction between lycopene loaded nanoparticles and skin, the skin samples underwent 3 h long penetration experiment, then fixed with gluteraldehyde and consecutively fixed with osmium tetroxide (OsO_4). The samples were subsequently subjected to harsh processing of dehydration by ethanol and embedding in resin prior to morphologic evaluation under TEM. Fixation converted soluble cellular contents such as proteins, carbohydrates, nucleic acids and lipids into insoluble networks and rendered preservation of cellular morphology.

The ultrastructural findings at stratum corneum after 3 h-incubation with lycopene loaded chitosan coated liposome nanoparticles are illustrated in Figure 35A-C. In Figure 35A presents the overview of keratinocytes after treatment with irregular widening of intercellular spaces. Figure 35B reveals a spindle structure about 250 nm situated between the keratinocytes. This structure had membrane that surrounded with the electron dense spot. There were few electron dense particles observed inside this structure. Figure 35C, Ellipsoidal shapes which resemble stacked flattened vesicles were observed within bilayers oriented perpendicular to skin lipid bilayers and found some oval shape with membrane bound in the intracellular. However, the intracytoplasmic one was located near cell membrane but not blend with it, while the intercellular one exhibited ability to interact with lipid bilayer of cell membrane. It could be proposed that these characteristics informed the lycopene loaded chitosan coated liposome nanoparticles. The penetration of liposomes throughout epidermal layers was explained previously (Biruss and Valenta, 2005; Contreras et al., 2005; Foco et al., 2005; Song and Kim, 2006). In brief, the encapsulation in liposomes influences the distribution of lipophilic drug throughout the different skin layers and the phospholipid component can mix with the intercellular lipids, thereby causes swelling of intercellular lipids without altering the multilayer structure of stratum corneum. The presence of the lamellar stacks throughout the stratum corneum lead to disorganize the skin lipid bilayers, by pushing them apart, which could created possible penetration pathway. Moreover, the swollen lipids may cause drug accumulation and form intercellular depot (Sinico et al., 2005; Verma et al., 2003).

Berg et al. (1999) postulated three main mechanisms that vesicles interact with stratum corneum: (1) penetration of intact vesicles into the stratum corneum where the vesicles either localize or pass on to the dermis; (2) adsorption or fusion of vesicles on the surface of the skin; and (3) penetration of vesicles constituents into the skin which may affect the ultrastructure and the intercellular regions in the stratum corneum.

A. B.

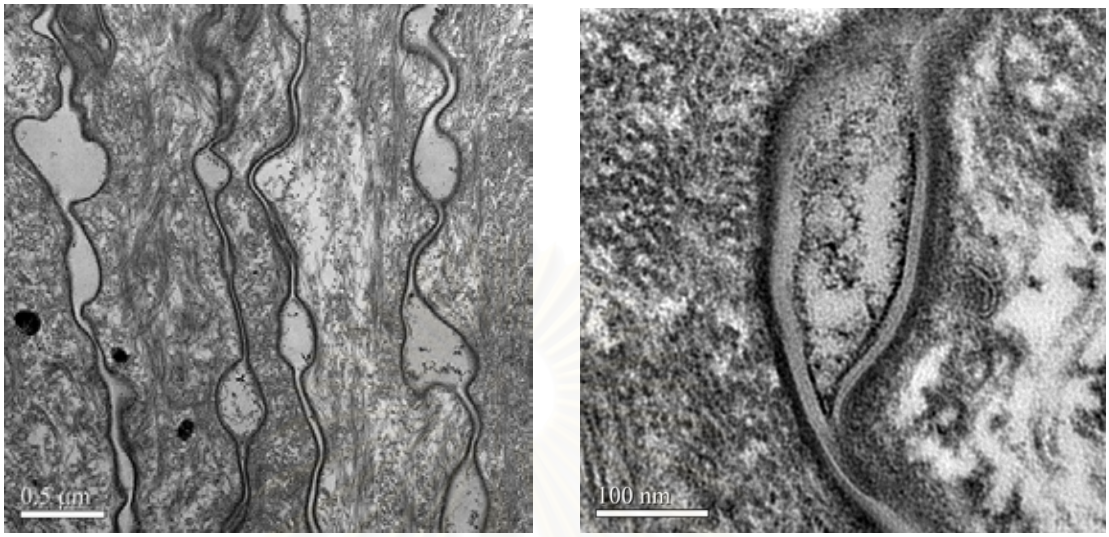

C.

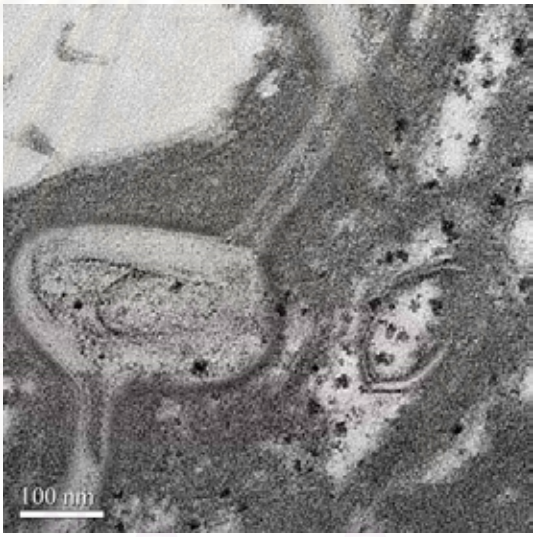

Figure 35 Transmission electron micrographs of keratinocytes at stratum corneum after 3 h of treatment with lycopene loaded chitosan coated liposome nanoparticles.
A: an overview of keratinocyte with irregular widening of intercellular spaces (x 22,000).
B: intercellular spindle membrane bound structure, vesicle, containing a few electron dense particles situated between the keratinocytes (x 150,000).
C: intercellular spaces filled with stacked flattened of lycopene loaded chitosan coated liposome were observed oritented perpendicular to skin lipid bilayers and found an oval shape vesicle in cytoplasm (x 110,000).

A.

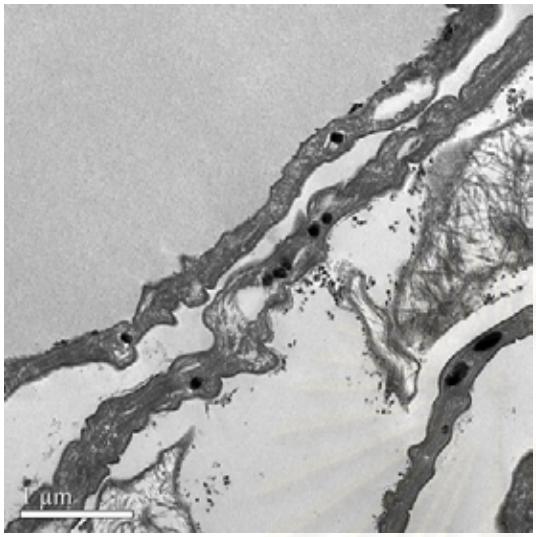

B.

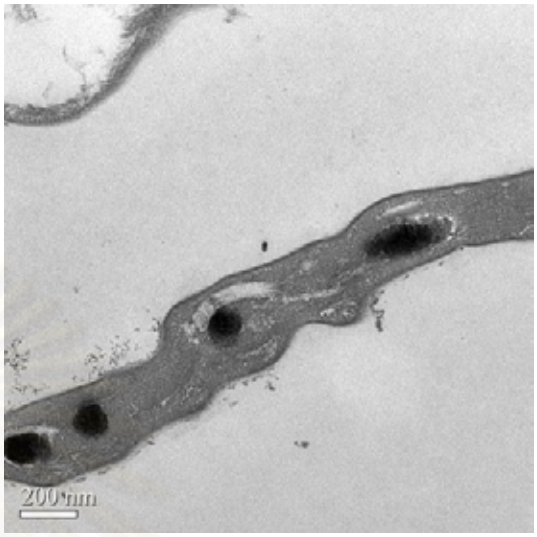

C.

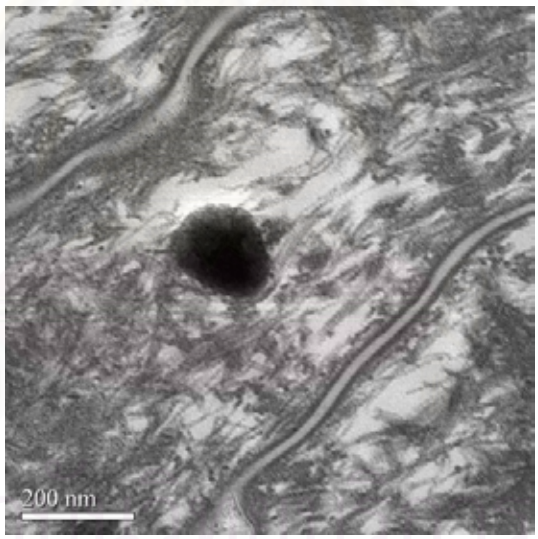

Figure 36 Transmission electron micrographs of keratinocytes at stratum corneum after 3 h of treatment with lycopene loaded chitosan alginate nanoparticle.

A: an overview of stratum corneum with containing electron dense materials of lycopene loaded chitosan alginate nanoparticles deposited in corneocyte (x 15,000). B: the high magnification of the upper part of stratum corneum with a spherical electron dense of lycopene loaded chitosan alginate nanoparticles in the corneocyte (x 35,000). C: the presence of a spherical electron dense of lycopene loaded chitosan alginate nanoparticles in the lower stratum corneum (x 75,000).

TEM analysis has provided a reliable microscopic estimation of the human skin after treatment with lycopene loaded chitosan alginate nanoparticles. As can be seen in Figure 36, a spherical shape of electron dense was found in the stratum corneum and epidermal cell of human skin after treated with lycopene loaded chitosan alginate nanoparticles for 3 h. These particles showed the nanospheres characteristic with size in range of 200 nm. The TEM micrographs in Figure 36 clearly show corneocyte, flattened cells characterized by the absence of cell organelles and the presence of the tightly packed keratin pattern. Figures 36A shows an overview of stratum corneum with containing a spherical electron dense material of lycopene loaded chitosan alginate nanoparticles. Figure 36B shows at high magnification of stratum coeneum containing spherical with a specific molecular of nanospheres and some of the particle was found in the lower part of stratum corneum (Figure 36C). The mechanisms involved in chitosan alginate nanoparticles and skin interaction is not obviously explained. In this study the particles that found in the stratum corneum can be discriminate from the cell and other materials or organelles in cells.

To sum up, the result from in vitro penetration study and ultrastructural observation demonstrated that lycopene loaded chitosan coated liposomes and lycopene loaded chitosan alginate nanoparticles were able to penetrate into epidermis of human skin which lead to appearance of lycopene loaded nanoparticles in the stratum corneum. Both of them could be entering the stratum corneum intactly. Hence, chitosan coated liposome and chitosan alginate nanoparticles can act as drug carriers to deliver encapsulated lycopene into or across the stratum corneum. TEM showed a distinct difference in penetration pathways after treatment of lycopene loaded chitosan coated liposomes and lycopene loaded chitosan alginate nanoparticles. The two mechanisms possible to facilitate the penetration of lycopene were suggested. Lycopene loaded chitosan coated liposome nanoparticles could be able to penetrate through the intercellular between the corneocyte whereas lycopene loaded chitosan alginate nanoparticles might be able to penetrate into the stratum corneum or transcellular route.

The mechanism of intercellular pathway involved interaction of vesicles with intercellular lipids due fundamentally to affinity of the lipid composition. This study suggested that encapsulated lycopene in chitosan coated liposome nanoparticles enter the stratum corneum in channel-like regions, intercellular lipid, and carry thereby lycopene into the skin.

The basic mechanisms of transcellular pathway include passive transport of small molecule and active transport of ionic and polar compound. Passive transport is the movement of a solute along its concentration gradient. As a result of cell membranes are permeable to some small, water soluble molecule. This chitosan alginate nanoparticle might be penetration by passive and active transport. In adddition, chitosan alginate nanoparticles might be making the membrane more fluid and thus more permeable of cell membrane. Thus, result in penetration of encapsulated lycopene via the transcellular pathway.

CHAPTER V

CONCLUSIONS

Lycopene has very low water solubility which makes it problematic to formulate with adequate bioavailability. For this reason, nanotechnology was used to improve the solubility and increase bioavailability in this study. The promising classes of nano-sized carriers that have been considered in drug delivery applications are chitosan coated liposome and chitosan alginate.

In this study lycopene was encapsulated into nanoparticles in order to improve its stability and penetration through the stratum corneum. Two types of nanoparticles were prepared, lycopene loaded chitosan coated liposome nanoparticles and lycopene loaded chitosan alginate nanoparticles. They were characterized for particle size, morphology and encapsulation efficiency. The mean particle sizes of lycopene loaded chitosan coated liposome nanoparticles and lycopene loaded chitosan alginate nanopatricles, when varing lycopene loading concentration, were in range of 320-463 and 323-500 nm, respectively. From TEM micrographs, lycopene loaded chitosan coated liposome showed a spherical or ellipsoidal shape with presence of unilamellar and multilamellar vesicles. According to the lipophilic property of lycopene, it would be encapsulated in the lipid bilayers of liposomes. In case of lycopene loaded chitosan alginate nanoparticles, TEM micrograph showed a relatively homogeneous population with spherical shape and with a highly porous structure. It indicated that lycopene may be encapsulated in the nanospheres as a droplet of nanosphere surrounded by chitosan. Therefore, the percentage of encapsulation efficiency of lycopene loaded chitosan alginate nanoparticles was higher than that of lycopene loaded chitosan coated liposomes. The initial concentration of lycopene influenced the percentage of encapsulation efficiency of lycopene loaded chitosan coated liposome and lycopene loaded chitosan alginate nanoparticles. The increase in loading lycopene

concentration, increase in the percentage of encapsulation efficiency of lycopene loaded chitosan alginate nanoparticles. On the other hand, lycopene loaded chitosan coated liposome nanoparticles showed the optimum encapsulation efficiency at the initial lycopene concentration of 200 µg/mL of core to wall ratio of 1:150 by weight. The percentage of recovery of lycopene loaded chitosan coated liposome nanoparticles and lycopene loaded chitosan alginate nanoparticles were about 10-56% and 47-73%, respectively.

In term of stability, the membrane disruption of lycopene loaded chitosan alginate nanoparticles occurred after storage for 12 weeks in refrigerator. Some nanoparticles ruptured into small fragment of polymer or erosion of membrane after storage for 12 weeks in dark and visible light at room temperature. As a result, the percentage of remaining of lycopene in chitosan alginate nanoparticles showed the highest when storage in refrigerator. In the same way, the outer layer of chitosan coated liposome nanoparticles appeared as porous vesicles and might induce the lycopene leakage from nanoparticles. This feature correlated with no lycopene was detected after storage of the lycopene loaded chitosan coated liposomes nanoparticles for 12 weeks in all conditions. To sum up, lycopene loaded chitosan alginate nanoparticles storaged in refrigerator exhibited greater stability than lycopene in ethanol and lycopene loaded chitosan coated liposome nanoparticles. The stability of lycopene in nanoparticles is much more influenced by storage temperature than by light.

In vitro penetration of lycopene nanoparticles were performed on human epidermis membrane using Franz diffusion cells. Chitosan coated liposome nanoparticles exhibited the higher penetration of lycopene through epidermis membrane than that from chitosan alginate nanoparticles. The percentage of penetration of lycopene loaded chitosan coated liposome and lycopene loaded chitosan alginate nanoparticles were 75.46% and 70.49%, respectively. The lycopene nanoparticles which penetrated through the epidermis were demonstrated using TEM. In conclusion, lycopene loaded nanoparticles prepared by chitosan alginate nanoparticles and chitosan coated liposome nanoparticles could pass through the

human stratum corneum. TEM images of the epidermis suggested different pathways of penetration. It seems that lycopene loaded chitosan coated liposome nanoparticles might be able to penetrate through the intercellular space between the corneocyte, while lycopene loaded chitosan alginate nanoparticles might be able to penetrate into the stratum corneum or transcellular route. Liposomes seem to be useful carrier to topical delivery of lycopene.

The lack of very pure commercial lycopene product and its high cost, the sensitivity of lycopene to sunlight, atmospheric air and temperature, caused several problems in the preparation, storage and handling of lycopene solutions. However, lycopene loaded chitosan alginate nanoparticles have shown adequate percentage of encapsulation efficiency, good storage stability in refrigerator. In further study, the chitosan alginate nanoparticles might be stabilized by optimizing the binding conditions either by prolonging the exposure time to chitosan. Moreover, lyophilization may be used to overcome the stability during storage and keep at low temperature with protection from light and heat.

REFERENCES

Agnihotri, S. A., Mallikarjuna, N. N., and Aminabhavi, T. M. 2004. Recent advances on chitosan-based micro- and nanoparticles in drug delivery. Journal of Controlled Release 100: 5-28.

Anal, A. K., and Stevens, W. F. 2005. Chitosan-alginate multilayer beads for controlled release of ampicillin. International Journal of Pharmaceutics 290: 45-54.

Andreassi, M., Stanghellini, E., Ettorre, A., Stefano, A. D., and Andreassi, L. 2004. Antioxidant activity of topically applied lycopene. European Academy of Dermatology and Venereology 18: 52-55.

Balachandran, B., and Rao, A. V. 2003. Time-dependent uptake and antiperoxidative potential of lycopene in multilamellar liposomes. Food Research International 36: 611-616.

Barbaroux, O. Production, properties, and uses of alginate, carrageenan and agar [Online]. Available from: www.fao.org/docrep/field/003/AB728E/AB728E09.htm[2006, April 10]

Beniha, S. 1996. Microencapsulation: method and industrial application. New York: Marcel Dekker.

Bergstrand, N. 2003. Liposomes for drug delivery: from Physico-chemical studies to application. Comprehensive Summaries of Uppsala Dissertation from the Faculty of Science and Technology. Acta Universitatis Upsaliensis.

Bhatia, K. S., and Singh, J. 1999. Effect of linolelic acid/ethanol or limonene/ethanol and iontophoresis on the in vitro percutaneous absorption of LHRH and ultrstructure of human epidermis. International Journal of Pharmaceutics 180 (2): 235-250.

Biruss, B., and Valenta, C. 2005. Skin permeation different steroid hormones from polymeric coated liposomal formulations. European Journal of Pharmaceutics and Biopharmaceutics: In press.

Blum, A., Monir, M., Wirsansky, I., and Ben-Arzi, S. 2005. The beneficial effects of tomatoes. European Journal of Internal Medicine 16: 402-404.

Brain, K. R., Walters, K. A., and Watkinson, A. C. 1998. Investigation of skin permeation in vitro. In M. S. Robert, K. A. Walters (eds.), Dermal absorption & toxicity assessment, Drug & the pharmaceutical science, pp.161-178. New York: Marcel Dekker.

Bramley, P. M. 2000. Is lycopene beneficial to human health ?. Phytochemistry 54: 233-236.

Brisaert, M., Gabriels, M., Matthijs, V., and Plaizier-Vercammen, J. 2001. Liposome with tretinoin: a physical and chemical evaluation. Journal of Pharmaceutical and Biomedical Analysis 26 (5-6): 909-917.

Bronaugh, R. L., Hood, H. L., Krealing, M. E. K., and Yourick, J. 1999. Determination of Percutaneous Absorbtion by In Vitro Techniques. In R. L. Bronaugh, and H. I. Maibach (eds.), Percutaneous Absorption: Drug-Cosmetics-Mechanism-Methodology, Drug and pharmaceutical sciences, pp.229-233. New York: Marcel Dekker.

Carpenter, K. L. 2004. A novel skin imaging technique and the transdermal delivery of melanin. Master's thesis. Department of Chemical Engineering. The Florida State University.

Cevc, G. 2004. Lipid vesicles and other colloids as drug carriers on the skin. Advance Drug Delivery Reviews 56: 675-711.

Chen, H., Chang, X., Du, D., Liu, W., Liu, J., Weng, T., Yang, Y., Xu, H., and Yang, X. 2006. Podophylotoxin-loaded solid lipid nanoparticles for epidermal targeting. Journal of Controlled Release 110: 296-306.

Contresas, M. J., Soriano, M. M. J., and Dieguez, A. R. 2005. In vitro percutaneous absorbtion of all-trans retionic acid applied in free form or encapsulated in stratum corneoum lipid liposomes. International Journal of Pharmaceutics 297: 134-145.

Das, S., Otani, H., Maulik, N., and Das, D. K. 2005. Lycopene, tomatoes, and coronary heart disease. Free Radical Research 39 (4): 499-55.

de Berker, D. (n.d.). Preview of understanding eczema [Online]. Family doctor books: British Medical Association. Available from: www.familydoctor.co.uk/.../ eczema_specimen.html[2006, April 10]

De, S., and Robinson, D. 2003. Polymer relationships during preparation of chitosan-alginate and poly-l-lysine-alginate nanospheres. Journal of Controlled Release 89: 101-112.

Douglas, K. L., and Tabrizian, M. 2005. Effect of experimental parameters on the formation of alginate-chitosan nanoparticles and evaluation of their potential application as DNA carrier. Journal of Biomaterials. Science. Polymer Edition16 (1): 43-56.

Eichler, O., Sies, H., and Stahl, W. 2002. Divergent optimum levels of lycopene, beta-carotene and lutein protecting against UVB irradiation in human fibroblasts. Photochemistry and Photobiology 75 (5): 503-506.

Fawcett, D. W. (1994). A textbook of histology. 12 th ed. New York: Chapman & Hall.

Fazekas, Z., Gao, D., Saladi, R. N., Lu, Y., Lebwohl, M., and Wei, H. 2003. Protective Effects of lycopene against ultraviolet B-induced photodamage. Nutrition and Cancer 47 (2): 181-187.

Fish, W. W., Perkins-Veazie, P., and Collins, J. K. 2002. A Quantitative Assay for Lycopene That Utilizes Reduced Volumes of Organic Solvents. Journal of Food Composition and Analysis 15: 309-317.

Foĉo, A., Gasperlin, M., and Kristl, J. 2005. Investigation of liposomes as carriers of sodium ascorbyl phosphate of cutaneous photoprotection. International Journal of Pharmaceutics 291: 21-29.

Gåserød, O., Sannes, A., and Skjåk-Bræk, G. 1999. Microcapsules of alginate-chitosan. II. A study of capsule stability and permeability. Biomaterials 20: 773-783.

Goddard, E. D., and Gruber, J. V. 1999. Principles of polymer science and technology in cosmetics and personal care. vol. 22. Cosmetic science and technology series. New York: Mercel Dekker.

Grit, M., and Crommelin, D. J. A. 1993. Chemical stability of liposomes: implication for their physical stability. Chemistry and Physics of Lipids 64: 3-18.

Hans, M. L., and Lowman, A. M. 2002. Biodegradable nanoparticles for drug delivery and targeting. Current Opinion in Solid State and Materials Science 6: 319-327.

Hart, D. J., and Scott, K. J. 1995. Development and evaluation of and HPLC method for the analysis of carotenoids in food, and the measurement of the carotenoid content of vegetables and fruit commonly consumed in the UK. Food Chemistry 54: 101-111.

Heber, D., and Lu, Q. Y. 2002. Overview of mechanism of action of lycopene. Experiment Biology and Medicine 227: 920-923.

Henriksen, I., Smistad, G., and Karlsen, J. 1994. Interactions between liposomes and chitosan. International Journal of Pharmaceutics 101: 227-236.

Hernandez-caselles, T., Villalain, J., and Gomez-fernandez, J. C. 1990. Stability of liposomes on long term Storage. Journal of Pharmaceutical Pharmacology 42: 397-400.

Junqueira, L. C., Carneiro, J., and Long, J. A. 1986. Basic histology. 5 th ed. California: Lange Medical Publications.

Kjøniksen, A. L. 2006. Publications on Alginate [Online]. Polymer Research Group: Department of Chemistry University of Oslo Norway. Available from: www.kjemi.uio.no/.../Research/Alginate.htm[2006, April 10]

Klein, E. A. 2005. Chemoprevention of prostate cancer. Critical Reviews in Oncology/Hematology 54: 1-10.

Konings, E. J. M., and Roomans, H. H. S. 1997. Evaluation and validation of and LC method for the analysis of carotenoids in vegetables and fruit. Food Chemistry 59: 599-603.

Lambert, G. 2002. Oligonucleotide and Nanoparticles Page [Online]. Available from: http://ajetudes.club.fr/nano/index.html[2006, April 10]

Lasic, D. D. 1997. Liposomes in Gene Delivery. New York: CRC Press LLC.

Liu, C., Lian, F., Smith, D. E., Russell, R. M., and Wang, X. D. 2003. Lycopene supplementation inhibits lung squamous metaplasia and induces apoptosis via up-regulating insulin-like growth factor-binding protein 3 in cigarette smoke-exposed ferrets. Cancer Rerearch 63: 3138–3144.

López-León, T., Carvalho, E. L. S., Seijo, B., Ortega-Vinuesa, J. L., and Bastos-González, D. 2004. Physicochemical characterization of chitosan nanoparticles: electrokinetic and stability behavior. Journal of Colloidal and Interface Science 283: 344-351.

Loukas, Y. L., Jayasekera, P., and Gregoriadis G. 1995. Novel liposome-based multicomponent systems for the protection of photolabile agents. International Journal of Pharmaceutics 117: 85-94.

Martins, O., Sebben, M., Raffin, A., Pohlmann, R., and da Silveira, N. P. 2005. Production of soybean phosphatidylcholine-chitosan nanovasicles by reverse phase evaporation: a step by step study. Chemistry and Physics of Lipids 138: 29-37.

Moghimi, H. R., Barry, B. W., and Williams, A. C. 1999. Stratum corneum and barrier performance : A model lamellar structure approach. In R. L. Bronaugh, and H. I. Maibach (eds.), Percutaneous Absorption: Drug-Cosmetics-Mechanism-Methodology, Drug and the pharmaceutical sciences, pp.515-545. New York: Marcel Dekker.

Müller-Goymann, C. C. 2004. Physicochemical characterization of colloidal drug delivery systems such as reverse micelles, vesicles, liquid crystal and nanoparticles for topical administration. European Journal of Pharmaceutics and Biopharmaceutics 58: 343-356.

Murley, G. 2003. Skin structure and function [Online]. Department of Podiatry: La Trobe University. Available from: www.latrobe.edu.au/podiatry/skin-structure.htm[2006, April 10]

NEW, R. R. C. 1997. Liposomes a practical approach. New York: Oxford University Press.

Nijhawan, K., and Holt, P. L. 1999. Introduction Chemistry II Laboratory: Isolation of lycopene and β-carotene. Department of Chemistry and Physics Bellarmine University.

Offord, E. A., Gautier, J. C., Avanti, O., Scaletta, C., Runge, F., Krämer, K., and Applegate, L. A. 2002. Photoprotective potential of lycopene, β-carotene, vitamin E, vitamin C and carnosic acid in UVA-irradiated human skin fibroblasts. Free Radical Biology and Medicine 32: 1293-1303.

Olives Barba, A. I., Hurtado, M. C., Mata, M. C. S., Ruiz, V. F., and de Tejada, M. L. S. 2006. Application of a UV-vis detection-HPLC method for a rapid determination of lycopene and b-carotene in vegetables. Food Chemistry 95 (2): 328-336.

Omoni, A. O., and Aluko, R. E. 2005. The anti-carcinogenic and anti-atherogenic effects of lycopene: a review. Trends in Food Science and Technology 16: 344-350.

Pinell, S. R., Durham, M. D., and Carolina, N. 2003. Cutaneous Photodamage, oxidative stress, and topical antioxidant protection. Journal of the American Academy of Dermatology 48 (1): 1-11.

Plessis, J. D., Ramachandran, C., Weiner, N., and Muller, D. G. 1996. The influence of lipid composition and lamellarity of liposomes on the physical stability of liposomes upon storage. International Journal of Pharmaceutics 127: 273-278.

Polk, A., Amsden, B., Yao, K. D., Peng, T., and Goosen, M. F. A. 1994. Controlled release of albumin from chitosan-Alginate Microcapsules. Journal of Pharmaceutical Sciences 83 (2): 178-185.

Pu, Y., and Lin, P. 1998. Water permeation barrier in isolated cutaneous newborn rat epidermis. Journal of Pharmacological and Toxicological Methods 40: 145-149.

Rajaonarivony, M., Vauthier, C., Couarraze, G., Puisieux, F., and Couvreur, P. 1993. Development of a new drug carrier made from alginate. Journal of Pharmaceutical Sciences 82 (9): 912-917.

Ranade, V. V., and Hollinger, M. A. 2003. Drug delivery systems. 2 nd ed. New York: CRC Press LLC.

Ribaya-Mercado, J. D., Garmyn, M., Gilchrest, B. A., and Russell, R. M. 1995. Skin lycopene is destroyed preferentially over β-carotene during ultraviolet irradiation in humans. Journal of Nutrition 125: 1854-9.

Ribeiro, A. J., Neufeld, R. J., Arnaud, P., and Chaumeil, J. C. 1999. Microencapsulation of lipophilic drugs in chitosan-coated alginate microspheres. International Journal of Pharmaceutics 187: 115-123.

SCCNFP/0750/03. Basic criteria for the in vitro assessment of dermal absorption of cosmetic ingradients. The Scientific Committee on Cosmetic Products and Non-Food Products Intended for Consumers (2003): 1-9.

Scott, K. J., Finglas, P. M., Seale, R., Hart, D. J., and Froidmont-Gortz, I. D. F. 1996. Interlaboratory studies of HPLC procedures for the analysis of carotenoids in foods. Food Chemistry 57: 85-90.

Sesso, H. D., Buring, J. E., Norkus, E. P., and Gaziano, J. M. 2004. Plasma lycopene, other carotenoids, and retinol and the risk of cardiovascular disease in women. American Journal of Clinical Nutrition 79 (1): 47-53.

Sesso, H. D., Buring, J. E., Zhang, S. M., Norkus, E. P., and Gaziano, J. M. 2005. Dietary and plasma lycopene and the risk of breast cancer. Cancer Epidemiology Biomarkers and Prevention 14 (5): 1074-81.

Shai, A., Maibach, H., and Baran, R. 2001. Handbook of cosmetic skin care. Martin Dunitz.

Sharma, S. K., and Maguer, M. L. 1996. Kinetic of lycopene degradation in tomato pulp solids under different processing and storage conditions. Food Research International 29: 309-315.

Shi, J. Maguer, M. L., Kakuda, Y., Liptay, A., and Niekamp, F. 1999. Lycopene degradation and isomerization in tomato dehydration. Food Research International 32: 15-21.

Shu, B., Yu, W., Zhao, Y., and Liu, X. 2005. Study on microencapsulation of lycopene by spray-drying. Journal of Food Engineering: In press.

Singh, A. K., and Das, J. 1998. Liposomes encapsulated vitamin A compounds exhibit greater stability and diminish toxicity. Biophysical Chemistry 73: 155-162.

Sinico, C., Manconi, M., Peppi, M., Lai, F., Valenti, D., and Fadda, A. M. 2005. Liposomes as carriers for dermal delivery of tretinoin: in vitro evaluation of drug permeation and vesicle-skin interaction. Journal Controlled Release 103: 123-136.

Snyder, L. R., Kirkland, J. J., and Glajch, J. L. 1997. Practical HPLC Method development. 2 nd ed. New York: John Wiley & Sons.

Socaciu, C., Bojarski, P., Aberle, L., and Diehl, H. A. 2002. Different ways to insert carotenoids into liposomes affect structure and dynamics of the bilayer differently. Biophysical Chemistry 99: 1-15.

Song, Y. K., and Kim, C. H. 2006. Topical delivery of low-molecular-weight heparin with surface-charged flexible liposomes. Biomaterials 27: 271-280.

Stacewicz-Sapuntzakis, M., and Bowen, P. E. 2005. Role of lycopene and tomato products in prostate health. Biochimica et Biophysica Acta 1710 (2): 101-107.

Stahl, W., and Sies, H. 2004. Bioactivity and protective effects of natural carotenoids. Biochimica et Biophysica Acta 1710 (2): 101-107.

Stahl, W., Heinrich, U., Skeila, W., Eichler, O., Sies, H., and Tronnier, H. 2001. Dietary tomato paste protects against ultraviolet light-induced erythema in humans. Journal of Nutrition 131: 1449-1451.

Swarbrick, J., and Boylan J. C. (1994). Microsphere technology and applications to nuclear magnetic resonance in pharmaceutical technology. vol. 1. Encyclopedia of pharmaceutical technology. New York: Marcel Dekker.

Tan, C. P., and Nakajima, M. 2004. β-Carotene nanodispersions: preparation, characterization and stability evaluation. Food Chemistry.

Taungbodhitham, A. K., Jones, G. P., Wahlqvist, M. L., and Briggs, D. R. 1998. Evaluation of extraction method for the analysis of carotenoids in fruit and vegetables. Food Chemistry 63 (4): 577-584.

Toor, R. K., and Savage, G. P. 2005. Antioxidant activity in different fractions of tomatoes. Food Research International 38: 487-494.

Tzouganaki, Z. D., Atta-Politou, J., and Koupparis, M. A. 2002. Development and validation of liquid chromatographic method for the determination of lycopene in plasma. Analytica Chimica Acta 467: 115-123.

United States Pharmacopeia Convention. The United States Pharmacopeia 27: The National Formulary NF 22. 2004. Asian edition. Canada: Webcom.

van den Bergh, B. A. I., Vroom, J., Gerritsen, H., Junginger, H. E., and Bouwstra, J. A. 1999. Interactions of elastic and rigid vesicles with human skin in vitro: electron microscopy and two-photon excitation microscopy. Biochimica et Biophysica Acta 1461: 155-173.

Venter, J. P., Muller, D. G., Plessis, J. D., and Goosen, C. 2001. A comparative study of an in situ adapted diffusion cell and an in vitro Franz diffusion cell method for trans dermal absorption of doxylamine. European Journal of Phamaceutical Sciences 13: 169-177.

Verma, D. D., Verma, S., Blume, G., and fahr, A. 2003. Particle size of liposomes influences dermal delivery of substances into skin. International Journal of Pharmaceutics 258: 141-151.

Visioli, F., Riso, P., Grande, S., Galli, C., and Porrini, M. 2003. Protective activity of tomato products on in vivo markers of lipid oxidation. European Journal of Nutrition 42 (4): 201-6.

Wertz, K., Siler, U., and Goralczyk, R. 2004. Lycopene: modes of action to promote prostate health. Archives of Biochemistry and Biophysics 430: 127-134.

Willcox, J. K., Catignani, G. L., and Lazarus, S. 2003. Tomatoes and cardiovascular health. Critical Reviews in Food Science and Nutrition 43 (1): 1-18.

Wilson, C. G., and Washington, N. 1989. Physiological pharmaceutics: biological barriers to drug absorption. Chichester: Ellis Horwood Limited.

Wilt, A. 2005. Equipment that measures permeation through membranes: Franz cells [Online]. PermeGear. Available from: www.permegear.com/ flange.htm[2006, April 10]

Wu, Z. H., Ping, Q. N., Wei, Y., and Lai, J. M. 2004. Hypoglycemic efficacy of chitosan-coated insulin liposomes after oral administration in mice. Acta Pharmacologica Sinica 25 (7): 966-972.

Wu, Y., Yang, W., Wang, C., Hu, J., and Fu, S. 2005. Chitosan nanoparticles as a novel delivery system for ammonium glycyrrhizinate. International Journal of Pharmaceutics 295: 235-245.

Xu, Y., and Du, Y. 2003. Effect of molecular structure of chitosan on protein delivery properties of chitosan nanoparticles. International Journal of Pharmaceutics 250: 215-226.

Zang, L. Y., Sommerburg, O., and van Kuijk, F. J. G. M. 1997. Absorbance Changes of Carotenoids in Different Solvents. Free Radical Biology & Medicine 23 (7): 1086-1089.

Zang, L. 2005. Liposome [Online]. Available from: blog.case.edu/linda.zhang/2005/09/03/lopisomes [2006, April 10]

APPENDICES

APPENDIX I

The data of lycopene and encapsulation efficiency study

Lycopene (Redivivo™ 10% FS) Data

Description

Lycopene (Redivivo™ 10% FS) is a dark red, viscous oil, containing micronized crystals of lycopene dispersed in corn oil. dl-α-Tocopherol is added as an antioxidant.

Product identification

Chemical name: ψ,ψ-carotene; 2, 6, 10, 14, 19, 23, 27, 31-octamethyl-2, 6, 8, 10, 12, 14, 16, 18, 20, 22, 24, 26, 30-dotriacontridecane

Empirical formula: $C_{40}H_{56}$

Molecular mass: 536.88 g/mol

Specification

Appearance: dark red, viscous oil

Light absorption (in n-hexane): Maximum absorption at 468-472 nm

Lycopene content: min. 10%

Solubility: slightly soluble in oils and fats

Table I-1 Compositions of lycopene (Redivivo™ 10% FS) used in the formulation**.**

Compositions	**1 g contains**
Lycopene	100 mg
DL-alpha-Tocopherol	15 mg
Corn oil	885 mg

Lycopene from tomato (Sigma®) Data

Empirical formula: $C_{40}H_{56}$

Molecular mass: 536.87 g/mol

Appearance: Brown powder with a red cast

Solubility: Clear red-orange solution at 1 mg/mL in chloroform

Table I-2 The exact concentration and % purity of the standard solution.

Theoretical Concentration (µg/ml)	Absorbance	Exact concentration	% Purity
3.2	1.116	3.23	100.93
3.2	1.116	3.23	100.93
3.2	1.116	3.23	100.93

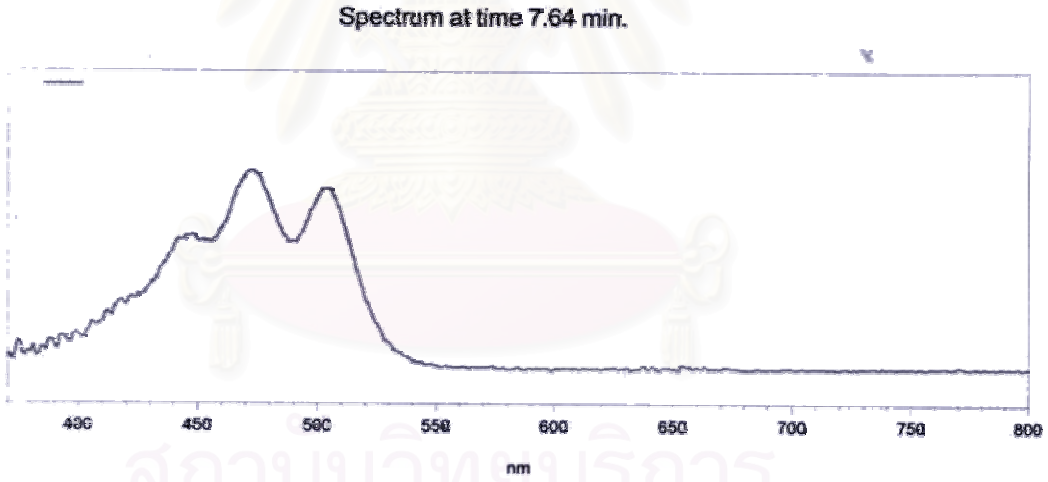

Figure I-1 The spectrum of lycopene determined using HPLC at retention time, 7.64 min.

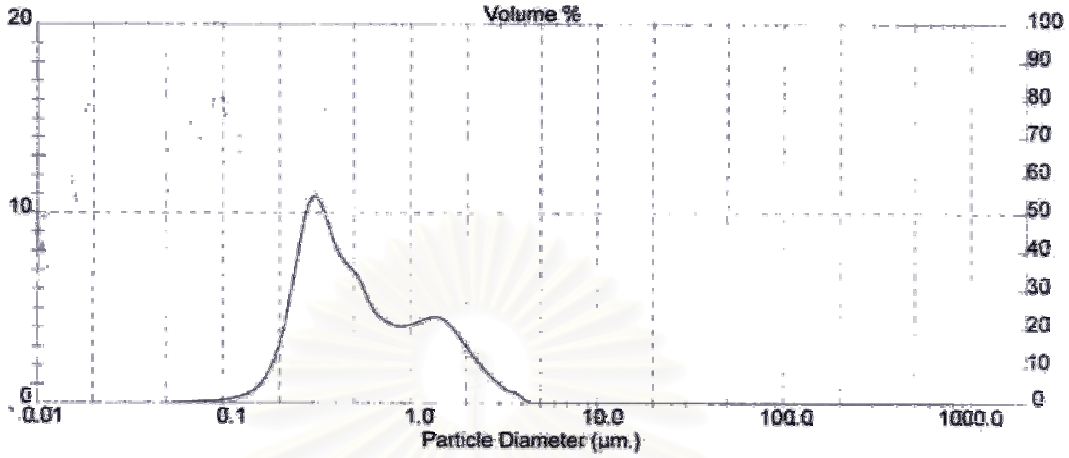

Figure I-2 The mean particle size and particle size distribution of chitosan coated liposome nanoparticles of lycopene initial concentration 45.75 µg/mL.

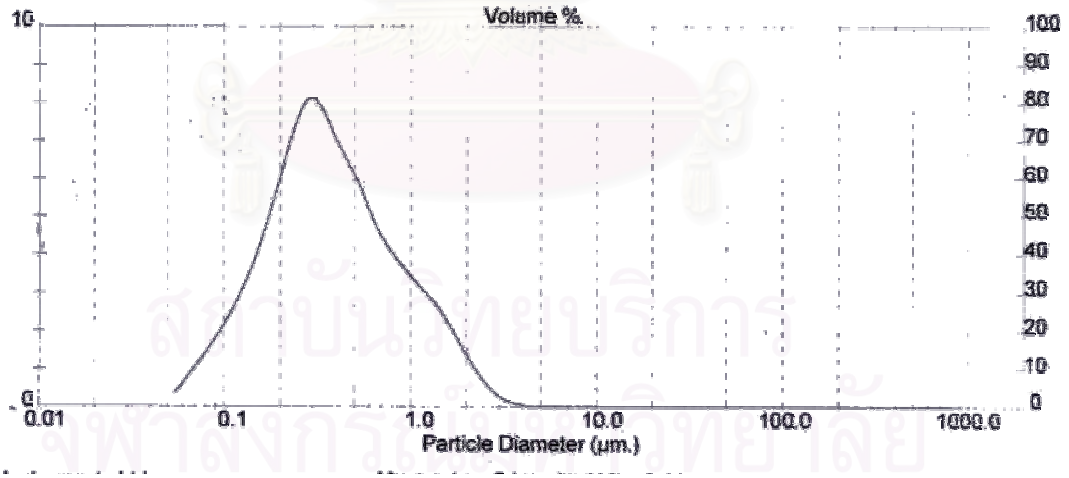

Figure I-3 The mean particle size and particle size distribution of chitosan coated liposome nanoparticles of lycopene initial concentration 88.98 µg/mL.

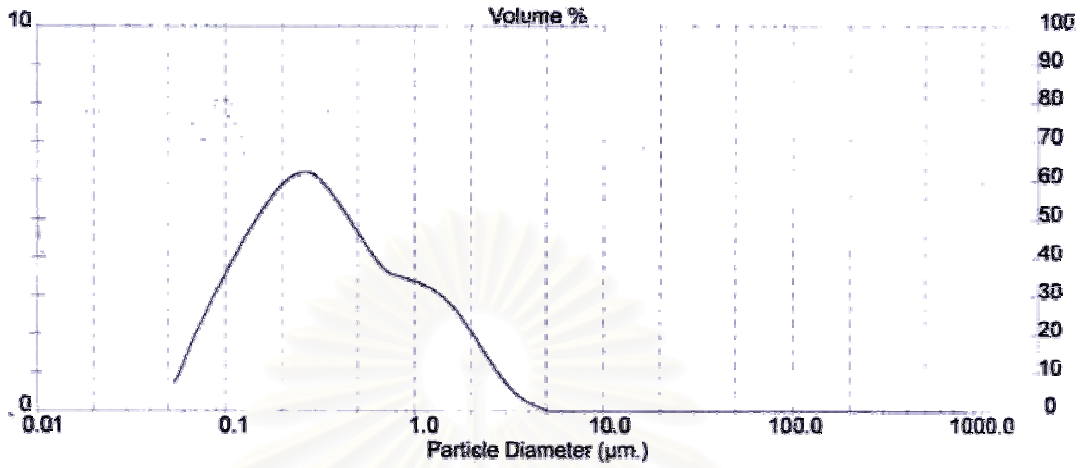

Figure I-4 The mean particle size and particle size distribution of chitosan coated liposome nanoparticles of lycopene initial concentration 140.56 µg/mL.

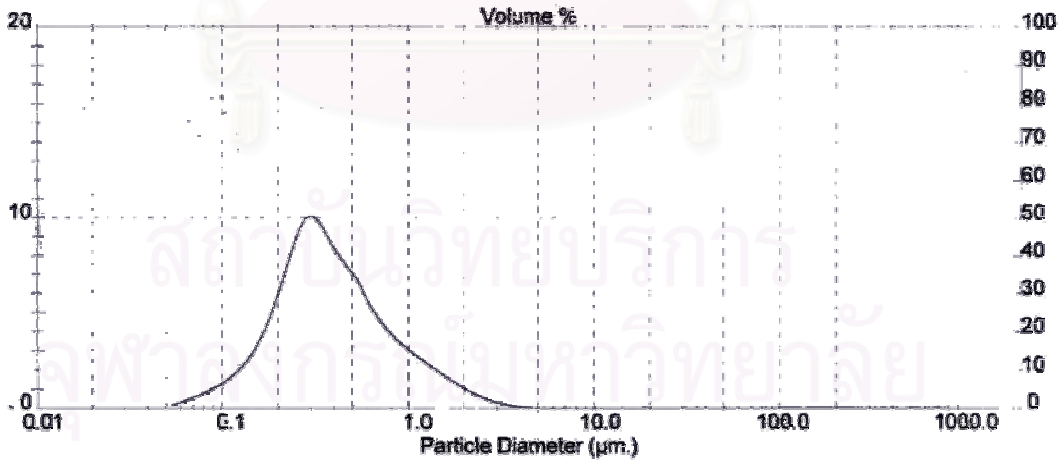

Figure I-5 The mean particle size and particle size distribution of chitosan coated liposome nanoparticles of lycopene initial concentration 200.28 µg/mL.

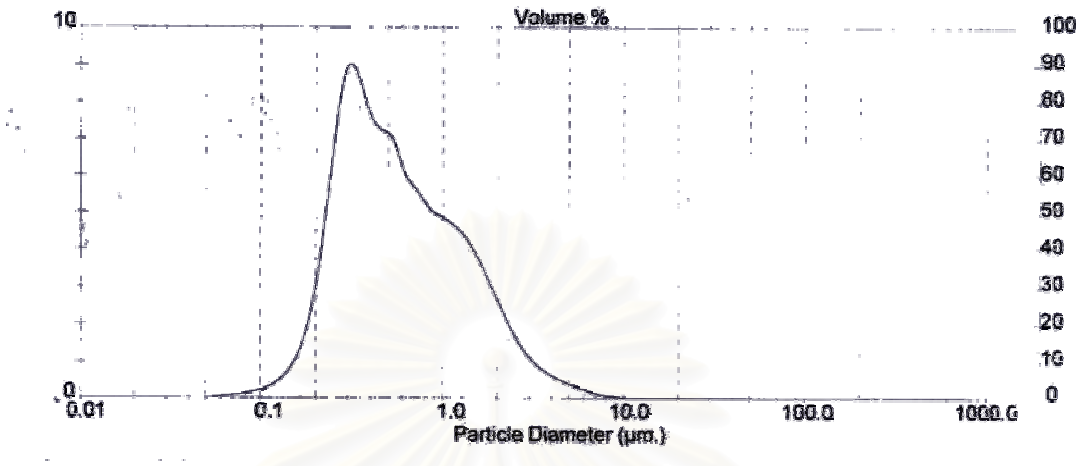

Figure I-6 The mean particle size and particle size distribution of chitosan coated liposome nanoparticles of lycopene initial concentration 234.16 µg/mL.

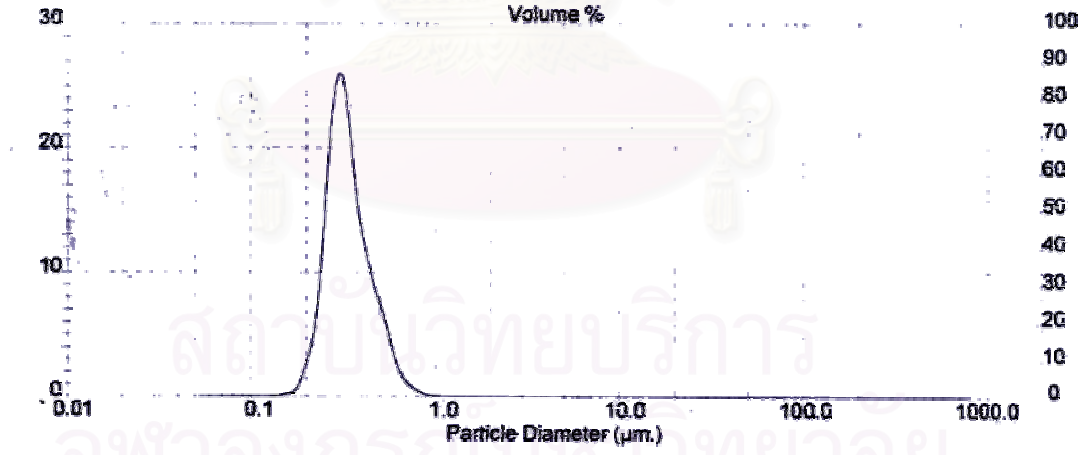

Figure I-7 The mean particle size and particle size distribution of chitosan alginate nanoparticles of lycopene initial concentration 45.75 µg/mL.

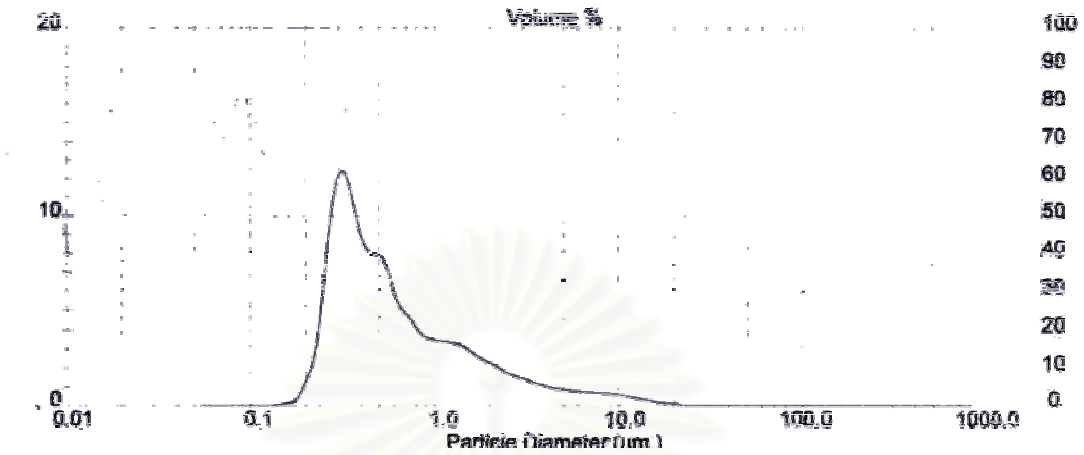

Figure I-8 The mean particle size and particle size distribution of chitosan alginate nanoparticles of lycopene initial concentration 88.98 µg/mL.

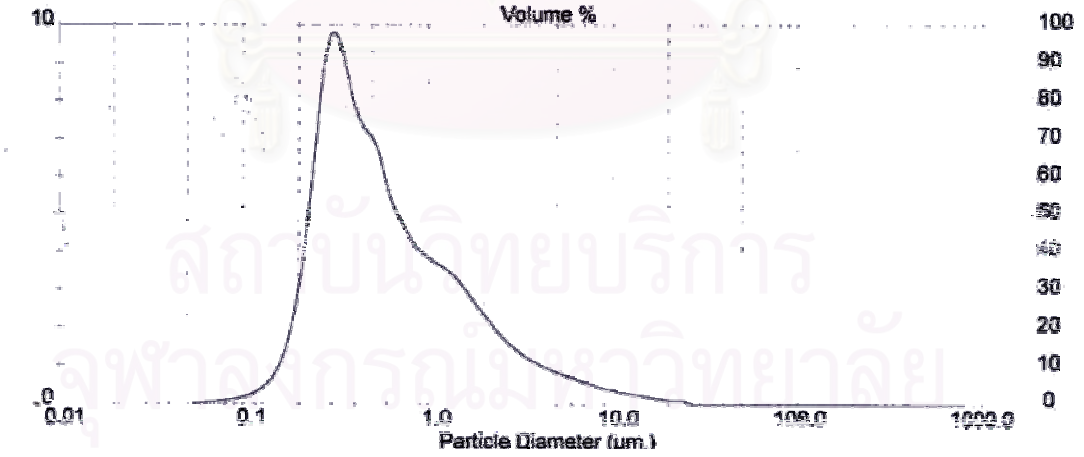

Figure I-9 The mean particle size and particle size distribution of chitosan alginate nanoparticles of lycopene initial concentration 140.56 µg/mL.

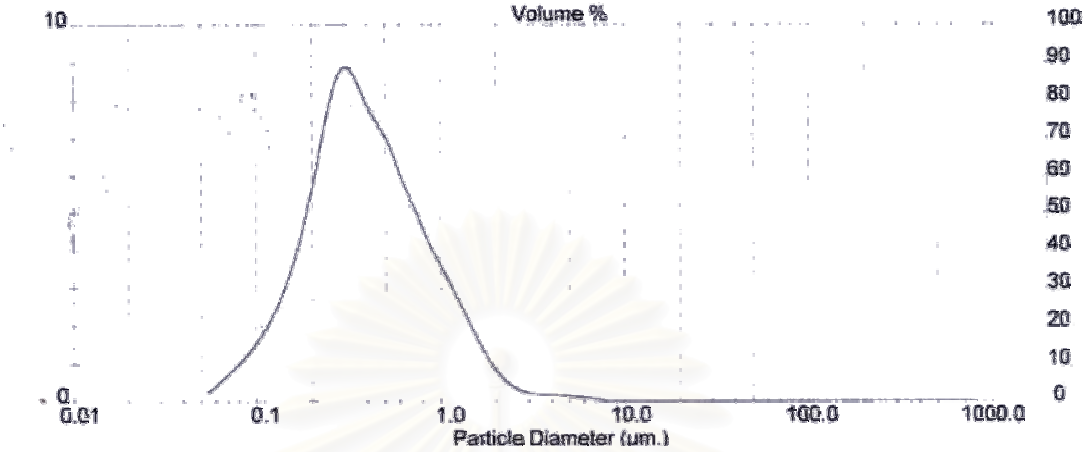

Figure I-10 The mean particle size and particle size distribution of chitosan alginate nanoparticles of lycopene initial concentration 200.28 µg/mL.

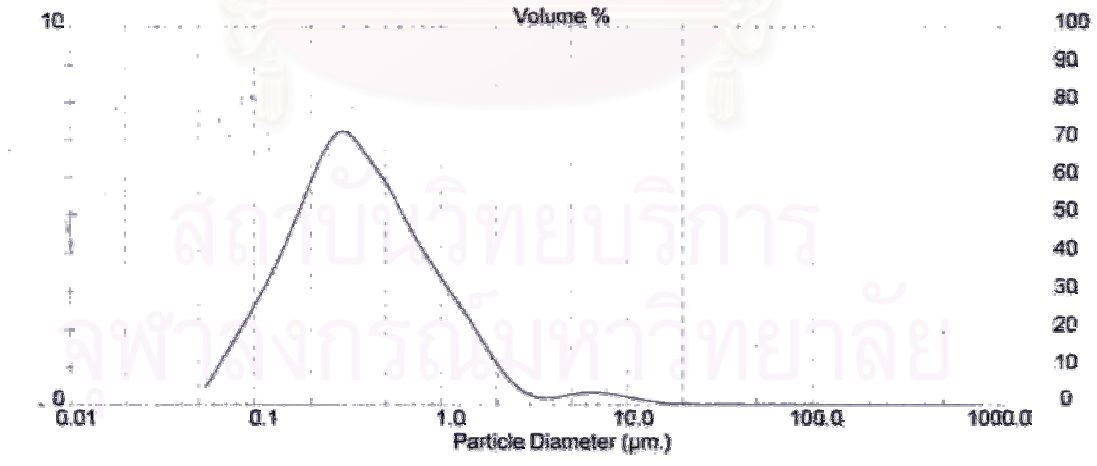

Figure I-11 The mean particle size and particle size distribution of chitosan alginate nanoparticles of lycopene initial concentration 234.16 µg/mL.

Figure I-12 Lycopene loaded chitosan coated liposome nanoparticle suspensions after centrifuge at 3,500 rpm for 1 h at 4^{o}C. CL1-5 is prepared from the initial lycopene concentration of 45.75, 88.98, 140.56, 200.28 and 234.16 µg/mL, respectively.

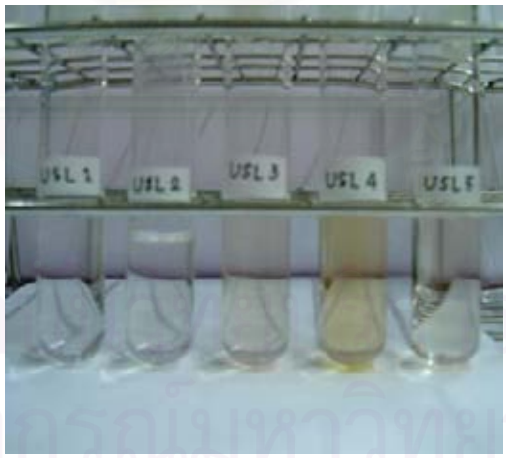

Figure I-13 The supernatant of lycopene loaded chitosan coated liposome nanoparticles after ultracentrifuge at 60,000 rpm for 2 h at 4^{o}C. USL1-5 is prepared from the initial lycopene concentration of 45.75, 88.98, 140.56, 200.28 and 234.16 µg/mL, respectively.

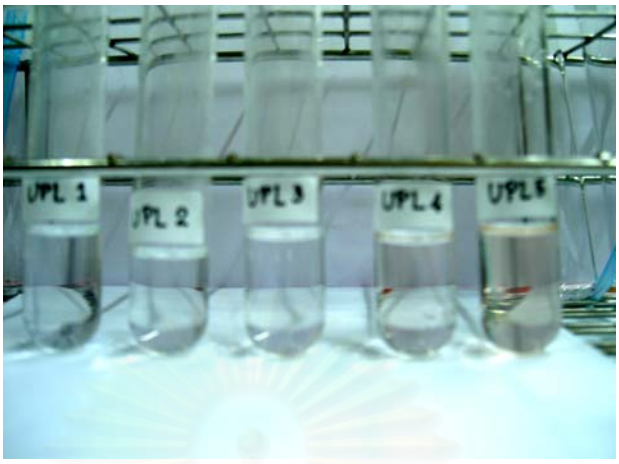

Figure I-14 The precipitant of lycopene loaded chitosan coated liposome nanoparticles after ultracentrifuge at 60,000 rpm for 2 h at 4^{o}C. UPL1-5 is prepared from the initial lycopene concentration of 45.75, 88.98, 140.56, 200.28 and 234.16 µg/mL, respectively.

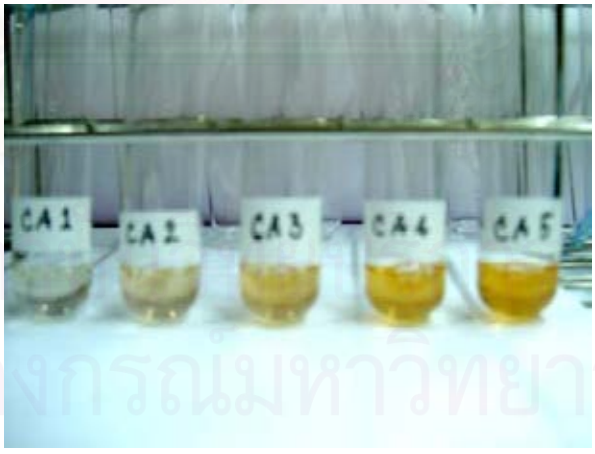

Figure I-15 Lycopene loaded chitosan alginate nanoparticle suspensions after centrifuge at 3,500 rpm for 1 h at 4^{o}C. CA1-5 is prepared from the initial lycopene concentration of 45.75, 88.98, 140.56, 200.28 and 234.16 µg/mL, respectively.

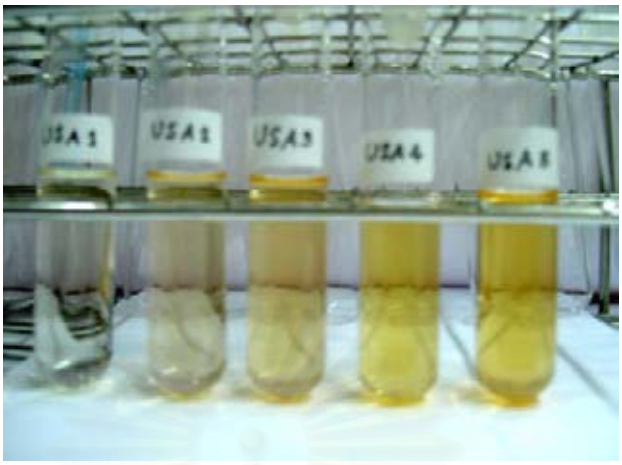

Figure I-16 The supernatant of lycopene loaded chitosan alginate nanoparticles after ultracentrifuge at 60,000 rpm for 2 h at 4^{o}C. USA1-5 is prepared from the initial lycopene concentration of 45.75, 88.98, 140.56, 200.28 and 234.16 µg/mL, respectively.

Figure I-17 The precipitant of lycopene loaded chitosan alginate nanoparticles after ultracentrifuge at 60,000 rpm for 2 h at 4^{o}C. UPA1-5 is prepared from the initial lycopene concentration of 45.75, 88.98, 140.56, 200.28 and 234.16 µg/mL, respectively.

A. B.

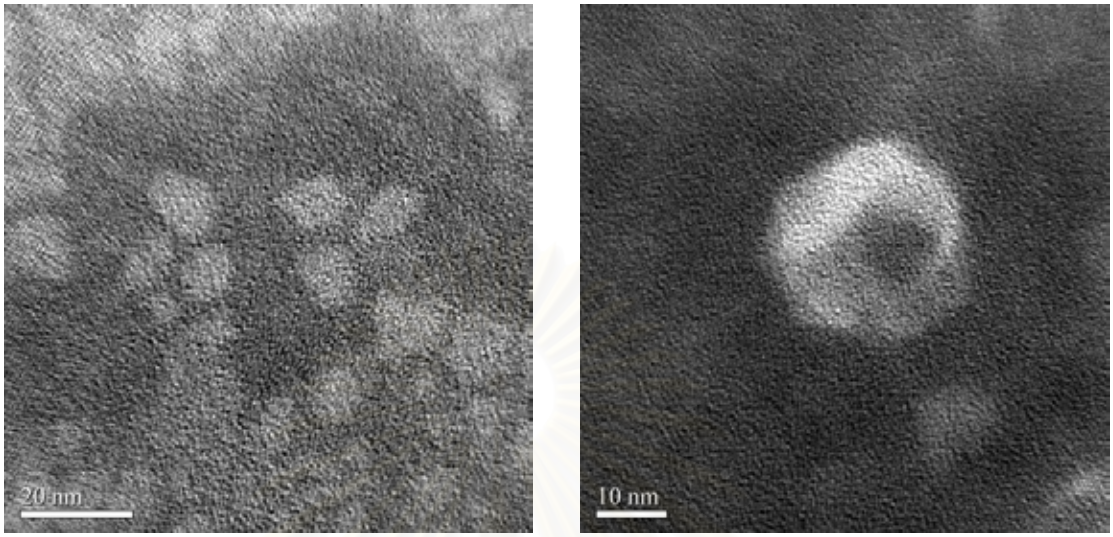

Figure I-18 Transmission electron micrographs of the supernatant of lycopene loaded chitosan coated liposome nanoparticles after ultracentrifuge at 60,000 rpm for 2 h. A: vesicles structure with a small particles with a homogeneous distribution of diameter about 10 nm (x 750,000),
B: individual vesicle structure at high magnification (x 900,000).

A. B.

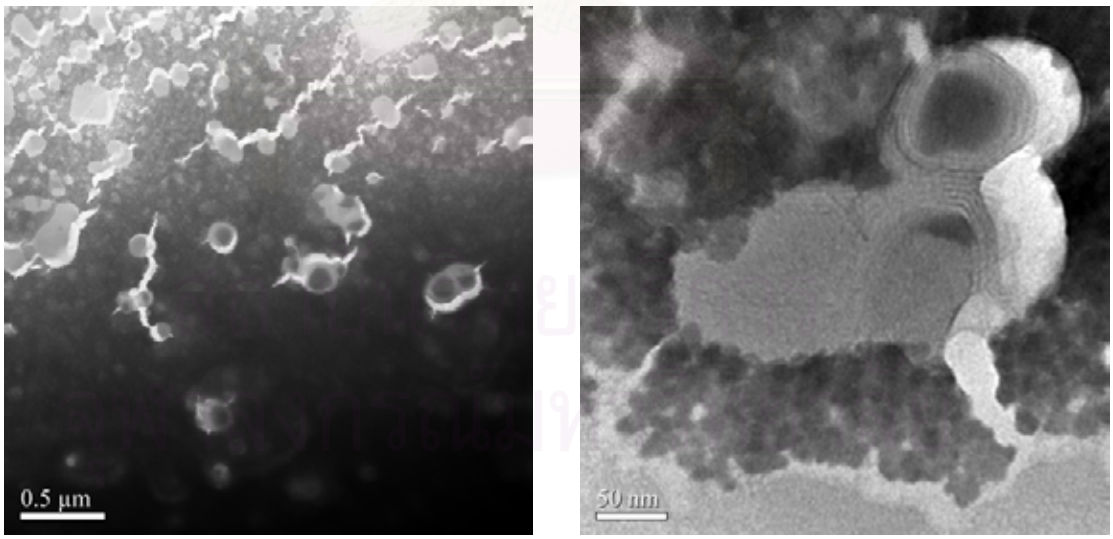

Figure I-19 Transmission electron micrographs of the precipitant of lycopene loaded chitosan coated liposome nanoparticles after ultracentrifuge at 60,000 rpm for 2 h. A: an overview of small vesicles with a homogeneous distribution (x 22,000),
B: overlapping of vesicle and presented of multilamellar vesicles at high magnification (x 180,000).

A. B.

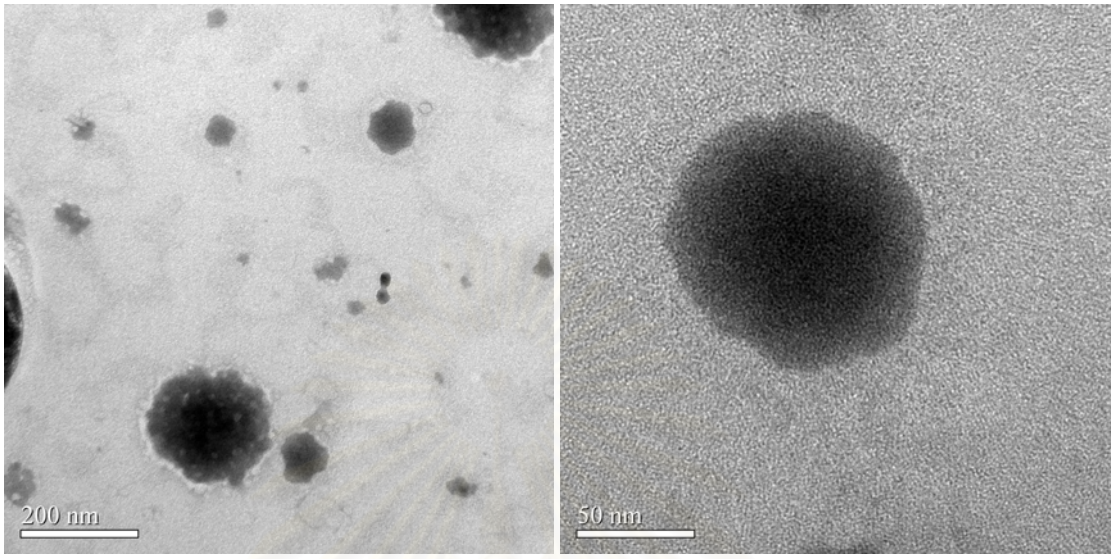

Figure I-20 Transmission electron micrographs of the supernatant of lycopene loaded chitosan alginate nanoparticles after ultracentrifuge at 60,000 rpm for 2 h.
A: a spherical structure with a various particles sizes up to 200 nm (x 75,000),
B: individual particle present a nanosphere structure (x 300,000).

A. B.

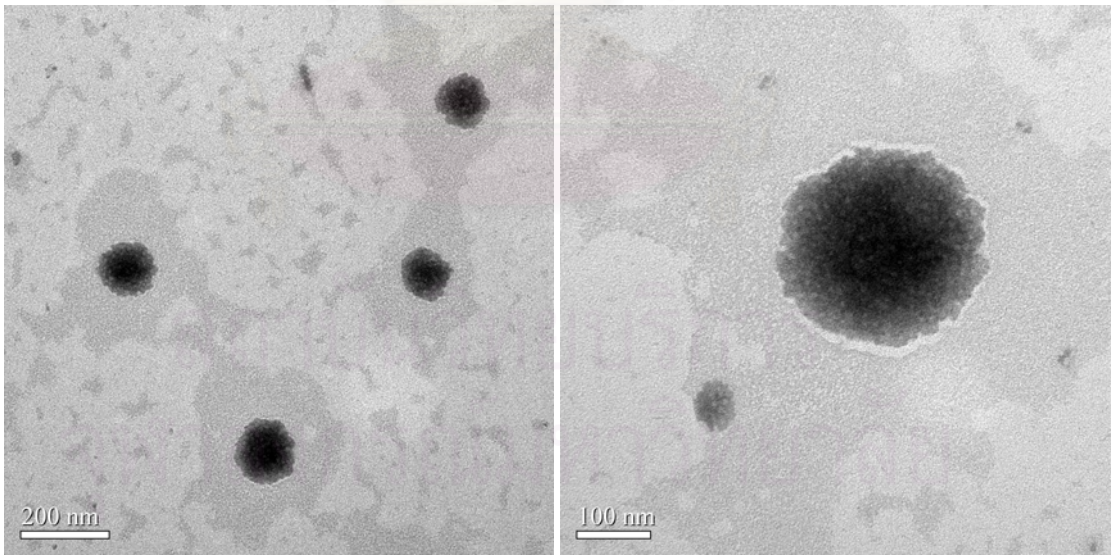

Figure I-21 Transmission electron micrographs of the precipitant of lycopene loaded chitosan alginate nanoparticles after ultracentrifuge at 60,000 rpm for 2 h.
A: spherical structure with a homogeneous distribution in diameter 100-200 nm (x 55,000), B: individual particle (x 90,000).

APPENDIX II

The data of stability study

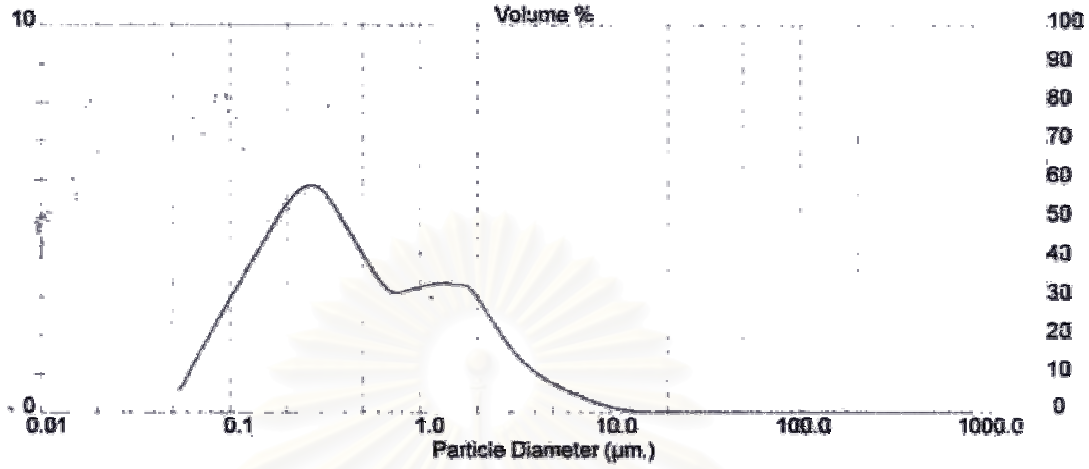

Figure II-1 The mean particle size and particle size distribution of lycopene loaded chitosan coated liposome nanoparticles after storage for 12 weeks in refrigerator.

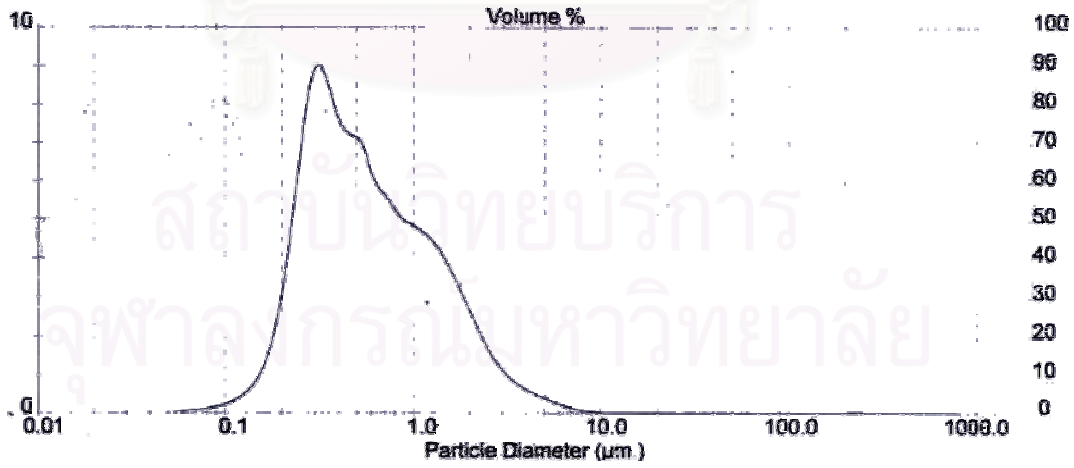

Figure II-2 The mean particle size and particle size distribution of lycopene loaded chitosan coated liposome nanoparticles after storage for 12 weeks in dark at room temperature.

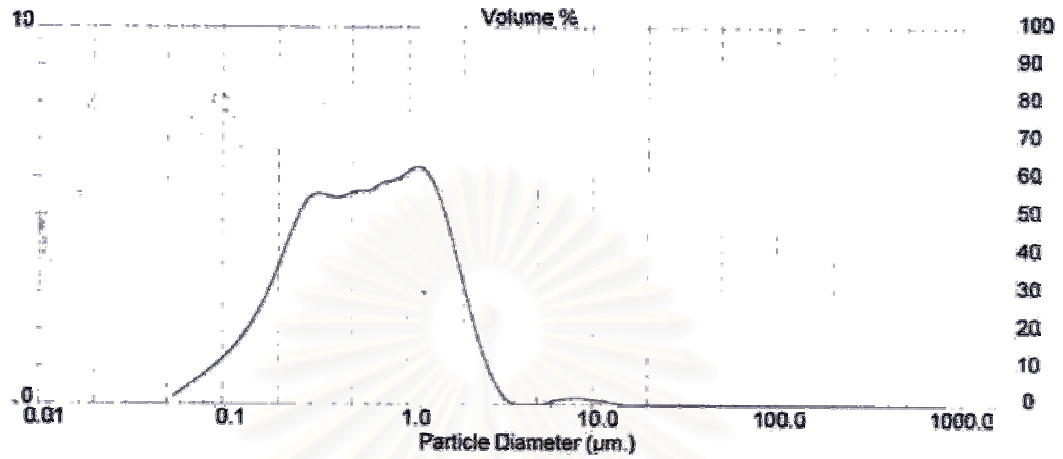

Figure II-3 The mean particle size and particle size distribution of lycopene loaded chitosan coated liposome nanoparticles after storage for 12 weeks visible light at room temperature.

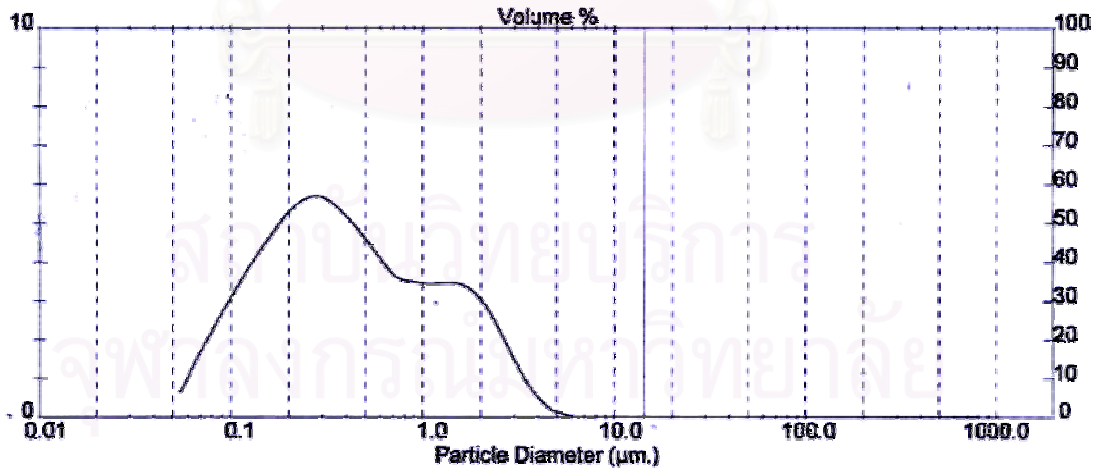

Figure II-4 The mean particle size and particle size distribution of lycopene loaded chitosan alginate nanoparticles after storage for 12 weeks in refrigerator.

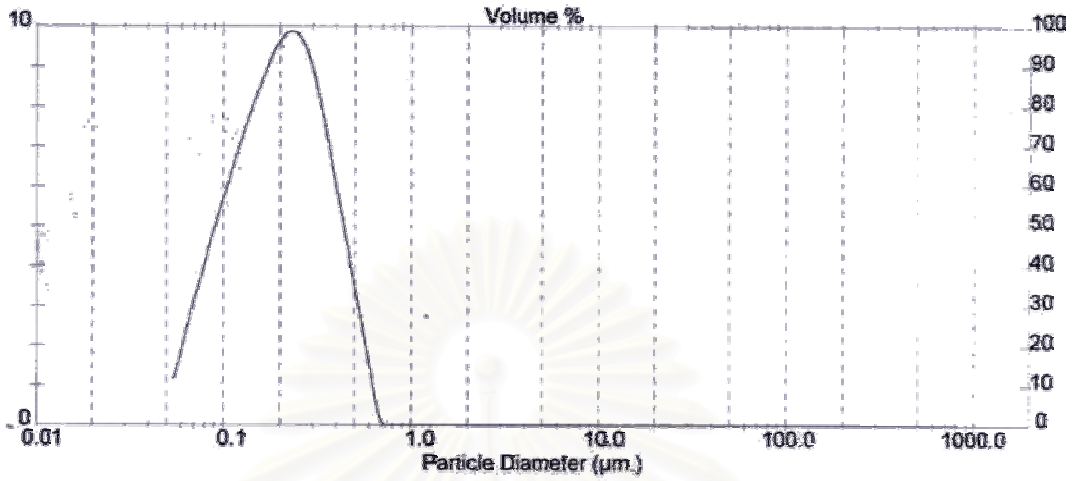

Figure II-5 The mean particle size and particle size distribution of lycopene loaded chitosan alginate nanoparticles after storage for 12 weeks in dark at room temperature.

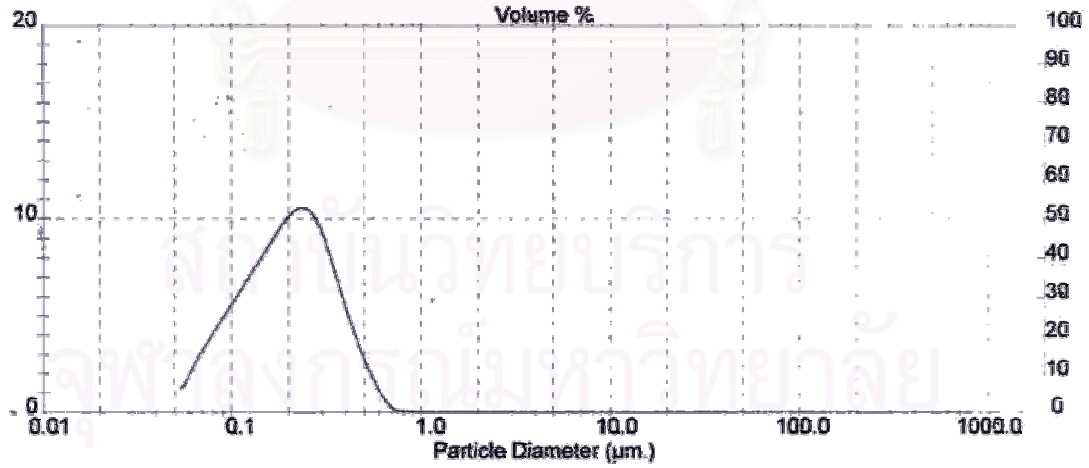

Figure II-6 The mean particle size and particle size distribution of lycopene loaded chitosan alginate nanoparticles after storage for 12 weeks in visible light at room temperature.

Table II-1 The lycopene content and % remaining of lycopene in chitosan coated liposome nanoparticles during storage for 12 weeks in refrigerator, in dark and visible light at room temperature (n=2).

Condition	Week	Lycopene content (µg/mL)				% Remaining of lycopene			
		n 1	n 2	Mean	SD	n 1	n 2	Mean	SD
Refrigerator	1	0.0679	0.0747	0.0713	0.0048	86.81	95.54	91.18	6.17
	2	0.0668	0.0781	0.0724	0.0080	85.40	99.84	92.62	10.21
	3	0.0607	0.0676	0.0641	0.0049	77.60	86.43	82.01	6.24
	4	0.0486	0.0551	0.0519	0.0046	62.18	70.49	66.33	5.88
	8	0.0133	0.0118	0.0125	0.0011	17.01	15.09	16.05	1.36
	12	UD	UD	UD	UD	UD	UD	UD	UD
Dark	1	0.0670	0.0669	0.0669	0.0001	85.62	85.51	85.57	0.08
	2	0.0574	0.0670	0.0622	0.0068	73.46	85.74	79.60	8.68
	3	0.0464	0.0576	0.0520	0.0080	59.28	73.69	66.48	10.19
	4	0.0425	0.0465	0.0445	0.0029	54.31	59.51	56.91	3.68
	8	0.0104	0.0102	0.0103	0.0002	13.33	13.03	13.18	0.21
	12	UD	UD	UD	UD	UD	UD	UD	UD
Visible light	1	0.0634	0.0711	0.0673	0.0055	81.06	90.95	86.00	7.00
	2	0.0612	0.0534	0.0573	0.0055	78.26	68.34	73.30	7.01
	3	0.0457	0.0431	0.0444	0.0018	58.38	55.08	56.73	2.33
	4	0.0423	0.0504	0.0464	0.0057	54.10	64.49	59.29	7.35
	8	UD	UD	UD	UD	UD	UD	UD	UD
	12	UD	UD	UD	UD	UD	UD	UD	UD

UD = Undetectable

Table II-2 The lycopene content and % remaining of lycopene in chitosan alginate nanoparticles during storage for 12 weeks in refrigerator, in dark and visible light at room temperature (n=2).

Condition	Week	Lycopene content (µg/mL)				% Remaining of lycopene			
		n 1	n 2	Mean	SD	n 1	n 2	Mean	SD
Refrigerator	1	3.0619	3.4514	3.2566	0.2754	95.83	108.02	101.93	8.62
	2	3.1431	3.1390	3.1410	0.0029	98.37	98.24	98.31	0.09
	3	2.7984	2.8025	2.8004	0.0029	87.58	87.71	87.65	0.09
	4	2.6509	2.7328	2.6918	0.0579	82.97	85.53	84.25	1.81
	8	2.1955	2.1366	2.1660	0.0416	68.71	66.87	67.79	1.30
	12	1.9179	1.9757	1.9468	0.0409	60.03	61.84	60.93	1.28
Dark	1	3.0737	3.1734	3.1236	0.0705	96.20	99.32	97.76	2.21
	2	2.9452	2.8162	2.8807	0.0913	92.18	88.14	90.16	2.86
	3	2.7233	2.8208	2.7720	0.0689	85.23	88.28	86.76	2.16
	4	2.4716	2.4620	2.4668	0.0068	77.36	77.06	77.21	0.21
	8	1.6222	1.5337	1.5780	0.0625	50.77	48.00	49.39	1.96
	12	1.0845	1.0583	1.0714	0.0186	33.94	33.12	33.53	0.58
Visible light	1	2.8130	2.8042	2.8086	0.0062	88.04	87.77	87.90	0.20
	2	2.7301	2.7816	2.7558	0.0364	85.44	87.06	86.25	1.14
	3	2.6399	2.7107	2.6753	0.0501	82.62	84.84	83.73	1.57
	4	2.5616	2.5429	2.5523	0.0132	80.17	79.59	79.88	0.41
	8	0.8596	0.9550	0.9073	0.0675	26.90	29.89	28.40	2.11
	12	UD	UD	UD	UD	UD	UD	UD	UD

UD = Undetectable

Table II-3 The lycopene content and % remaining of lycopene in ethanol during storage for 12 weeks in refrigerator, in dark and visible light at room temperature (n=2).

Condition	Week	Lycopene content (µg/mL)				% Remaining of lycopene			
		n 1	n 2	Mean	SD	n 1	n 2	Mean	SD
Refrigerator	1	6.8623	7.0228	6.9425	0.1135	99.06	101.37	100.22	1.64
	2	6.7059	6.8033	6.7546	0.0689	96.80	98.21	97.50	0.99
	3	6.2524	6.3980	6.3252	0.1030	90.25	92.36	91.30	1.49
	4	4.8268	5.0132	4.9200	0.1318	69.67	72.37	71.02	1.90
	8	3.6887	3.8483	3.7685	0.1129	53.25	55.55	54.40	1.63
	12	3.6199	3.8036	3.7117	0.1299	52.25	54.90	53.58	1.88
Dark	1	6.7386	7.2896	7.0141	0.3896	97.27	105.22	101.25	5.62
	2	6.1031	6.3829	6.2430	0.1978	88.10	92.14	90.12	2.86
	3	5.9601	6.3200	6.1400	0.2545	86.03	91.23	88.63	3.67
	4	5.3936	5.5606	5.4771	0.1181	77.86	80.27	79.06	1.70
	8	1.6472	1.7956	1.7214	0.1049	23.78	25.92	24.85	1.51
	12	0.9100	1.0275	0.9687	0.0831	13.14	14.83	13.98	1.20
Visible light	1	5.9985	6.1773	6.0879	0.1264	86.59	89.17	87.88	1.83
	2	5.4737	5.8147	5.6442	0.2412	79.01	83.94	81.47	3.48
	3	5.2287	5.3548	5.2918	0.0891	75.48	77.30	76.39	1.29
	4	4.4776	4.7832	4.6304	0.2161	64.63	69.04	66.84	3.12
	8	1.4587	1.5576	1.5082	0.0700	21.06	22.48	21.77	1.01
	12	0.6974	1.0072	0.8523	0.2190	10.07	14.54	12.30	3.16

APPENDIX III

The data of *in vitro* skin penetration experiment

Table III-1 Cumulative amount (µg) and % penetration of lycopene loaded chitosan coated liposome nanoparticles (n=3).

Time	n 1		n 2		n 3		Mean	SD
	Cumulative amount	% Penetration	Cumulative amount	% Penetration	Cumulative amount	% Penetration		
0.5	1.2005	36.06	1.2559	37.73	1.2821	38.51	37.43	1.25
1	1.3692	41.13	1.4756	44.32	1.4992	45.03	43.50	2.08
1.5	1.9386	58.23	2.0463	61.47	2.0807	62.50	60.73	2.23
2	2.0098	60.37	2.1672	65.10	2.1260	63.86	63.11	2.45
4	2.3155	69.55	2.4075	72.32	2.3997	72.09	71.32	1.53
6	2.3387	70.25	2.4653	74.06	2.4464	73.49	72.60	2.05
8	2.3548	70.74	2.5097	75.39	2.5383	76.25	74.12	2.97
12	2.4025	72.17	2.5677	77.13	2.5657	77.07	75.46	2.85

Table III-2 Cumulative amount (µg) and % penetration of lycopene loaded chitosan alginate nanoparticles (n=3)

Time	n 1		n 2		n 3		Mean	SD
	Cumulative amount	% Penetration	Cumulative amount	% Penetration	Cumulative amount	% Penetration		
0.5	2.5339	28.23	2.4648	27.46	2.4363	27.14	27.61	0.56
1	3.6954	41.17	3.4562	38.50	3.5476	39.52	39.73	1.35
1.5	4.7449	52.86	4.4013	49.03	4.4518	49.60	50.50	2.07
2	5.1181	57.02	4.9073	54.67	4.9760	55.43	55.71	1.20
4	5.9909	66.74	5.7145	63.66	5.6271	62.69	64.36	2.12
6	6.4719	72.10	6.0881	67.82	6.0826	67.76	69.23	2.49
8	6.4418	71.76	6.1476	68.49	6.0836	67.77	69.34	2.13
12	6.5190	72.62	6.2598	69.74	6.2026	69.10	70.49	1.88

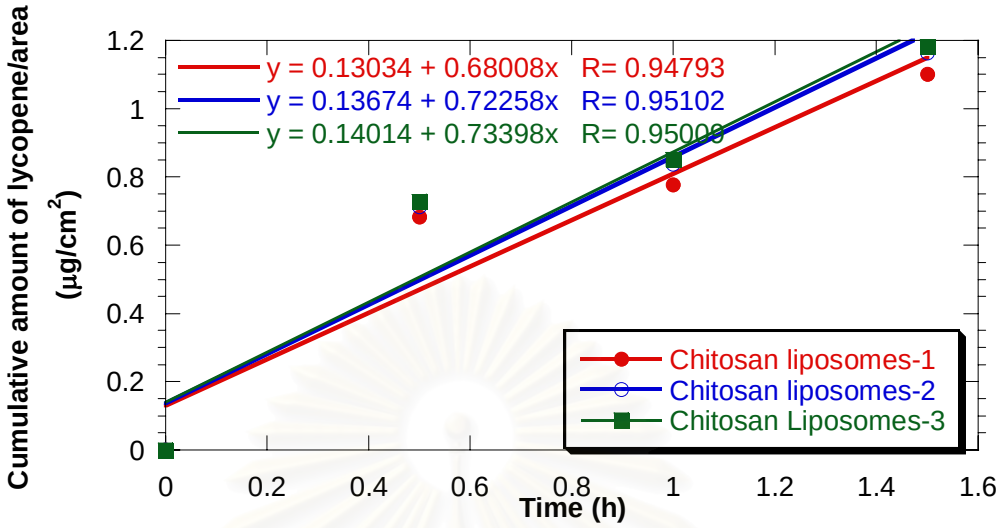

Figure III-1 Flux of lycopene loaded chitosan coated liposome nanoparticles (n=3).

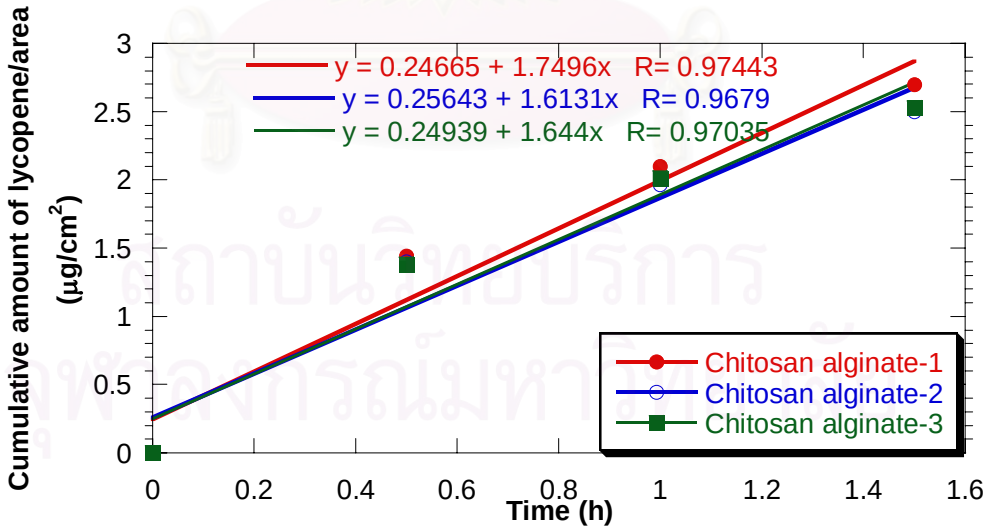

Figure III-2 Flux of lycopene loaded chitosan alginate nanoparticles (n=3).

Table III-3 The statistical analysis of permeability coefficient of lycopene loaded chitosan coated liposome nanoparticles and lycopene loaded chitosan alginate nanoparticles.

Student's t-test for unpaired data with unequal variance

Group 1: permeability coefficient of lycopene loaded chitosan coated liposome nanoparticles

Group 2: permeability coefficient of lycopene loaded chitosan alginate nanoparticles

	Group 1	Group 2
Count	3	3
Mean	0.296567	0.264033
Variance	0.000139523	0.000128
Std. Dev.	0.011812	0.011325
Std. Err	0.00681966	0.006538
Mean Difference	0.0325333	
Degrees of Freedom	3	
t Value	3.4436	
t Probability	0.02628	
F Value	1.088	
F Probability	0.9579	

Table III-4 The statistical analysis of flux of lycopene loaded chitosan coated liposome nanoparticles and lycopene loaded chitosan alginate nanoparticles.

Student's t-test for unpaired data with unequal variance

Group 1: flux of lycopene loaded chitosan coated liposome nanoparticles

Group 2: flux of lycopene loaded chitosan alginate nanoparticles

	Group 1	Group 2
Count	3	3
Mean	0.712233	1.6689
Variance	0.000807	0.005123
Std. Dev.	0.028406	0.071576
Std. Err	0.0164	0.041324
Mean Difference	-0.95667	
Degrees of Freedom	2	
t Value	-21.518	
t Probability	0.000514	
F Value	6.349	
F Probability	0.2721	

Table III-5 The statistical analysis of percentage of penetration of lycopene loaded chitosan coated liposome nanoparticles and lycopene loaded chitosan alginate nanoparticles.

Student's t-test for unpaired data with unequal variance

Group 1: the percentage of penetration of lycopene loaded chitosan coated liposome nanoparticles

Group 2: the percentage of penetration of lycopene loaded chitosan alginate nanoparticles

	Group 1	Group 2
Count	3	3
Mean	75.4567	70.4867
Variance	8.10253	3.51574
Std. Dev.	2.8465	1.87503
Std. Err	1.64342	1.08255
Mean Difference	4.97	
Degrees of Freedom	3	
t Value	2.5255	
t Probability	0.07464	
F Value	2.305	
F Probability	0.6052	

VITA

Miss Suda Limvongsuwan was born on August 1, 1979 in Bangkok, Thailand. She received her Bachelor's Degree of Science in Pharmacy from the Faculty of Pharmacy, Mahidol University in 2001. After graduation, she worked at Klongyai hospital, Trat, Thailand for 3 years before entering the Master's Degree program in Pharmaceutical Technology at Chulalongkorn University.